POTENTIAL OF PERVAPORATION FOR THE CONVERSION OF A METHYL ACETATE-METHANOL WASTE INTO N-BUTYL ACETATE

Giuseppe GENDUSO

Supervisor:
Prof. B. Van der Bruggen

Co-Supervisor:
Prof. P. Luis

Members of the Examination Committee:
Prof. A. Bultheel, chairman
Prof. J. Degrève
Prof. P. Izák
Prof. P. Pescarmona
Prof. G. Stefanidis

Dissertation presented in partial fulfilment of the requirements for the degree of Doctor in Engineering Science

February 2016

Uitgegeven in eigen beheer, Giuseppe Genduso, Rue Van Hammée 77, 1030 Schaerbeek (Brussels).

ACKNOWLEDGEMENTS

This is the final act of my Ph. D. experience: writing all about my research; or at least what has been achieved through a patient work and can be shown as a major result. The hidden rest of my research comprises a lot of mess, errors, stress, missed experiments, missed points, confusion, misunderstandings, deleted sentences and so on. According to my limited experiences, research is most of the time a *rough* learning process, surrounded by few but very intense feelings of accomplishment.

However, hereinafter I am going to skip the research for a moment in order to talk about people; all the people that have been around me during these intense three years of my Ph. D. research. In particular, I am going to talk about all the people that made me a better person, both from a professional and an every-day-life point of view, and both directly and indirectly.

How did I end up in Belgium? During October 2012, I was in Berlin, where I was studying for the *chemical engineering license exam* (what in Italy is called "abilitazione alla professione di ingegnere") and looking for a job; meanwhile enjoying living together with my girlfriend Miriam. One day she wanted to work alone for her thesis and *kicked me* out of the apartment. Therefore, I went to the library of the Humboldt University where, for the first time after, I decided to look for a possible Ph.D. position and not for a job in industry (at that time I was more than convinced that I should avoid doing a Ph. D.). One of the first applications I wrote was in fact directed to Prof. Bart Van der Bruggen, as reply to his announcement that attracted my attention. The selection procedure went quite fast and, according to the schedule of my *chemical engineering*

license exam, I was able to start my Ph. D. in Belgium in February 2013. Therefore, I would like to express my gratitude to Prof. Van der Bruggen for selecting me for this Ph. D. position and introducing me to the world of membranes. During these three years, he has given me the chance to believe in my ideas and to have the freedom and time to recognize them, finding a solution. I could always count on his deep understanding. With his help, I have learned how to write scientific communications and present my work in the best manner. Moreover, I have been always deeply fascinated from his commitment to employ people from all over the world for his research group; and in particular, people coming from those regions of the word that suffer from a very slow and obstructed economic growth. I believe that, even bigger than Prof. Van der Bruggen's fundamental scientific contribution to today's membrane technology, it is his contribution to the creation of a more equal world.

I would also like to thank my co-promoter, Prof. Patricia Luis for her work of supervision; and in particular during the first year of my Ph. D., when my lack of experience led to commit a number of infinite errors, which she was always willing to discuss and help finding a solution. In a way, during the first year, she has been the person who taught me how to deal with my future Ph. D. difficulties.

Concerning the members of the Ph. D examination committee, I would like to thank Professor Adhemar Bultheel for chairing my Ph. D. Moreover, I would like to express my gratitude to Professors Paolo Pescarmona, Pavel Izák and Georgios Stefanidis, for the time spent in evaluating my thesis manuscript, providing interesting and helpful suggestions.

For their help and scientific input I would like to thank all Professors of the *Chemische Ingenieurstechnieken* (CIT). In particular, I would like to acknowledge the help of Prof. Jan Degrève for giving always punctual and reasonable critics regarding my research work and, according to his deep knowledge about the chemical engineering technology, for having acted as a perfect mentor for one of the chapters of this thesis. In addition, I would like to acknowledge Prof. Degrève's, very helpful, work of evaluation of my thesis manuscript as a member of the Ph. D. examination committee. Sincere and deep is also the gratitude I want to express to Prof. Carlo Vandecasteele for his help during my job search; his advices and critics turned out to be fundamental in order to find new and interesting work opportunities. Prof. Simon Kuhn, thanks for your help with the calculation of the Reynold's number of the pervaporation cell setup and for being so kind to show me your impressive research work. Prof. Ilse Smets and Koenraad Muylaert, thanks for your interest in my micro-*algae* idea and for sending your contacts; unfortunately my proposal was not further considered. I would also like to acknowledge the help of Prof. Tom Van Gerven for his impressive work as manager of the ProcESS division and for proposing a Ph.D. position within his group to my friend Corrado (unfortunately Corrado opted for another position in the United Arab Emirates).

My special thanks are extended to the administrative staff of CIT, *i.e.*, Alena Vaes, Marie-Claude Deflem and Beatrice De Geest, always ready in solving any administrative matter. I would also like to offer my special thanks to the technician of CIT: Hanne Geunes, Herman Tollet and Marc Van Overloop, for their daily work assuring the CIT-machine is working. Marc, thanks for allowing me to describe my fantastic Sicily; I hope I will meet you there once, I would be more than honoured to show you around

(at least what you still have not visited yet). Thanks to Michèle Vanroelen who, during these years, was much more than just a very professional laboratory technician to me. I enjoyed discussing with her about running and her advices about baby-managing resulted to be very helpful. My gratitude goes also to Christine Wouters, who made a fantastic job analyzing my samples.

A particular acknowledgement goes to Tony Debecker of the mechanical workshop of the Chemical Department. I could have never run some of my experiments without the mechanical laboratory pieces he built for me. It was very interesting to design and try to find a creative solution to mechanical problems regarding the pervaporation laboratory unit I have used.

During my experience at CIT, I have been in contact with quite a large number of people that, for a more or less long time, have been good colleagues to me and some of them also friends. I would like to acknowledge people like: Nora Jullok, Priyanka Mondal, Thi Kim Anh Tran, Tadesse Getahun, Alemayehu Haddis, Wenyuan Ye, Jiuyang Lin, Abdellah Ammisaid, Henrik Tækker Madsen, Siavash Darvishmanesh, Anita Rugaika, Dessalegn Dadi Olani, Oded Nir, Bjorn Gielen, Bart Van den Bogaert, Chenna Rao Borra, Jeroen Jordens, Jinu Joseph John, Anca Roibu, Aditi Potdar, Christos Xiouras, Milad Mottaghi, Rodolfo Marin Rivera, Van Loy Steff, Senne Fransen and Afsoon Jamali and many more. They have been a pleasant company during my work at CIT, creating an incredibly multicultural environment that allowed all the most interesting discussions about our world.

Thanks to Hasan Farrokhzad for his help with polymer technology and membrane synthesis. The collaboration with Hasan resulted to be very

fruitful because it led to the publication of two scientific papers. Moreover, I have to acknowledge him for the nice discussions we had (even about spiritual matters).

Johan Vanneste, you have been an acquaintance just for a short time. It is a pity we did not have enough time to get to know each other better. I believe that my culture of the underground bike world would have benefited a lot from your friendship (I wish you all the best there in USA).

For the category "office mates", I acknowledge Wouter Van Aeken. I hope there will be the possibility to get to know you better in the future; I have really appreciated your respectful way of sharing our office. Kerwin Wong was also a nice presence in my office before leaving for Canada. At that time, Ruixin Zhang was also an office companion. She has been a friend before being a colleague, always willing to discuss problems and to find reasonable solutions: she was also a bit of a supervisor. I have really enjoyed her company in our office (room 03.45) before her graduation.

For the category "crazy discussions group", I acknowledge Saeed Mazinani, Fred Molelekwa and Shadi Hamdan. Individually, these three persons can be very quiet and discrete. However, every time I found them all together, the craziest discussions started. It is a pity we could not get more of this. A particular acknowledgment goes to Shadi who has been a real friend throughout my entire time at CIT. We have discussed, argued, drunk nice coffee, laughed and also asked each other for advices in all critical work and personal-related situations. Shadi, it is a pity I cannot insert the image of "the wind" here in this section of my manuscript.

For the category "it is lunch time, why don’t we go to make some healthy blues", I acknowledge Enis Leblebici. It was great to play with you. It was

short but it also gave me the necessary kick to start playing again. Enis is a great guitar player and I will miss the chance to gig with him. It has been also a pleasure to meet his wife, Pelin Leblebici, a person of elegant humour.

For the category "we go running during lunch break", I need to express all my deep gratitude to Bram Verbinnen and Pieter Billen, who gave me the chance to become a bit less fat than I am. Pieter and Bram are two wonderful friends that gladdened my heart at work and after work time with nice discussions, running breaks, bike tours and much more. I have enjoyed very much doing all this with you both! Pieter, it was a joy to be present to your wedding. Bram, somewhere in the future we will run again the Velpe-Mene trail; I had a very good time that day.

In the category "friendship and wedding", I include Carlos Andecochea Saiz and Antonio Amelio. Antonio is the first person I have met at CIT. Besides the work collaborations we had, which gave very interesting results, I feel like our friendship has grown increasingly during these three years. We had very nice moments in Poland for the *IV International Scientific Conference on Pervaporation, Vapor Permeation and Membrane Distillation* (during the end of September 2014). On this occasion, I also met Rafal Grzelewski, to whom goes my gratitude for hosting me in Warsaw, sharing his bright soul and humour. Carlos instead, is a person of strong believes and passionate living. I have enjoyed our discussions about music, politics and guitars. Moreover, I thank him and his nice spouse Zoe, for having me selected to be an important pillar of their wedding. Antonio together with Carlos became two solid mates to share my free time at CIT with. I will never forget Carlos' bachelor party: a celebration of joy and happiness, embracing people of all over the world

in the scenario of Brussels historical centre. I still have to defeat you both in our next go-kart session! In addition, I need to express my gratitude to Zoe, Carlos and Antonio for the wonderful moments we had during our trip to Spain (for Carlos' fabulous wedding), where we were visiting the beautiful Cantabria.

In the category "thesis students", I have got Sebastien Rauss, Ylke Bruggeman, Vicente Osorio, Yannick Latré and Erik Colombini. I could never obtain most of my research results without their help. In particular, to these last two persons I would like to dedicate my gratitude for being friends to me and not only two special students. They were very beloved persons at CIT, from colleagues and technical staff alike. One of the members of the technical staff group said once: "Giuseppe, you had no better students than Yannick and Erik".

Apart from the time I have spent working in Leuven, all the most beautiful and meaningful moments derived from my after-work in Brussels. It is in fact there, that Miriam and I decided to live; a place as far as possible from the world of university in order to separate home life from work. I believe that was the right decision, since (besides the lost time waiting always for delayed trains [NMBS, thanks for that!]) it allowed me to maximize the number and variety of nice people that I could get in contact with.

Treated chronologically, the first people I have met in Brussels were Annelies Boddez and Evelien De Bal. In fact, at the very end of 2012, they hosted Miriam and me in their apartment, after having accepted our CouchSurfing request. They were also so kind to invite us for the *New Year's Eve* of 2013 they would celebrate with their friends. This event constituted the first real contact we had with Belgium and in particular

with Brussels people. We felt like being among friends and we enjoyed a funny and happy night. During this occasion we also had the chance to meet Dorien and Quentin Smets. We could not have expected how strong the friendship with these people may become. With Dorien and Quentin we have shared a lot and much more we could have done. It was more than a pleasure and honour to be invited to their lovely wedding. Quentin, you have been a great friend. I have enjoyed biking with you (up until I could keep up!). Moreover, I will never forget the rainy-jungle-style paint-ball afternoon, which we enjoyed during your bachelor party.

The day after the *New Year's Eve* of 2013, Miriam and I were already busy looking for an apartment. We found something, but it turned out to be fraud. Hence, in order to start working in February at CIT, I had to find another accommodation via CouchSurfing. It is in this way that I have found Theun, who has become one of my closest friends. He is an incredible person, out of any scheme, always positive and helpful. He entered my life with a big noisy smile and I keep enjoying his company during any moment of the week. We can discuss everything. There is not limitation of any kind in our friendship and sometimes I feel like having found a new brother. In addition, Elmar (my son) loves him and elected him to be his *geuzenpeter*; which is some kind of non-religious flamish godfather invented by Theun's father. I am also grateful to Theun's adorable family for hosting us in their house in the "far-west" of Belgium; during this occasion we felt at home, enjoying happy moments and interesting discussions.

Along with Theun's acquaintance came also another wonderful couple: Anne Dewaele and Pieter van Den Broek. Their way of travelling is an

inspiration for me. I keep enjoying their company during our meetings, listening stories about their numerous journeys.

I would also like to thank the German speaking friends that I have met thanks to Miriam: namely Esther Bohé, Dhana Irsara, Sophia Kabir, Marion Bergerman and Lisa Wiedemann. I have enjoyed their presence during our parties in my house in Brussels. I loved to practice my modest German with them. Lisa, thanks for being such a nice person and friend.

Although the companions I met during this period in Belgium may seem numerous, the number of friends I have left behind in Italy is even higher. I am not going to list them all. I will just acknowledge those who endured showing me their friendship, no matter how far the distance. I would like to start with Serafino who is the friend I care the most. It is difficult to describe the joy I felt hosting him here in Brussels and having him as Elmar's godfather. Dario, we didn't get any chance to be together here in Brussels, I hope we will have the possibility to enjoy Saudi Arabia together. I miss humiliating you in a soccer match! Corrado, you were here in Belgium for a too short visit; I will literally cross the desert to meet you in Abu Dhabi (or maybe, you will do it). To Roberto I would like to say that playing with him is one of the things I miss the most. Peppe Colletti, I was very happy to have you here in Belgium for a while and to have had the chance of enjoying hanging around with you, which is a something that deeply amuses me. A particular acknowledgment goes to Martina who came to visit me at the very beginning of my Ph. D. experience (when my apartment walls were of an ugly brown and she had to sleep on the ground). You are a special friend who I really care for. I feel very happy for you having found your love in Luigi. I am very much looking forward to be present at your wedding.

To Maurizio goes my gratitude for having me invited to Tilburg, besides being such a nice companion. In this context, I would like to thank Prof. Andrea Cipollina (Maurizio's Ph.D. co-promoter), for the patience he showed during Euromembrane 2015, for listening to my ideas and for being so kind with me, proposing some interesting research topics. I hope in the future there will be a chance to work together. The experience of Euromembrane 2015 gave me the chance to meet two other incredibly nice persons: Luigi Gurreri and Gianluca Mannella. It has been a long time I have laughed so much in a single night.

I am not going to miss the chance to thank my "Bloofi-Generation" friends: Francesco G., Francesco M., Rossella, Oriana, Veronique, Eloise, Clémentine and Michele. Some of them came to Brussels in a couple of memorable reunion days, during May 2015. In these days, one of the funniest memories regards Elmar, remaining astonished for a couple of minutes, being unable to understand why there was a person (Francesco G.) who looked so much like his father.

I am also indebted to my entire family, a pillar that supports any decision I have taken so far. My best possible expression of love goes to: Nonna Rosina, aunt Lilla and Maria and uncles Vincenzi, to my cousins Sergio, Claudio, Carmelo, Pietro and Maria Chiara. I also want to thank my cousin Valentina (who is like a sister to me) for being such a nice godmother for Elmar. To my uncle Giuseppe and in particular to my aunt Liliana goes a special thought: they are a symbol of endurance and strength, a beautiful couple; the value of their actions is worth a thousand of words.

I would also like to include my family-in-law for their support and warm presence. Wilma, Christopher, Lilith and Timea thanks for being such a nice family for Elmar and making me always feel at home when we have

the chance to meet. In addition, I have to say that I feel very honoured to be Elias' godfather. I hope to have the ability to show the right way to such a good guy like Elias.

It is impossible to describe the gratitude and love towards my parents, Alberto and Lucia, and my wonderful brothers Damiano and Andrea. I miss you the most. You are my strength and my shelter.

My final words go to Miriam, my very love and perspective. She is the person that every day gives me her light, clearing my thoughts. There would not have been any of this without her, helping me taking the right decision. I am indebted with my life for living in such a harmony with her.

Miriam and Elmar, you are my every day and future.

I sincerely hope I have not forgotten anybody who accompanied me during these three years, however even if not mentioned here, to them goes my gratitude too.

Giuseppe Genduso

Brussels, February 2016

ABSTRACT

In order to study the industrial application of the transesterification reaction between *n*-butanol and methyl acetate, the pervaporative concentration of the MM20 waste (~16 mole% methyl acetate in methanol) was assessed. This was done with the intent of producing a reagent stream of higher methyl acetate content, which is necessary in order to shift the reaction equilibrium. For this scope polyvinylidene fluoride (PVDF) pervaporation membranes were synthesized and tested. The outcomes demonstrate that methyl acetate selective membranes based on PVDF are realistic and can be used in order to concentrate low content methyl acetate-methanol industrial waste streams. The PVDF membranes were also compared to two other in-house synthesized membranes, selected based on the Hansen solubility parameters theory. The pervaporative separation of all chosen membranes revealed the inadequacy of the Hansen solubility parameters theory for selection of membranes to be used in pervaporation of alcohol/ester mixtures.

Membranes are often the main limitation of pervaporation. In general, the selection, synthesis and improvement of membranes is an operation that may require an extensive effort in terms of time and cost. Frequently membranes have a limited separation performance and a pure product is not attainable as permeate, especially for pervaporation of organic-organic mixtures. Thus, when the objective is to obtain a pure product, the permeate of a membrane stack is first condensed and then further purified in a following stage. However, a condenser is needed in between each stage making the cost of a long series of stacks economically unacceptable. The use of an alternative approach is proposed in this thesis, by exploring the concept of multi-stage-batch-pervaporation

(MSBP) as a unit operation. In this configuration, the permeate obtained after each batch-stage is recycled back to the feed tank in order to increase the permeate product purity in a following stage. In this thesis it is described how a multi-stage-batch-pervaporation unit is able to meet product purity requirements, by varying the stage-termination condition and the number of stages, using a single membrane-module and a single condenser. The separation of the MM20 waste was chosen as a case study proving that, by using the MSBP approach, it is possible to obtain high quality products even with medium-low performance membranes.

Currently, in the industry the MM20 waste is converted into acetic acid in a continuous-mode operation. Extractive distillation units are used in order to recover methyl acetate from this waste stream, before feeding it to the reactor. In view of producing *n*-butyl acetate instead of acetic acid, in a third part of this thesis a pervaporation module was used in order to study the feasibility of a retrofitting operation. The retrofitted unit uses the columns of the extractive system; the solvent is not longer necessary since the azeotrope is now overcome by pervaporation. The membrane chosen for the retrofitting, *i.e.*, the PolyAl TypM1®, was found to have a medium/low separation factor and high fluxes at the methanol/methyl acetate azeotropic composition. This ensured the simulation of a very challenging condition for the retrofitting from an energetic point of view (*i.e.,* for moderate or low separation factor membranes: the higher the flux, the higher the process energy requirement).

During comparison of the retrofitted hybrid pervaporation-distillation unit with the industrial extractive distillation unit, an overall energy saving up to ~38% was demonstrated (~23% when only the energy of the heaters is taken into account). In addition, major hydraulic

modifications could be avoided using a structured packing and membranes with a higher separation factor.

In the final part of this thesis, in order to propose a low energy consumption flow scheme for the production of *n*-butyl acetate from the MM20 waste stream, three pervaporation-based processes schemes were simulated and energetically compared with two conventional systems, on the basis of the same values of inlet-outlet flow rates and product concentrations. The energy consumption of the three pervaporation-based flow schemes resulted in many cases markedly lower than in the conventional processes, with an overall energy saving up to 27%. Further savings are suggested by heat integration. In addition, it was possible to demonstrate that membranes with a similar separation factor and average total flux values (in the entire range of feed concentrations) influence process design and profitability in a way that depends on the total flux trend at low concentrations in the component selective for the membrane. The higher the total flux in these regions, the lower is the membrane area requirement and the higher is the profitability of the plant designed, even when feeding the system with the streams of low methyl acetate concentration.

SAMENVATTING

De pervaporatieve concentratie van de zogeheten MM20 afvalstroom (bestaande uit 16 mol% methylacetaat in methanol) werd onderzocht in het kader van industriële toepassing van de transesterificatiereactie tussen n-butanol and methylacetaat. De doelstelling is de productie van een reagensstroom met een hogere concentratie van methylacetaat, die nodig is om het reactie-evenwicht te verleggen. Hiertoe werden polyvinylideen fluoride (PVDF) pervaporatiemembranen gesynthetiseerd en getest. De resultaten hiervan tonen aan dat PDVF gebaseerde membranen selectief voor methylacetaat realiseerbaar zijn en kunnen ingezet worden om methylacetaat-methanol industriële afvalstromen op te concentreren. De geteste PVDF membranen werden vergeleken met andere, in dezelfde onderzoeksgroep gesynthetiseerde membranen, geselecteerd op basis van de oplaasbaarheidsparameterstheorie van Hansen. De pervaporatieve scheiding gebruik makend van elk van deze membranen toonde aan dat de theorie van Hansen niet geschikt is voor het selecteren van membranen voor dergelijke scheiding van alcohol/ester mengsels. Membranen zijn vaak de belangrijkste beperking van pervaporatie. De selectie, synthese en verbetering van membranen vereist in het algemeen een significante investering in tijd en middelen. De scheidingsperformantie van membranen is vaak beperkt en een zuiver permeaat kan niet bereikt worden, voornamelijk bij pervaporatie van mengsels van organische vloeistoffen. Wanneer het verkrijgen van een zuiver product de doelstelling is, wordt het permeaat van een membraanconfiguratie eerst gecondenseerd en pas in een latere stap verder gezuiverd. De benodigde condensor tussen elke stap maakt echter de kost van lange series membraanconfiguraties economisch onacceptabel. Als alternatief stelt deze thesis het concept ‘meertraps

batch pervaporatie' (Multi-Stage-Batch-Pervaporation, MSBP) voor als eenheidsoperatie. In deze configuratie wordt het permeaat, product van elke batch-trap, gerecycleerd naar de voedingstank om het in een volgende trap verder te zuiveren. Deze thesis beschrijft hoe een MSBP eenheid de zuiverheidsspecificatie van producten kan halen, door het variëren van de voorwaarde voor trapbeëindiging en het aantal trappen, gebruik makend van één enkele membraanmodule en één condensor. De scheiding van de MM20 afvalstroom was gekozen als gevalstudie om aan te tonen dat de MSBP eenheidsoperatie hoogwaardige producten kan opleveren, zelfs bij middel- tot laagperformante membranen.

De MM20 afvalstroom wordt momenteel in de industrie omgezet tot azijnzuur in een continu proces. Het methylacetaat wordt uit de afvalstroom gewonnen door middel van extractieve distillatie alvorens het naar de reactor te sturen. Met het oog op het produceren van n-butylacetaat in plaats van azijnzuur, werd in het derde deel van deze thesis de mogelijkheid onderzocht om een pervaporatie-eenheid in bestaande systemen in te bouwen. De nieuw ingebouwde eenheid maakt gebruik van de kolommen van het extractieve systeem, maar het is niet langer nodig een solvent te gebruiken, aangezien de azeotroop wordt doorbroken door pervaporatie. Het membraan dat hiervoor werd gekozen, PolyAl TYP MA®, vertoonde een lage tot gemiddelde verdelingscoëfficiënt en een hoge flux bij de azeotroop van het methanol-methylacetaat mengsel. Vanuit energetisch standpunt zorgt de inbouw van de pervaporatie-eenheid voor uitdagende condities: voor lage tot gemiddelde verdelingscoëfficiënten is de energiebehoefte van het proces stijgend bij stijgende flux.

Een energetische vergelijking van de hybride pervaporatie/distillatie installatie met de industriële extractieve distillatie, toont aan dat de hybride opstelling een winst in energieverbruik oplevert van ~38% (~23% wanneer enkel de energie nodig voor verwarming wordt meegerekend). Bovendien kunnen grote aanpassingen aan de hydraulica vermeden worden door gebruik te maken van een gestructureerde pakking en van membranen met hogere verdelingscoëfficiënten.

In het laatste deel van deze thesis wordt op zoek gegaan naar de energetisch meest efficiënte manier om n-butylacetaat uit de MM20 afvalstroom te produceren. Hiervoor worden drie processen op basis van pervaporatie gesimuleerd en energetisch vergeleken met twee conventionele systemen. De vergelijking gebeurt steeds op basis van gelijke in- en uitgaande stromen en productconcentraties. De drie processen op basis van pervaporatie scoren in de meeste gevallen energetisch beter dan de conventionele processen, het energieverbruik ligt gemiddeld 27% lager. Een verdere vermindering van het energieverbruik kan mogelijks bereikt worden door het integreren van warmterecuperatie. Bovendien werd er aangetoond dat membranen met gelijke verdelingscoëfficiënten en een gemiddelde totale flux (voor alle mogelijke concentraties in de voedingsstroom) het procesontwerp en de winstgevendheid kunnen beïnvloeden, op een manier die afhangt van de totale flux bij lage concentraties van de component waarvoor het membraan selectief is. Hiervoor geldt dat hoe lager de totale flux, hoe kleiner het vereiste membraanoppervlak moet zijn, en hoe hoger de winstgevendheid van de installatie, zelfs wanneer het systeem gevoed wordt met stromen met een lage methylacetaat concentratie.

LIST OF ABBREVIATIONS

BPTI	Batch pervaporation time index
BuOAc	*n*-butyl acetate
BuOH	*n*-butanol
ClPP	Chlorinated polypropylene
Luyben_CSTR	The conventional distillation-based process studied in literature and employing a CSTR reactor
Luyben_RD	The conventional distillation-based process studied in literature and employing a reactive distillation unit
MeOAc	Methyl acetate
MeOH	Methanol
Module0	Pervaporation module that precede the reactor (SIM3)
Module1	Pervaporation module that follow the reactor (methanol selective membrane)
Module2	Pervaporation module that follow module1 (methyl acetate selective membrane)
MSBP	Multi-stage-batch-pervaporation
PVDF	Polyvinylidene fluoride
PVOH	Polyvinyl alcohol
R (subscript)	Retentate
SIM1, SIM2, SIM3	The three different block flow schemes discussed in this work
sqm	Square meter

STP	Standard temperature (0 °C) and pressure (1 atm) conditions
Type-1 orM1	1st type of total flux trend studied in this work
Type-2 or M2	2nd type of total flux trend studied in this work

LIST OF SYMBOLS

$\alpha_{i/j}$	Selectivity of the membrane between *i* and *j*-compound
$\beta_{i/j}$	Separation factor
θ	Cell-cut
λ	Heat of vaporization [J/mol]
v_i^G	Molar volume of the *i*-gas at STP conditions
A_{tot}	Area of the pervaporation membrane module [m^2]
$BPTI_{98}^{o}$	Standardized version of the batch pervaporation time index for separations that start from an initial feed concentration of 50mole% and end when the purity of the component enriched in the retentate reaches a value of 98 mole% [h*m^2*kmol]
$BPTI_{98}^{MM20}$	Batch pervaporation time index employed for separations in which each stage ends once a constant purity of the component enriched in the retentate is reached [h*m^2*kmol]
$BPTI_{rec,98}^{MM20}$	Batch pervaporation time index employed for separations in which each stage ends once a constant value of stage-recovery of the component enriched in the permeate is reached [h*m^2*kmol]
C_{BM}	Bare module equipment cost [$]
C_{GR}	Grass roots cost [$]
C_i	Generic voice of *i*-cost [$]

C_{MR}	Cost of membrane replacement [$]
C_{OL}	Cost of operating labour [$]
COM	Cost of manufacturing [$]
c_p^L	Heat capacity at constant pressure for liquids [J*mol^{-1}*K^{-1}]
C_{RM}	Cost of raw materials [$]
C_{TM}	Total module cost [$]
C_{UT}	Cost of utilities [$]
C_{WT}	Cost of waste treatment [$]
$(D/F)_i$	Distillate to feed ratio of the *i*-column
DCFROR	Discounted cash flow rate of return
d_h	Hydraulic diameter [m]
DSTWU	Aspen Plus distillation unit block that performs a Winn Underwood Gilliland shortcut design calculation for a single feed
E_{att}	Activation energy of permeation process [kJ/mol]
F	Instantaneous amount in the feed tank or feed flow rate [kmol] or [kmol/h]
F_0	Initial amount in the feed tank
f (subscript)	Feed
FCI	Fixed capital investment [$]
h, H	Enthalpies of liquid and vapour, respectively [J]
J	Membrane total flux [kg*m^{-2}*s^{-1}]
j_1	Instantaneous flux of the component enriched in the permeate

m	Solvent to feed flow ratio of column 1
MACRS	Modified accelerated cost recovery system
MM20	~16 mole% methyl acetate in methanol waste stream
MM80	60 mole% methyl acetate in methanol stream
N_i	Number of stages of the *i*-column
Nf_i	Feed stage of the *i*-column
Ns	Solvent stage inlet (column 1 of the extractive unit)
Np	Permeate stage inlet (column 1 of the retrofitted unit)
NPV	Net present value [$]
P	Permeate flow rate [kmol/h]
PBP	Payback period [years]
$\frac{P_i}{l}$	Permeance [GPU]
$\frac{P_i^{\infty}}{l}$	Permeance at infinite temperature [GPU]
P_{cond}	Pervaporation condenser total pressure [Pa]
P_i^{sat}	Saturation pressure of the *i*-component [Pa]
PSI	Pervaporation separation index [$kg*m^{-2}*s^{-1}$]
PM_i	Molecular weight of the *i*-component [kg/mol]
$Q_{c,Ci}$	*i*-column condenser duties [kW]
$Q_{H,C2M}$	Duty of the heat exchanger treating the distillate of column 2 recycled to the pervaporation module [kW]
$Q_{H,Ci}$	*i*-column reboiler duty [kW]

Qm	Pervaporation module duty (*i.e.*, the energy required from the process of pervaporation) [kW]
R	Retentate flow rate [kmol/h]
RADFRAC	Aspen Plus distillation unit block that performs a rigorous estimation of all thermodynamic and chemical-physical outcomes of the separation
ReR	Reagents molar ratio
RR	Reflux ratio
RR^m	Minimum value of RR_1 that allows respecting the limit condition of 94.4 mole% methyl acetate in the distillate of column 1 of the extractive distillation unit (to not be confused with the minimum reflux ratio)
S	Solvent flow rate [kg/s]
T	Temperature [°C]
x	Generic molar concentration
x_1	Instantaneous molar concentration in the feed tank
$x_{1,0}$	Initial concentration in the feed tank
$x_{B,i}$	Mole fraction concentration of the *i*-column bottom
$x_{D,i}$	Mole fraction concentration of the *i*-column head
y_1	Instantaneous molar concentration in the permeate tank
y_i	Molar concentration of the permeate in the basis of *i*-component selective for the membrane
cm^3(STP)]	Cubic centimetre volume of a gas at STP conditions
[cmHg]	Pressure in centimetre of mercury units
[GPU]	Gas permeance units.

Table of Contents

Chapter 1

INTRODUCTION AND SCOPE OF THE THESIS

1.1. From the polyvinyl alcohol production to the MM20 waste

Polyvinyl alcohol (PVOH) is a synthetic linear polymer with condensed structural formula: $[CH_2CH(OH)]_n$. It pertains to the class of commodity polymers; during 2006 the demand has reached a value of about 152 millions of kg (Kirschner, 2007). From 2012 to 2020, PVOH demand is forecast to grow at an average annual rate of 3.6% (IHS-Chemical, 2013) and it is estimated that the global production of PVOH can reach up to 650,000 tons/ year (Zhang and Yu, 2004, Aoi et al., 1997).

The PVOH production can be divided in two phases. The first step is the polymerization of vinyl acetate ($CH_3CO_2CHCH_2$). In Equation 1 the second step is shown, *i.e.*, the partial or complete alcoholysis (methanolysis) of polyvinyl acetate into PVOH.

$$[CH_2CHOAc]_n + MeOH \leftrightarrow MeOAc + [CH_2CHOH]_n$$

Equation 1

The amount of hydroxylation (*i.e.*, degree of removal of the acetate groups) and the molecular weight determine the chemical-physical and mechanical properties of the PVOH material (Baker et al., 2012).

The resistance of PVOH against organic solvents and the aqueous solubility makes this polymer specific for many applications. During 2007, it was reported that the main uses of PVOH are: 35% for polyvinyl

butyral production, 21% for textile and warp sizing, 20% adhesives, 10% for polymerization aids, 8% for paper coating and sizing and the remaining 6% for miscellaneous applications (Kirschner, 2007).

Equation 1 shows the role of methanol and methyl acetate during PVOH production. Methyl acetate and methanol are two components of the *saponification mother liquor* and form the so-called MM20 stream (Jiménez and Costa-López, 2002, Fuchigami, 1990). This stream is removed from the PVOH process with a concentration of ~30 wt% methyl acetate in methanol (*i.e.*, ~16 mole% methyl acetate at 40 °C). In the past it was sold as solvent but volatile organic compound legislation has drastically decreased this market (Jiménez and Costa-López, 2002) so that it is now considered a waste product (Fuchigami, 1990).

During polyvinyl acetate alcoholysis (Equation 1), methyl acetate (CH_3COOCH_3) is formed at a ratio of 1.68 tons of methyl acetate per ton of PVOH (Jiménez and Costa-López, 2002, Fuchigami, 1990). Looking at this number it is evident that for the PVOH industry it is crucial to (i) define a process for methyl acetate (MeOAc) conversion into a more valuable compound and (ii) recycling methanol to the methanolysis reaction step.

1.2. The MM20 waste stream conversion

The separation of a mixture of methyl acetate and methanol is an interesting and challenging issue, since these two components form an azeotrope. Currently, in a PVOH production plant the MM20 stream is first concentrated to a higher purity methyl acetate reagent stream that is then hydrolyzed through a strong acid catalyst into acetic acid and methanol. Diluted acetic acid is concentrated by azeotropic distillation

(Jiménez and Costa-López, 2002) and methanol is recycled for the methanolysis reaction.

Another possibility is the transesterification conversion of the MM20 stream to: (i) *n*-butyl acetate, by transesterification of methyl acetate with *n*-butanol (Bożek-Winkler and Gmehling, 2006, Yang et al., 2015); (ii) or ethyl acetate, by transesterification of methyl acetate with ethanol (Peng et al., 2014). In particular the economically favourable production of *n*-butyl acetate from methyl acetate/methanol waste mixtures, studied hereinafter in this thesis, has received some attention from the scientific community but it is yet not implemented in the industry (Jiménez et al., 2002, Fuchigami, 1990, Steinigeweg and Gmehling, 2004, Luyben, 2010). This economically favourable transesterification reaction (Figure 1) is a challenging reaction since the conversion is limited by the equilibrium (*i.e.*, when the equilibrium is reached, the rate of the forward reaction becomes equal to the rate of the backward reaction). As shown in Figure 2 when using Amberlyst 15® as catalyst, the chemical equilibrium constant K_a of this reaction is quite independent from the variation of temperature (Bożek-Winkler and Gmehling, 2006).

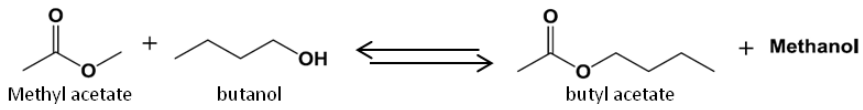

Figure 1. Representation of chemical equation of the transesterification reaction proposed.

A black boxes representation of this waste stream conversion is shown in Figure 3, where the first block represents the concentration step of the MM20 to higher concentrations of methyl acetate. This step is needed to obtain high conversions into *n*-butyl acetate. The azeotropic nature of this mixture, made of 32 mole% methanol in methyl acetate at ~1 atm

and ~54 °C (Tu et al., 1997), suggests the use of advanced distillation methods, *e.g.*, extractive distillation (Berg and Yeh, 1986) with water or ethylene glycol, to obtain pure methyl acetate (Jiménez and Costa-López, 2002). Pervaporation may be also considered for the same purpose and also in order to separate and recycle reagents to the reaction unit, as described in this thesis.

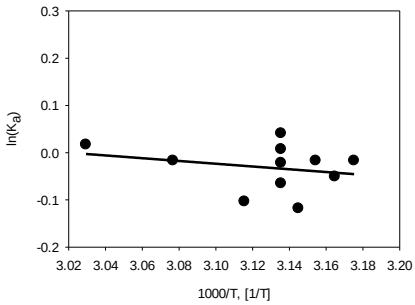

Figure 2. Chemical equilibrium constant Ka (♦) from data obtained by Ewa Bożėk-Winkler and Juergen Gmehling (—) when using Amberlyst 15 as catalyst of the transesterification reaction between methyl acetate and n-butanol (Bożek-Winkler and Gmehling, 2006).

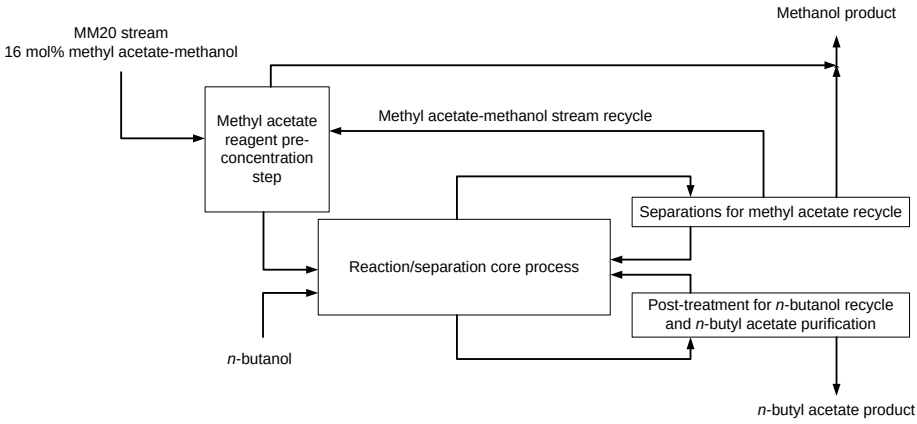

Figure 3. Block scheme of the process of conversion of the MM20 waste stream to n-butyl aceate.

1.3. Pervaporation, technology background and difference with vapour permeation

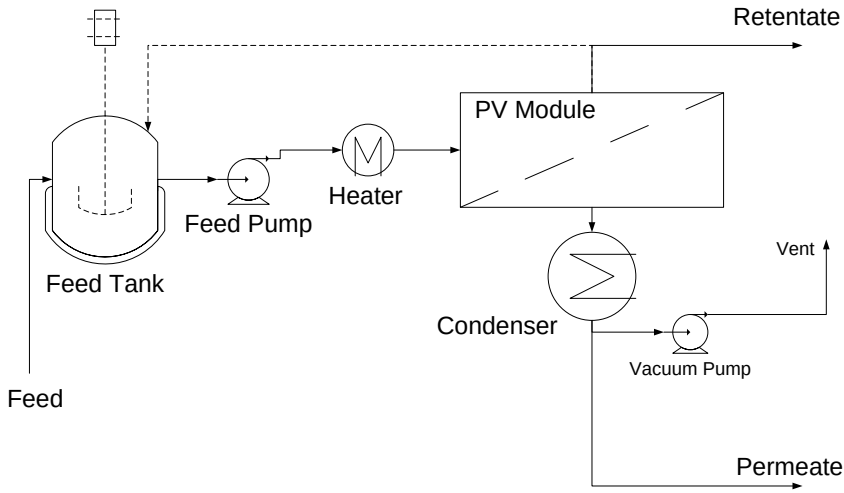

Figure 4. Scheme of a pervaporation unit working in continuous or in batch mode (dashed lines)

A pervaporative separation consists of two steps: selective dissolution and diffusion of the components of a liquid charge through a dense membrane and its consequent partial evaporation. The driving force for permeation is the difference in chemical potential of components at the two sides of the membrane (Wijmans and Baker, 1995). A common dense membrane consists of a dense layer oriented towards the feed/retentate side (in the pervaporation cell) on top of a porous supporting layer oriented towards the permeate side, in which vaporization occurs (McCabe et al., 2005). The selectivity of a pervaporative separation depends on the different transport rates of compounds, which depend on their diffusivity and solubility in a dense membrane layer. Thus, the separation is not affected by the presence of an azeotrope (Vandi et al., 2012, Uragami et al., 2011, Anjali Devi et al., 2005, El-Zaher and Osiris, 2005).

A pervaporation unit working in batch or continuous mode (represented in Figure 4) is commonly made of a feed pump, a membrane module and a vacuum system. Industrially, the vacuum system is made of a condenser and a vacuum pump. This pump is normally used to remove the incondensables that continuously accumulate in the condenser, lowering the separation performance of a pervaporation unit.

The energy required from the pervaporation separation is the enthalpy of vaporization of the permeate. The energy is taken from the feed side. Hence, the retentate that comes out from a membrane stack is cooler than the feed and needs to be re-heated in order to be sent to the next membrane stack (shown in Figure 5a). For ideal membranes with perfect separation performance, the energy requirement can be reduced to the minimum, which is the energy to vaporize the amount contained in the feed of the component selective for the membrane. In any case, even for membranes with a modest separation performance, in comparison with distillation the energy required from a pervaporative separation is much lower, so that pervaporation is classified as a low energy consumption technology (Lipnizki et al., 1999, McCabe et al., 2005).

Vapour permeation is similar to pervaporation (Figure 5b) and the only difference is that the feed is in a gaseous state. This means that no energy is required during components permeation. In the case of vapour permeation, then, energy is spent to vaporize the entire feed to be sent to the vapour permeation membrane module. Vapour permeation has to be preferred to pervaporation when the feed is coming from a unit in which vaporization has already occurred. For example, the head product of a distillation column, in the vapour state, can be directly sent to a vapour

permeation module obtaining an inexpensive separation, from an energetic point of view.

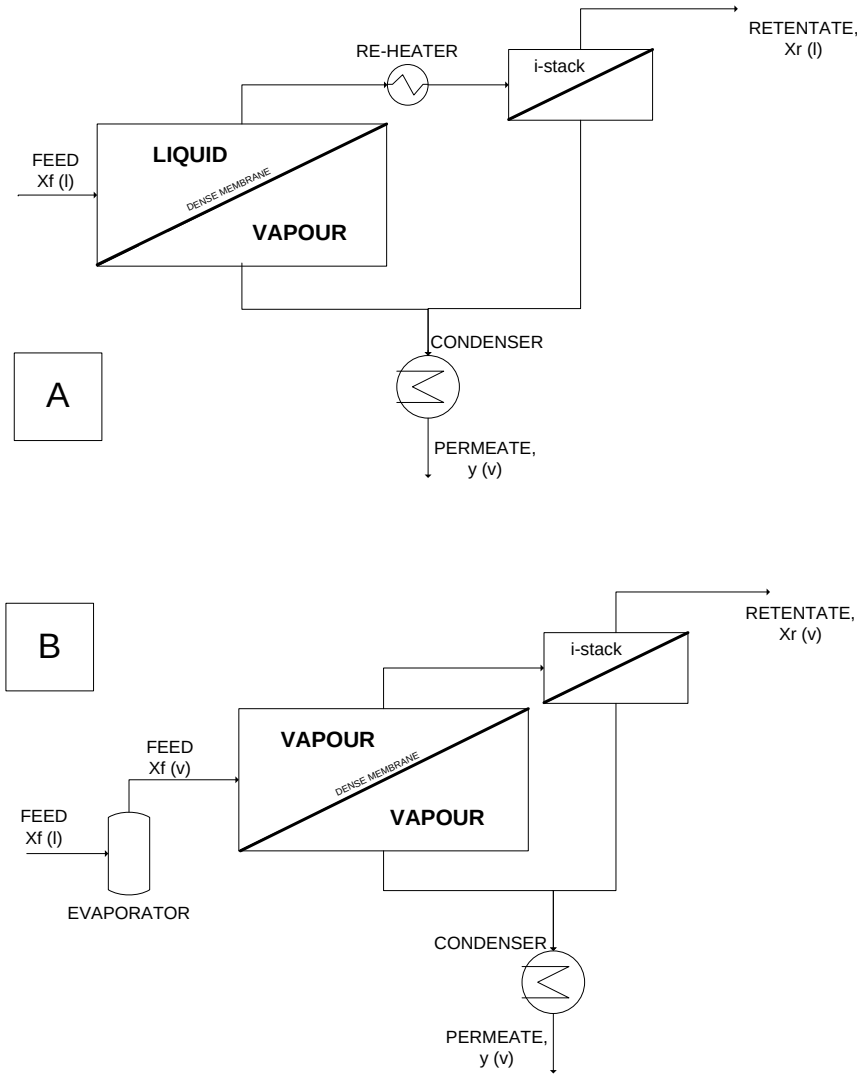

Figure 5. (a) pervaporation and (b) vapour permeation unit operations.

1.4. Membrane selection

As shown in Figure 3, in the context of conversion of the methyl acetate-methanol waste streams into *n*-butyl acetate, pervaporation could be used: (i) during separation of methanol from methyl acetate in the pre-concentration step; (ii) during the removal of methanol (by-product of the reaction) from the 4 components transesterification medium; and (iii) during the separation (from the same reaction medium) and recycle of methyl acetate to the reactor. A fourth case can be considered: the separation of *n*-butanol/butyl acetate mixtures in order to obtain pure *n*-butyl acetate and recycle *n*-butanol to the reactor. However, in the literature there is no trace of pervaporation of these two compounds and therefore this case is not considered in this thesis.

Taking into account that the MM20 binary mixture is made for the greatest part of methanol, selective pervaporation of methyl acetate should be preferred from an energetic point of view (*i.e.*, a methyl acetate selective membrane should be used). So far, the literature about the pervaporative separation of methyl acetate/methanol mixtures is limited. Some studies aimed at methanol selectivity (since methanol is a small and fast diffusing molecule) using in-house-prepared and commercial membranes: Gorri et al. (2006) studied the commercial Sulzer Chemtech™ membrane Pervap 2255-30® obtaining separation factors methanol/methyl acetate ranging between about 4 and 7 with total fluxes ranging between 0.97 and 7.9 $kg.m^{-2}.h^{-1}$ at 40 °C; Steinigeweg and Gmehling (2004) used the Sulzer Chemtech membranes Pervap 2255-40®, 2255-50® and 2255-60® at 45 °C, where the first and the second membrane types resulted in the best flux (an average of about 5.2 $kg.m^{-2}.h^{-1}$) and the best separation factor for methanol (an average of about

4.4), respectively; Sain et al. (1998) applied the commercial Cuprophan® membranes (supplied by AKZO™, Germany) obtaining a methanol separation factor of 4.7 and a flux of about 2.2 $kg.m^{-2}.h^{-1}$ (on average) at 45 °C and fluxes ranging between 0.1 and about 3.7 $kg.m^{-2}.h^{-1}$. Finally, Abdallah et al. (2013) reported about their in-house prepared nylon-6 membranes with outstanding properties (fluxes up to 80 $kg.m^{-2}.h^{-1}$ and separation factors up to 344 at 40 °C) . To date, the membranes proposed by this last group of authors may be the best solution when pervaporation is considered as separation technology for this mixture. Nevertheless, the study of the separation of methyl acetate/methanol mixtures by pervaporation is not complete. In fact, no methyl acetate selective membrane has yet been proposed. Only Penkova et al. (2013) studied the separation of a reactive quaternary mixture composed of acetic acid, methanol, water and methyl acetate, using in-house prepared poly-(2,6-dimethyl-1,4-phenylene oxide) membranes, obtaining separation factors methyl acetate/all the rest of values typically below 3. A review of permeate/feed concentration data, pervaporation McCabe-Thiele diagram, and total flux data of membranes used in the literature for pervaporation of methanol/methyl acetate mixtures is shown in Figure 6a-c. The figure reports also pervaporation data of polyvinylidene fluoride and PolyAl TypM1 membranes, which are further discussed in the next chapters of this thesis.

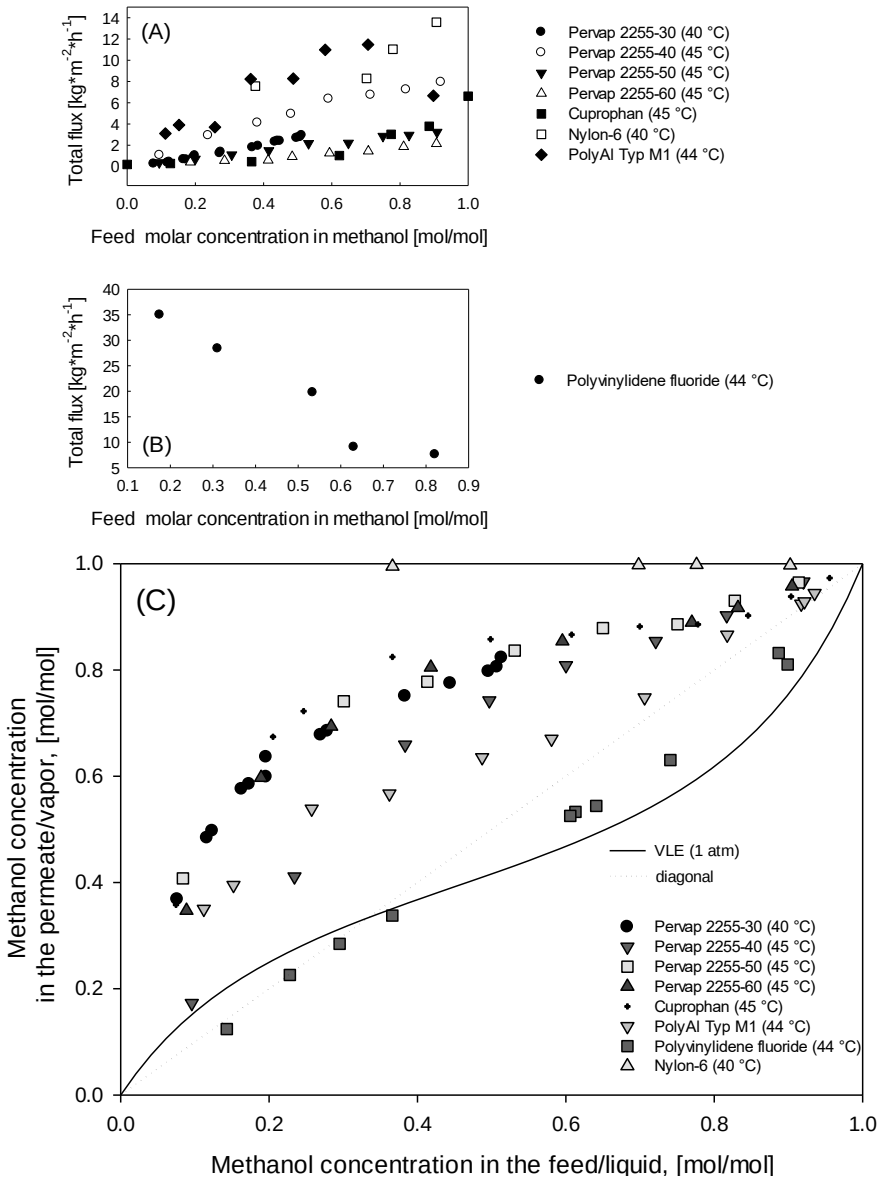

Figure 6. (a) and (b), total flux data (weight-basis) variation with feed methanol concentration of various commercial and in-house synthesized membranes employed during methanol/methyl acetate pervaporation; working temperature in the range 40-45 °C (Gorri et al., 2006, Sain et al., 1998, Steinigeweg and Gmehling, 2004, Abdallah et al., 2013). (c) permeate/feed concentration literature data of all these membranes. The same graph also reports the vapour-liquid equilibrium curve obtained using the UNIQUAC property method.

As shown in Figure 6, almost all the membranes tested in literature for this binary separation gave modest results in terms of delivered separation. In addition, it can also be considered that, more challenging than the separation of the binary methyl acetate/methanol mixture is the separation of methanol (or methyl acetate) from the remaining three components of the medium of the transesterification reaction between methyl acetate and *n*-butanol. The reason can be found in the intrinsic strong interaction between the four components of the transesterification reaction medium (Luis and Van der Bruggen, 2015).

Thus, in order to achieve these binary or quaternary alcohol/ester separations with enhanced performances (which also means, avoiding to treat the permeate in following pervaporation stacks), tailored membranes need to be developed. Consequently, when the intent is the in-house synthesis of a polymeric membrane to be used in pervaporation of a specific mixture, the selection of the best polymer has to be pursued according to the separation mechanism of pervaporation (*i.e.*, polymer-solvents affinity and components diffusivities inside the membrane have to be taken into account). In particular, when the membrane is made of a polymer in the rubbery-state (*i.e.*, the working temperature of the material is higher than the glass-transition temperature, T_g), the affinity of the material to the component to be selectively permeated should be used as selection parameter (Bell et al., 1988). In fact, in the case of rubbery-state polymers the main contribution to the pervaporative separation is given by component solubilization at the membrane feed-side. To date the best methodology to assess the solubility of a solvent in a polymeric membrane material is the procedure proposed by Hansen (1967). In the Hansen Solubility Parameters (HSPs) theory, the dispersion interactions energy (derived from atomic forces), the polar

cohesive energy and hydrogen bonding energy (δ_d, δ_p and δ_h, respectively) are considered as the main interaction energies between polymer and dissolved organics (Hansen, 2012). The HSPs method can be easily visualized in the energy density space (*i.e.*, the space having as axis δ_d, δ_p and δ_h), where the distance between the solvent and centre of the polymer solubility sphere reflects the affinity between polymer and solvent compounds (Hansen, 1967, Buckley-Smith, 2006).

The HSPs theory criterion was already applied (on a larger scale and with a high level of detail) by Buckley-Smith (Buckley-Smith, 2006) during selection of membrane materials for pervaporation of a model solution containing linalool and linalyl acetate (major components of lavender essential oil), in ethanol. This work shows that, when components with similar molecular size are pervaporated, the HSPs theory results to be a good membrane screening method. However, Buckley-Smith remarked that diffusivity (not considered in HSPs), having a fundamental impact on components pervaporation, should be also taken into account during this screening step.

1.5. Selection of the module arrangement: a limitation of pervaporation

Pervaporation membranes with very high performance can be found mainly in the pervaporative dehydration of organic solvents, because water is small and diffuses faster than organic compounds (2010, Jafar and Budd, 1997, Morigami et al., 2001, Bolto et al., 2011, Chapman et al., 2008). However, as reported by Smitha *et al.* (2004), successful separations have also been reported more recently in the pervaporation of organic-organic mixtures involving: aromatic-alicyclic compounds, *e.g.*,

benzene/cyclohexane; aromatic-aliphatic compounds, *e.g.*, benzene/*n*-hexane; isomers; and the separation of organic polar-apolar compounds, *e.g.*, methanol-toluene/benzene or ethanol/ethyl *tert*-butyl ether mixtures. The separation of methanol/organic compounds is an interesting sub-case. As an organic compound, methanol is more similar to water than any other organic compound, which may lead to the same high level of separation when the right membrane is applied. For example, the organic-organic separation of methanol from larger apolar molecules, *e.g.*, methyl *tert*-butyl ether or toluene was already proven in the literature to have high separation factors (Smitha et al., 2004, Mandal and Pangarkar, 2002).

However, in general, for medium low separation factor membranes, as is the case during organic-organic pervaporation of similar molecules, to obtain high purity products, a pervaporation unit should be arranged in a series/parallel configuration of membrane modules. In particular, when the objective is the depletion of a product from a retentate stream, a multi-*step* pervaporation configuration, *i.e.*, a series of membranes modules using the retentate of the previous module as the feed, is used (Baker et al., 1993). A historical case, reported by Rautenbach and Albrecht (1989), is the GFT™ pervaporation unit used for continuous dehydration of ethanol, where the retentate is depleted from water with a series of PVOH-PAN membrane steps, including re-heating after each step. In contrast, when the objective is to obtain a pure permeate, a multi-*stage* configuration can be designed, where the permeate product exiting a membrane module is first condensed and then further purified in a subsequent module (Baker et al., 1993). However, the need for a condenser after each stage makes a long series of pervaporation stages impractical and uneconomic.

From a theoretical point of view, pervaporation provides a promising partial replacement of distillation, as the separation based on the vapour liquid equilibrium can be enhanced by adding the contribution of the membrane-component affinity (Baker, 2012). However, pervaporation does not allow the design of a cascade of contacting stages, typical for a distillation column, or the design of a too long series of pervaporation stages. Thus, when high purity products are required, it is necessary to develop and use highly selective membranes with high separation factors. This means that pervaporation suffers from configuration limitations and the separation is strongly dependent on the separation performance of the membrane.

Operation of pervaporation in batch mode has one extra degree of freedom over continuous-mode operation, due the fact that time is a parameter in the separation. In particular, the purity of the retentate can be improved by varying the batch operation time. Nevertheless, component recoveries and the achievement of a high purity permeate are still strictly linked to the separation performance of the membrane.

In 1993, Baker *et al.* published a patent describing a batch pervaporation system, composed of different service tanks connected in a network and referring to the same membrane module. In this patent, it is also shown how by recycling the permeate to the membrane in consequent batch stages, it is possible to increase the purity of the permeate. However, although this configuration allows great flexibility, the idea has not been taken further up so far.

The separation of methyl acetate/methanol mixtures is an interesting case study to test a batch approach similar to the one suggested by Baker et al. (1993).

1.6. Hybrid PV-distillation units: debottlenecking and retrofitting

Stand-alone pervaporative separation of organic mixtures has been already discussed and studied for many years; however, up to date the applicability of this process (even if very promising) is not yet fully satisfactory, at least for industrial purposes. To the best of our knowledge, the only industrial application of organic-organic pervaporation is the separation of methanol/methyl tert-butyl ether mixtures (Kujawski, 2000). In many cases, and with more success, pervaporation modules were coupled with distillation units (or in general with other traditional separation technologies) in order to obtain the desired separation efficiency (Smitha et al., 2004). Lipnizki *et al.* (1999) reviewed such pervaporation-based hybrid processes (with a focus on industrial applications).

Apart from the design of *ex novo* distillation-pervaporation hybrid units, pervaporation can be used for debottlenecking of distillation units (Chemtech, 2004, Hoch et al., 2003, Eliceche et al., 2002, Pribic et al., 2006, Ho and Sirkar, 1992). By definition, the term *debottlenecking* indicates the action of "increasing the production capacity of existing facilities through the modification of existing equipment to remove throughput restrictions" (encyclo.co.uk, 2014). Pervaporation is one of the most promising technologies for debottlenecking purposes since it is not affected by the presence of an azeotrope (Vandi et al., 2012, Uragami et al., 2011, Anjali Devi et al., 2005, El-Zaher and Osiris, 2005) and because pervaporation is a low energy consumption technology (Lipnizki et al., 1999, McCabe et al., 2005). For pervaporation the only major

challenge can be the condensation of organics of high volatility, since very low refrigerant temperatures may be required.

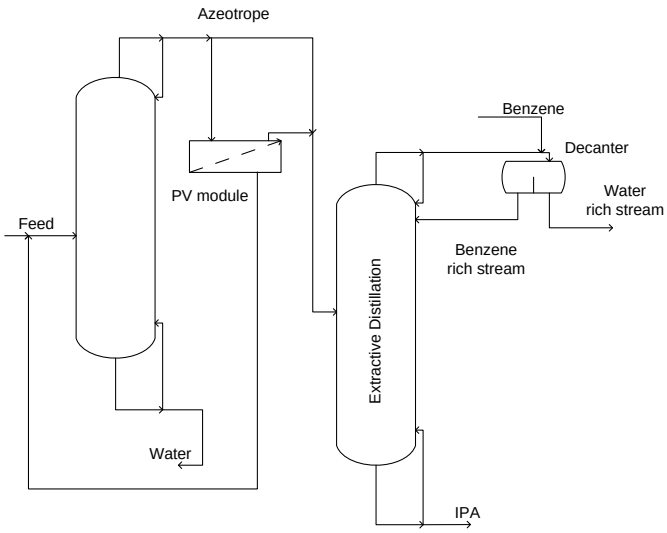

Figure 7. Texaco's IPA- dehydration system after retrofitting (Ho and Sirkar, 1992, Van Hoof et al., 2004).

An interesting case is the use of pervaporation in the context of the Hüls process (Eliceche et al., 2002, Chen et al., 1988, Chen et al., 1989, González González and Ortiz Uribe, 2001, Gonzalez and Ortiz, 2002) for the debottlenecking of the methanol/methyl tert-butyl ether (MTBE) distillation column, in which the azeotrope is classically obtained from the top head of the column. Eliceche et al. (2002) simulated this option and obtained a reduction of the operating costs by 9.7%. Another case is the debottlenecking of a Texaco isopropyl alcohol (IPA) dewatering unit by a membrane module (Ho and Sirkar, 1992, Van Hoof et al., 2004). In this case (see Figure 7) an azeotropic-extractive distillation system was debottlenecked employing a membrane module. The recovery of IPA of the azeotropic-pervaporation hybrid system (prior to feeding to the extractive column) rose from 85% up to 95%. This is beneficial for the

extractive column that now requires less solvent (benzene), resulting in an effective reduction of fluid treated by the column (lowering overall capital costs of the process).

Partially different from debottlenecking is retrofitting. Here the process unit is made more efficient and productive by radically transforming the unit and, at the same time, maintaining the greatest part of all structural and mechanical parts with a reasonable number of feasible modifications.

An interesting industrial case in which it is possible to consider retrofitting of advanced distillation systems with pervaporation is the MM20 stream separation. In fact, in order to increase the conversion of the MM20 stream into acetic acid, ethyl acetate or *n*-butyl acetate, the MM20 should be concentrated into pure methyl acetate. The azeotropic nature of the methanol/methyl acetate mixture suggests the use of advanced distillation methods. In particular, extractive distillation with water is the best option when the concentration step aims at obtaining acetic acid, since water (reagent for this conversion) is not an impurity for the methyl acetate head product of the extractive column. In the literature, ratios water/feed flow ranging between 0.3 and 4 were reported for this extractive distillation system (Finch, 1973, Langston et al., 2005).

1.7. The continuous production of *n*-butyl acetate by conventional processes: current situation

Among other interesting papers (Fuchigami, 1990, Steinigeweg and Gmehling, 2004, Wang et al., 2011, Wang et al., 2008), the studies of Luyben et al. (2004), Luyben (2010), Jiménez et al. (2002) and Jiménez

and Costa-López (2002) can be considered as a solid foundation for the industrial continuous production of *n*-butyl acetate from methyl acetate/methanol wastes, since they are based on well known distillation-based conventional methods. Figure 8 shows the three block flow schemes discussed by these authors. These three systems permit to obtain highly pure *n*-butyl acetate and methanol products (≥99 mole% purity). In particular, in Figure 8a the flow scheme proposed by Luyben et al. (2004) is reported, composed of a CSTR reactor connected with a series of columns working at different pressures. The same authors studied the flow scheme of Figure 8b; in this case two distillation service column work together with a reactive distillation column (*i.e.*, the Reactive C-2 distillation column). Both Luyben *et al.*'s systems are fed with the MM80 stream (60 mole% methyl acetate in methanol). Differently, the flow scheme simulated by Jiménez and Costa-López (2002) shown in Figure 8c is fed with the MM20 stream and uses an extractive-reactive distillation column linked with three service distillation columns. This last flow scheme was not considered further in this thesis since the work of Jiménez and Costa-López (2002) was found missing of a series of data, required during any comparison with process-flow schemes proposed in this manuscript.

Apart from these three distillation-based flow schemes (Figure 8), it is not possible to find any study in the literature dealing with reaction-pervaporation continuous systems for the conversion of methyl acetate into *n*-butyl acetate. This is due to the fact that a suitable methanol or methyl acetate selective membrane, having high separation factors, has not been commercialized yet.

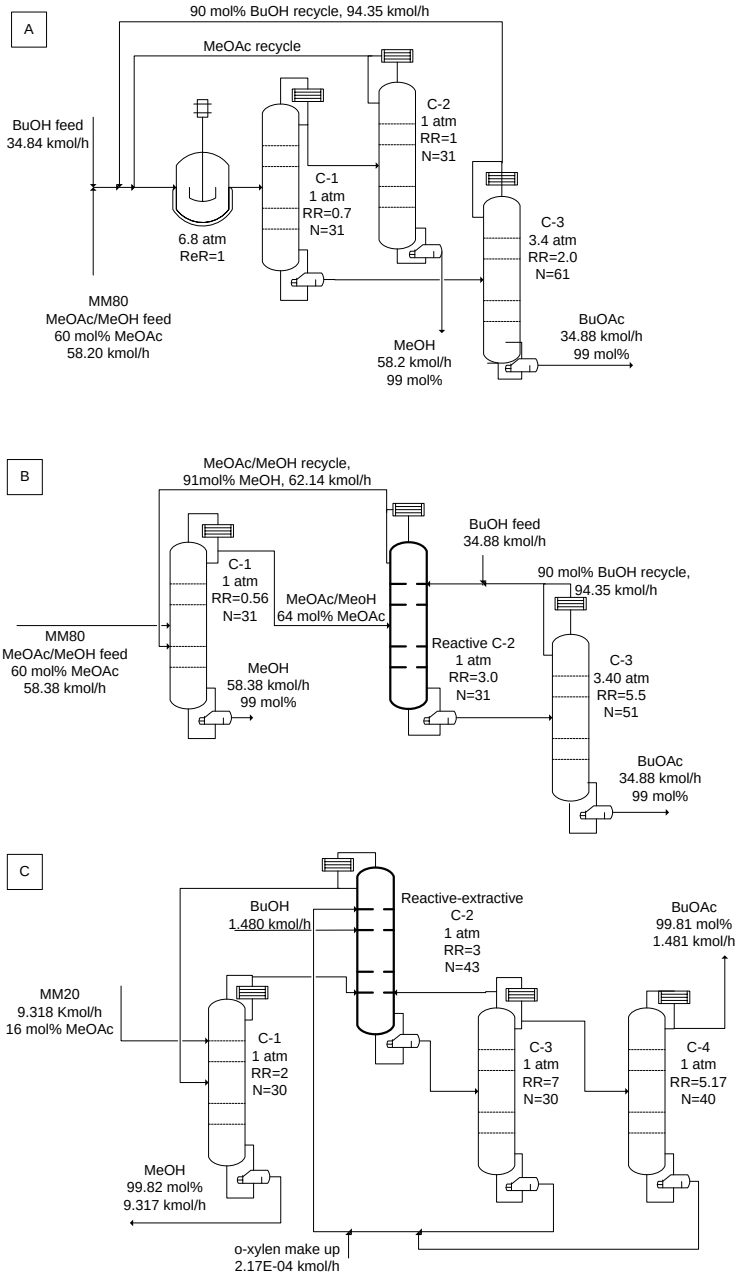

Figure 8. (a) block flow diagram of the reaction-distillation column train and (b) of the reactive distillation system described elsewhere by Luyben et al. (2004). (c) block flow scheme of the reactive-extractive distillation system proposed by Jiménez et al. (2002) and Jiménez and Costa-López (2002).

In addition, even if a hypothetical high quality membrane exists, in order to run simulations of reaction-pervaporation based systems, an operator faces difficulties in finding the right model, method or simulator to simulate pervaporation. For example, among all industrial computer programs for simulation of chemical processes, there is not any that offers a pervaporation unit block (or in general a membrane unit block).

Some generalities about pervaporation model-typologies and hybrid-pervaporation simulations were described elsewhere (Kreis and Górak, 2006, Schiffmann and Repke, 2015). Amelio et al. (2015) proposed and implemented an Aspen Plus module written in Aspen Custom Modeler, based on the pervaporation permeances equations (Baker et al., 2010). In this case the pervaporation module is divided in perfectly mixed 'cells' having constant physical-chemical properties. Isothermal conditions, a constant permeation activation energy and permeance at infinite temperature, were also assumed for the membranes studied.

1.8. Aim of the thesis

Hereinafter in this thesis, the reader will notice that in each chapter a particular aspect of the pervaporation technology is assessed and discussed in order to give answer to relevant questions, such as: "how difficult is it to select an appropriate polymeric material to be used to synthesize pervaporation membranes tailored for particular separations?" (Chapter 3); "how about flexibility of pervaporation in the absence of high quality membranes?" or "how about configuration and membrane limitations to separation?" (Chapter 4); "instead of thinking about pervaporation stand-alone separations, what about retrofitting of industrially operative distillation-based units, with the intention of improving their sustainability?" (Chapter 5); "how easy is it to apply pervaporation in an industrial process of conversion that consists of solely organic compounds?" and "is the celebrated energetic superiority of pervaporation enough for a conversion process also from an economic point of view?" (Chapter 6). These questions arise from issues that have been already discussed in literature in particular works, but never over a single case-study assessment that may give a more general understanding of the problematic and provide new, unexplored, solutions. Based on these questions, it can be stated that the aim of this thesis is double. On one side, the aim is the analysis of the MM20 to *n*-butyl acetate stream conversion using pervaporation based technologies, both from an energetic and economic point of view. On the other side, if it is assumed that the MM20 conversion is just a complex case-study, the aim of the thesis is the study of the ability of pervaporation to be flexibly/straight forwardly applied in all various aspects of an unexplored conversion process.

In addition, in this thesis pervaporation and distillation are analysed in parallel in a continuous and direct comparison, in order to understand how far is pervaporation from the flexibility demonstrated by the distillation technology.

1.9. Thesis outline

In **Chapter 2** of this thesis a detailed overview of materials and methods is provided, including: (i) polymeric membrane materials and selection methods; (ii) a general and detailed (chapter by chapter) description on pervaporation experiments methods; (iii) the description of computer assisted simulation methods used for the studies done on batch and continuous binary or quaternary alcohol/ester pervaporations.

In **Chapter 3** the Hansen Solubility Parameters theory is used as a method for the selection of pervaporation membranes. This is done mainly in order to synthesize a methyl acetate selective membrane to be used during concentration of the MM20 stream to be sent to the reactor or during recycle of methyl acetate to the reactor (see Figure 3). For this reason, the three polymeric materials, on which the discussion made in this chapter is based, were chosen among many materials because they have a good affinity for methyl acetate on the basis of the HSPs theory or on the basis of preliminary screening (for what concerns the polyvinylidene fluoride membrane). Then, the polymeric membranes were initially tested in order to assess the HSPs theory potential in selecting the appropriate material. The experimental tests of these membranes were pursued by pervaporation of the reaction medium mixture of the transesterification conversion of methyl acetate to *n*-butyl acetate (Steinigeweg and Gmehling, 2004, Bożek-Winkler and Gmehling,

2006, Jiménez and Costa-López, 2002), which was chosen since it contains two esters (methyl acetate is the component of interest) and two alcohols that differ by three carbon atoms (*i.e.*, methanol, *n*-butanol and methyl acetate, *n*-butyl acetate); this means that the separation of methyl acetate from this mixture is rather challenging for the membrane since the presence of the other compounds may lead to unwanted plasticization-swelling and/or coupling phenomena (Goethaert et al., 1993). The membrane showing the highest methyl acetate/methanol selectivity (values higher than one), was finally used in the pervaporation of methyl acetate/methanol binary mixtures throughout a wide feed concentration range. In the final part of Chapter 3 the applicability and future perspectives of this selected membrane are given.

The second goal of this thesis was to define a unit operation mode capable of being independent from unit configuration and membrane performances to be employed during pre-concentration of the MM20 stream. This is done in **Chapter 4** based on a reconsideration of Baker *et al.*'s batch pervaporation multi-tank apparatus (Baker et al., 1993) and using state-of-the-art of today's membranes. Hence, in the first part of this chapter, the *multi-stage-batch-pervaporation* (MSBP) unit is presented and simulated for the methyl acetate/methanol separation case-study, using all membranes reported in Figure 6. In particular two new MSBP operation modes are proposed showing MSBP unit application potential and limits. In addition, a new way to index batch pervaporation membrane separation effectiveness is also presented and discussed.

In **Chapter 5**, instead, the same pre-concentration is pursued retrofitting industrial extractive-distillation units addressed to the obtainment of methyl acetate reagents for acetic acid production. Therefore, in this

chapter an extractive distillation unit working in the acetic acid from MM20 production line is first designed using a new design procedure, different from what can be found in the literature (Wankat, 2006, de Figueirêdo et al., 2011, Wang et al., 2012, Langston et al., 2005, Brüggemann and Marquardt, 2004) and meant to optimize the design from an energetic point of view. The corresponding retrofitted unit is then investigated after inserting a pervaporation module to separate the components of the azeotrope, making the use of the solvent unnecessary. To the best of our knowledge, there are no similar cases of retrofitting in the literature. For this purpose, the PolyAl TypM1 membranes, already successfully applied in similar separations (Genduso et al., 2014, Luis et al., 2013), was tested for the separation of methanol/methyl acetate mixtures and then, after comparison with other membranes reported in the literature, was used for retrofitting simulations. This membrane showed a pervaporation performance that allows simulating an energy demanding retrofitting case. The energy optimized extractive distillation system is then compared with this retrofitting case which, based on the choice made on the membrane module, has still a great potential in terms of energy savings; *i.e.*, the success of this comparison proves the idea of retrofitting extractive distillation units with pervaporation modules.

In the final part of this chapter, a discussion on energy savings after retrofitting and feasibility of the operation (employing column hydraulic concepts) is made.

At this point of the thesis, the reader has already found solutions for the MM20 pre-concentration step issue; however, in order to obtain pure *n*-butyl acetate a low energy consumption process flow scheme needs to be simulated. This is discussed in **Chapter 6**, where two hypothetical high

performance membranes, the former methanol selective and the latter methyl acetate selective, are considered on the basis of background experience with such membranes (Abdallah et al., 2013, Penkova et al., 2013). Then, a realistic pervaporation module based on the pervaporation permeances equations (Baker et al., 2010), working in non-isothermal separation conditions and on membrane permeance properties that vary with the concentration of the component selective for the membrane, is elaborated. Computer assisted simulations permitted to obtain all design information necessary in order to carry out an energetic comparison with two distillation-based systems described in the literature (Luyben et al., 2004, Luyben, 2010) and fed with the MM80 stream.

The energy integration of a chosen pervaporation-based scheme is discussed together with a profitability analysis (also considering the effect of the total flux trend) leading to the final conclusions, where an answer to the question: "can a process that starts from the MM20 waste and produces *n*-butyl acetate be profitable?", is given.

In **Chapter 7**, future research advices and final conclusion are given.

Chapter 2

MATERIALS AND METHODS

2.1. Materials

2.1.1. Membrane synthesis

A. *Chapter 3 and Chapter 5: membranes and feed solution preparation methods*

The three membranes used in Chapter 3 were prepared by overnight stirring as follows: 10 wt% solution of chlorinated polypropylene (ClPP) in toluene, 10 wt% solution of PVOH in dimethyl sulfoxide (DMSO) and 10 wt% solution of polyvinylidene fluoride (PVDF) in N,N-dimethylformamide (DMF). Subsequently, air bubbles were removed from the polymeric solution by applying vacuum for a maximum of 30 minutes. Each solution was then poured in a glass Petri-dish and placed in a dynamic vacuum oven at 55 °C for at least 8 hours.

The PVDF membranes, to be used for the separation of the methyl acetate/methanol binary mixtures, were prepared by casting the polymer with a 250 μm thick knife on a glass plate and drying under vacuum atmosphere at 55 °C for at least 8 hours.

All prepared dense membranes were peeled off from the glass support by immersion in water.

Chlorinated polypropylene (Mw~100,000) was purchased from Sigma Aldrich™. Polyvinylidene fluoride Solef 6020® was provided by Solvay™.

Polyvinyl alcohol (PVOH, MW 72000) was purchased from AppliChem™. N,N-Dimethylformamide, toluene and dimethyl sulfoxide 99.9% (ACS grade) were purchased from VWR International™.

Nyssen Graphics™ 99.5% pure methanol, Alfa Aesar™ 99% pure methyl acetate, *n*-butanol AnalaR-Normapur® (VWR International) 99.9% pure and *n*-butyl acetate Chem-Lab™ (99+% pure), all without further purification, were blended to prepare all feed solutions for the pervaporation tests discussed in Chapter 3 and 5.

B. *Appendix I: membrane synthesis*

Poly [4,4' - methylenebis (phenylisocyanate) - alt - 1,4 - butanediol / di(propyleneglycol/polycaprolactone] (PU) and poly(hexano-6-lactam), this last having the commercial name of "nylon-6", were synthesized by overnight stirring, as follows: 10 wt% solution of PU in DMF and 20% nylon-6 in formic acid (FA). The nylon-6 solution was then poured in a glass Petri-dish and placed in a dynamic vacuum oven at 55 °C for at least 8 hours. The PU membrane was prepared by phase inversion procedure after casting a polymeric film of 250 μm. The non-solvent used is water, in which the membrane remained immersed for 4 hours. Once removed from this bath, the membrane was dried in air.

Poly [4,4' - methylenebis (phenylisocyanate) - alt - 1,4 - butanediol /di(propyleneglycol/polycaprolactone] and the 99% pure formic acid were bought from Sigma Aldrich. Poly(hexano-6-lactam) was kindly provided by RTP co. (Winona, Minnesota, USA).

2.2. Methods: membrane selection and pervaporation experiments

2.2.1. Membrane material assessment via HSPs theory

Table 1 reports the four solvents involved in the transesterification reaction of methyl acetate with *n*-butanol and the three membrane materials used in the pervaporation experimental tests of Chapter 3, together with the HSPs values and the glass-transition temperatures. The affinity of one of these solvents toward one of the chosen polymeric materials was first assessed based on the *solubility parameter distance* (R_a, Equation 2) developed by Skaarup (Hansen, 2012), which takes into account the distance between the polymer and the solvent in the HSPs 3D-energy density space (Hansen, 2012, Buckley-Smith, 2006).

$$(R_a)^2 = 4\,(\delta_{d,pol} - \delta_{d,solv})^2 + (\delta_{p,pol} - \delta_{p,solv})^2 + (\delta_{h,pol} - \delta_{h,solv})^2$$

Equation 2

Table 1. The Hansen Solubility Parameters (HSPs) (Hansen, 2012, Hiroshi, 2010, Hansen, 1971, Liu et al., 2011) and the glass-transition-temperatures (El-Zaher and Osiris, 2005, Solvay, 2014, Sigma-Aldrich, 2014) of all the organics and polymers reported in this work.

Material/Compound	δ_d *	δ_p *	δ_h *	R_o	T_g
Methanol	15.1	12.3	22.3	-	-
***n*-butanol**	16.0	5.7	15.8	-	-
methyl acetate	15.5	7.2	7.6	-	-
***n*-butyl acetate**	15.8	3.7	6.3	-	-
Chlorinated polypropylene (ClPP)	20.3	6.3	5.4	10.6	54 °C
Polyvinyl alcohol (PVOH)	14.7	14.1	14.9	10.5	88 °C
Polyvinylidene fluoride (PVDF)	17.4	13.7	11.3	5.0	-40 °C

* Unit: $(MPa)^{1/2}$

Consecutively this assessment was extended considering the *relative energy difference* (RED), showed in Equation 3 (where R_o is the *radius of interaction*, *i.e.*, the radius of the solubility sphere) that permits to distinguish solvents and non-solvents for the polymer. This means that when RED is lower than 1, the solvent (represented by an R_a value) lies inside the sphere of radius R_o, *i.e.*, the organic is a solvent for the polymer.

$$RED = \frac{R_a}{R_o}$$

Equation 3

2.2.2. Pervaporation experiments: general method

For each pervaporation experiment discussed in Chapter 3, Chapter 5 and Appendix I, the temperature was measured at the outlet of the pervaporation cell. Upstream, a centrifugal pump circulated the feed/retentate stream under turbulent conditions to maintain the system well mixed and in order to maximize the feed side diffusion rate. In this way the limiting step of the mass transfer process is the diffusion through the membrane dense layer and concentration polarization is not expected to affect the pervaporation process significantly (Baker et al., 2010, Van der Bruggen et al., 2004, Luis et al., 2013).

At the feed side, the pressure is atmospheric (no over pressure was applied). At the permeate side, vacuum is achieved by means of a vacuum pump.

Every *x* minutes, depending on the membrane flux, permeate was collected using a liquid nitrogen based condenser in a glass u-tube (*i.e.*, permeate collections were stopped just before the u-tube could be

overfilled). Once the overall flux resulted to be stationary three permeate samples of fixed feed concentration and pervaporation temperature were stored and then analyzed.

Each membrane, having an active area of 19.63 cm^2, was immersed in the feed solution at least 12 h before starting the experiment in order to obtain an equilibrium condition between the components in solution and the same absorbed into the membrane. U-glasses used to collect the produced permeate were weighed before and after each experiment by means of a Mettler Toledo AB204-S balance with an accuracy of 0.1 mg, obtaining the mass M [kg] of each pervaporation sample. The molar permeate concentration (y_i) and pervaporation feed molar concentration (x_i) were determined by gas chromatography (Perkin Elmer GC-autosystem with Headspace Sampler Turbomatrix 16 and FID detector).

The membrane flux was calculated as:

$$J = \frac{M}{\Delta t \cdot A}$$

Equation 4

where A is the membrane active area.

From membrane fluxes and permeate components concentrations, partial fluxes were calculated:

$$J_i = J \cdot y_i \cdot \frac{MW_i}{MW_T}$$

Equation 5

where MW_i is the molar mass of *i*- and MW_T is the total molar mass of the mixture.

The separation factor was calculated as:

$$\beta_{i/j} = \frac{y_i / y_j}{x_i / x_j}$$

Equation 6

This parameter gives quantitative information about the separation achieved. According to Baker et al. (2010), only by eliminating the effect of driving force it is possible to see the effect of the membrane on the pervaporative separation. The driving force for pervaporation of a component in a mixture is the difference of its chemical potential between the feed and the permeate side, which can be expressed as the difference in partial pressure of the component *i* between the two sides (Wijmans and Baker, 1995). Thus, the permeance can be defined as:

$$\frac{P_i}{l} = \frac{j_i}{(x_i \cdot \gamma_i \cdot P_i^o - y_i \cdot P_p)}$$

Equation 7

where, l is the thickness of the active layer, γ_i is the activity coefficient of component i, P_i^o is its vapour pressure at the permeation temperature and P_p is the pressure at the permeate side; j_i is the molar flux of component i, calculated following Baker et al. (2010) in [cm/s] at the standard condition of temperature and pressure STP (v_i^g = *22.58 dm³/mol*) as:

$$j_i = \frac{J_i \cdot v_i^g}{MW_i}$$

Equation 8

For the purpose of this work, permeance values are presented in GPU ($1\text{GPU} = 10^{-6}\text{cm}^3(\text{STP})/(\text{cm}^2 \cdot \text{s} \cdot \text{cmHg}) = 7.5005 \cdot 10^{-12}\text{m} \cdot \text{Pa}^{-1} \cdot \text{s}^{-1}$).

All activity coefficients were estimated by Aspen Plus® v7.2 UNIQUAC property method; vapour pressures and component densities at feed temperature were estimated with correlations reported in Perry's Chemical Engineers' Handbook, 8th edition (Perry and Green, 2008).

The membrane selectivity was calculated from the permeances of the components in the mixture:

$$\alpha_{i/j} = \frac{P_i}{l} \Big/ \frac{P_j}{l}$$

Equation 9

In this work the temperature influence on separation was studied using a simple Arrhenius-type equation [similarly to other pervaporation studies (Jullok et al., 2011, Luis et al., 2013)]:

$$\frac{P_i}{l} = \frac{P_i^{\infty}}{l} \cdot \exp\left(-\frac{1000 \cdot E_a}{R \cdot T}\right)$$

Equation 10

where E_a *[kJ/mol]* is the activation energy of the permeation process and P_i^{∞}/l is the permeance for an infinite temperature.

As defined by Huang (Wang et al., 2001, Huang and Yeom, 1991), the pervaporation separation index (PSI) is the product of separation factor and total flux values, for each feed concentration. In this thesis a modified version of this index widely accepted in literature is used (Sampranpiboon et al., 2000, Kopeć et al., 2013):

$$\mathrm{PSI} = \mathrm{J} * (\beta - 1)$$

Equation 11

In this version of the PSI-index, when $\beta = 1$, no separation occurs and PSI=0.

2.2.3. Pervaporation experiments chapter by chapter

A. *Chapter 3: membrane material selection via pervaporation tests on a reference quaternary mixture*

In order to select the appropriate membrane to be used in the separation of methyl acetate/methanol binary mixtures (discussed in Chapter 3), the three membranes were subjected to pervaporation tests using the equimolar quaternary reference mixture already mentioned in the introduction (Chapter 1) of this work and a pervaporation temperature of 40 °C, obtaining information of separation factor methyl acetate/all the rest ($\beta_{MeOAc/rest}$) and selectivity methyl acetate/methanol ($\alpha_{MeOAc/MeOH}$).

B. *Chapter 3: Pervaporation of methyl acetate-methanol binary mixtures*

For pervaporation of the methyl acetate/methanol binary mixtures discussed in Chapter 3, in order to be coherent with the industrial condition of methanolysis of polyvinyl acetate to PVOH [*i.e.*, temperatures ranging in between room temperature and 60 °C, as reported elsewhere (Snyder, 1960, Finch, 1973, Ter Jung et al., 1983)] and in order to work at least 10°C lower than the azeotropic temperature of ~54 °C at 1 atm, methyl acetate/methanol pervaporation experiments were performed at temperatures of 30, 36 and 44 °C. More information about the thermodynamic properties of the methyl acetate/methanol system is given in Figure 9 and Table 2. As Figure 9 indicates, the UNIQUAC property method (Aspen Plus v7.2 was used to work with this property

method) gives a good prediction of the experimental data (Tu et al., 1997).

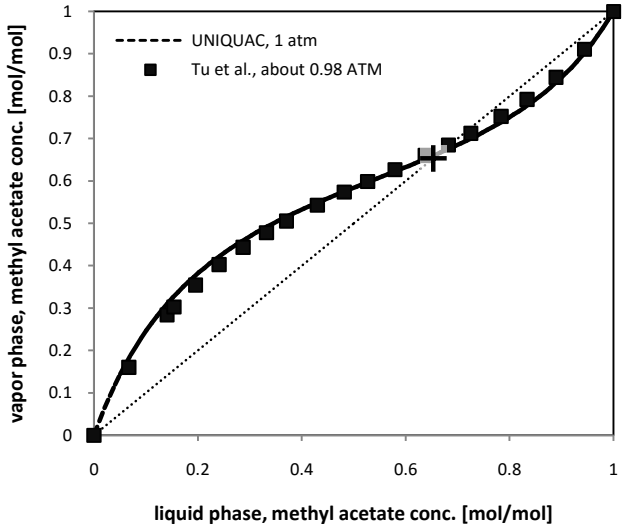

Figure 9. VLE data of the methanol/methyl acetate binary mixture, obtained from (i) the UNIQUAC predictive model at 1 atm and (ii) from experiments at about 0.98 atm (Tu et al., 1997).

Table 2. Azeotrope information obtained using the UNIQUAC property method at 1 atm.

Homogeneous	Temperature: 53.64 C	
	Classification: Unstable Node	
	[mol/mol]	[wt/wt]
Methanol	0.33	0.18
Methyl acetate	0.67	0.82

For all the three temperatures explored, five feed concentrations were chosen (*i.e.*, 11, 26, 38, 66 and 78 mole% methyl acetate) with a maximal variation of ±5 mole% between the expected and the resulted average

value. The test at 38 mole% methyl acetate in the feed was repeated three times employing 3 different membranes in order to study the variation in total flux due to the different average thickness of the membrane (this resulted in a high standard deviation for the fluxes, as discussed later). The vacuum was in the range 9-11 mbar, increasing with the temperature. About every 15 minutes permeate was collected in a cryo-trap. Three samples for fixed concentration and temperature were collected and then analyzed once the overall flux became stationary, observing average maximal standard deviations of 2 °C in temperature and 1.6 mbar in permeate pressure. The morphology of the membranes was evaluated by scanning electron microscopy (SEM) using a Philips XL 30 FEG SEM.

C. *Chapter 5: Pervaporation of methyl acetate-methanol binary mixtures*

The PolyAl TypM1 membranes, used in Chapter 5, are functionalized ultrafiltration poly acrylonitrile membranes with pores filled with a selected functional polymer (Matuschewski and Schedler, 2008).

Pervaporation experiments of the methyl acetate/methanol binary mixture were performed at 30, 36 and 44 °C (with a fluctuation of about ±1.5 °C).

For all the three temperatures, six feed concentrations were chosen (*i.e.,* 11, 26, 49, 58, 71, 90 mole% methyl acetate), with a ±5 mole% maximum variation between the expected and the average value calculated. The test at 90 mole% methyl acetate in the feed was repeated four times using 3 different pieces of the same membrane.

The vacuum was in the range 2-10 mbar, increasing with the working temperature. Permeate was collected every 10-15 min.

D. *Appendix I: Pervaporation of the equimolar quaternary alcohol/ester mixture of transesterification reaction*

The membranes Pervap 2255-30, 2255-50, 2255-80®, 4100/2565® and 2256/1768® were kindly provided by Sulzer Chemtech™; the Cuprophan® membrane by Akzo Nobel™; the PDMS (polydimethylsiloxane) membrane by Pervaptech™; and the PolyAl Typ M2® membrane was bought from PolyAn™.

A temperature of 40 °C and an equimolar concentration of 25±9 mole% feed were used for all membrane evaluations via pervaporation (reported in Appendix I).

2.3. Computer assisted simulation methods

2.3.1. A multi-stage-batch pervaporation unit (Chapter 4)

A. *Terminology and model equations*

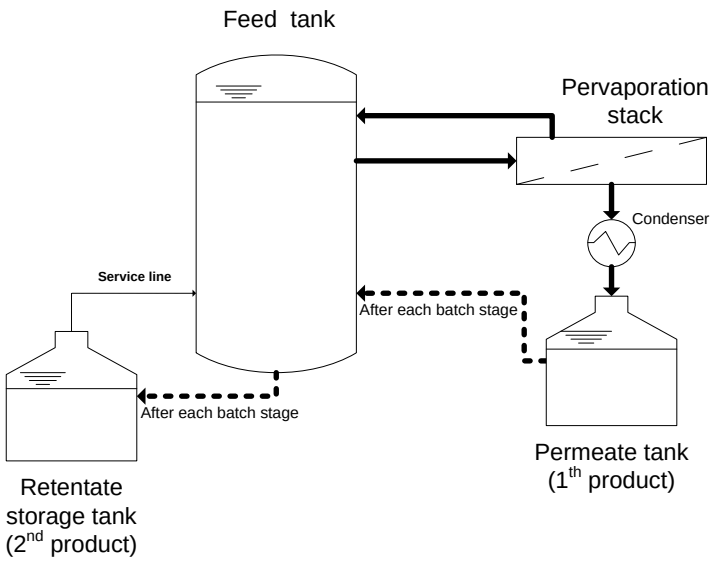

Figure 10. Scheme of the MSBP unit studied in Chapter 4.

The MSBP unit (Figure 10), discussed in Chapter 4, is made of three service tanks, in place of the four in the general version of Baker *et al.*'s apparatus (Baker et al., 1993); in fact, according with the new operation modes proposed (see Section 2.3.1B.), a 4th tank is not needed.

In a MSBP unit, in order to increase the purity of the permeate to be obtained as the product, at the end of each stage, what is left in the feed tank is sent to the storage tank, and what has been permeated, condensed and collected in the permeate tank, is returned to the feed tank for further purification. Therefore, the *retentate product* (hereinafter always reported referring to the concentration of the component not selective

for the membrane, *e.g.*, methyl acetate concentrations, if the membrane is methanol selective) is the product accumulated in the storage tank; the *permeate product* (hereinafter always reported in concentration unit of component selective for the membrane) is the product obtained at the end of the entire MSBP process and contained in the permeate tank; the *stage-termination condition* is the condition that terminates an MSBP stage; the *process-termination condition* is the condition that ends an MSBP process; the *operation mode* indicates the way in which the MSPB unit is run and depends on the stage-termination condition; a component *stage-recovery* and *total-recovery* are the ratios between the amount of the component at the end (in the respective tanks) over the amount of the same component (in the feed tank) at beginning of the stage or at the very beginning of the process, respectively.

Considering that the energy of permeation comes from the retentate-side and that during condensation the permeate rejects heat to the cooling utility, during each stage both retentate and permeate have to be heated in a heat exchanger system. However, this step was not assessed here as it is outside the scope of this study.

The model equations of this process unit are the same unsteady state mass balance equations of a batch-pervaporation unit (Figure 10), with the sole difference that in the case of MSBP-mode, for each stage the initial conditions result from the outcomes of the previous stage and the time is cumulative.

$$-\frac{\mathrm{d}F}{\mathrm{d}t} = \frac{j_1}{y_1} \times A$$

Equation 12

$$-\frac{\mathrm{d}(F \times x_1)}{\mathrm{d}t} = j_1 \times A$$

Equation 13

Where, A is the membrane area, F is the instantaneous amount in feed tank, j_1 *is* the instantaneous flux of the component enriched in the permeate, x_1 is the instantaneous molar concentration in the feed tank of the component enriched in the permeate, y_1 the instantaneous molar concentration in the permeate of the component enriched in the permeate. Combining Equation 12 and Equation 13 leads to Equation 14, which is similar to the Rayleigh equation for batch distillation (Henley et al., 2011); here however, the thermodynamic equilibrium relation between the vapour and liquid phases is replaced by the separation characteristic of the membrane.

$$\frac{\mathrm{d}F}{F} = \frac{\mathrm{d}x_1}{y_1 - x_1}$$

Equation 14

All membrane separation data were derived from experimentally obtained transport and separation data (see Figure 6), *i.e.*, methanol molar flux and the variation of permeate concentration with methanol feed concentration.

Fixing appropriate boundary conditions, *i.e.*, x_1 and the initial concentration in the feed tank $x_{1,0}$, Equation 14 results in Equation 15.

$$\ln\frac{F_0}{F} = \int_{x_1}^{x_{1,0}} \frac{\mathrm{d}x_1}{y_1 - x_1}$$

Equation 15

where,

$$F = F_0 \times \exp(-z)$$

Equation 16

and

$$z = \int_{x_1}^{x_{1,0}} \frac{\mathrm{d}x_1}{y_1 - x_1}$$

Equation 17

By combining Equations Equation 12 and Equation 15 the time dependency can be obtained (Equation 18).

$$t = \frac{F_0}{A} \int_{x_1}^{x_{1,0}} \frac{y_1}{y_1 - x_1} \frac{\exp(-z)}{j_1} \mathrm{d}x_1$$

Equation 18

B. *MSBP MATLAB simulations and termination conditions*

To simulate the MSBP-modus operandi, MATLAB® was used assuming that: (i) the storage and permeate tanks are perfectly mixed, (ii) the membrane adapts infinitely fast to the new concentrations in the feed, and (iii) the time required for liquid circulation is negligible compared to the processing time. All integrations were performed numerically on very short intervals of feed concentration, *i.e.*, lower than 0.01 mole% methanol, to minimize the integration error.

As mentioned above, medium-low performance membranes may lead to the design of expensive pervaporation units made of a long series of membrane modules, discouraging the use of this technology. The MSBP unit described in Section 2.3.1A. may allow overcoming this problem. Here, after each batch-stage it is possible to increase the purity of the permeate product by recycling to the feed tank using a single condenser.

Figure 11a-b, shows two proposed (basic) operation modes, represented schematically, to operate an MSBP unit. Table 3 includes all stage-termination conditions and process-termination conditions for both these operation modes. Figure 11a and b were produced simulating an imaginary membrane separation; in particular, Figure 11a shows the case in which each stage is terminated once a fixed stage-recovery of the component enriched in the permeate is reached, and Figure 11b the case in which each stage is terminated when reaching a desired retentate product purity. Starting from the feed point and following the time direction, for each stage it is possible to see the dynamics of the purity of permeate and retentate products. When terminating each stage at the desired retentate product purity (Figure 11b), at the end of the entire process it is possible to obtain both products, *i.e.*, storage and permeate tank products, with the desired purities. On the other hand, when terminating each stage after reaching a certain value of stage-recovery of the component enriched in the permeate, only the permeate product can be extracted pure as the membrane limits the retentate product purity. However, in this case the retentate product accumulated in the storage tank, can be recycled to the feed tank for further processing or be treated by other separation systems, *e.g.*, pervaporation, distillation, etc.

Table 3. Stage-termination conditions and process termination conditions of the two operation modes used in this work during MSBP simulations.

MSBP unit operation mode	End-stage condition	End-process condition
Constant purity of the component enriched in the retentate	fixed purity (*i.e.*, 98mole%) of the component enriched in the retentate	fixed purity (*i.e.*, 98 mole%) of the component enriched in the permeate
Constant stage-recovery of the component enriched in the permeate	fixed stage-recovery of the component enriched in the permeate	fixed purity (*i.e.*, 98 mole%) of the component enriched in the permeate

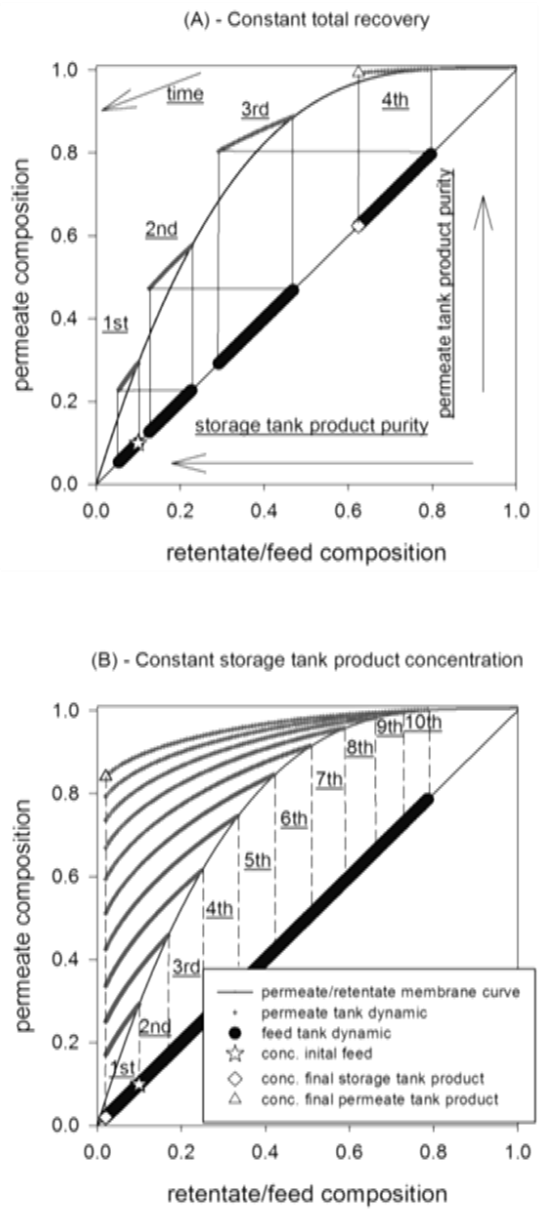

Figure 11. Two schemes for variation of compositions of permeate vs. retentate with the number of stages: (a) multi-stage-batch-pervaporation mode in which each stage is terminated after reaching a certain value of stage-recovery of the component enriched in the permeate; (b) each stage is terminated when a constant purity value of the retentate product is reached.

These two ways of operating the MSBP unit are basic examples. More elaborate combinations may be designed and employed depending on the particular separation. However, it is not the purpose of the present work to explore them.

2.3.2. The batch pervaporation time index (Chapter 4)

In the results and discussion of Chapter 4, all time data-points are reported in form of the so-called *batch pervaporation time index* (BPTI). Equation 19 shows the definition of the BPTI; the time is multiplied for the area of the cell (A) and divided for the amount of feed (F_0) used during membrane testing. This means that the time needed for a batch pervaporation can be calculated via the BPTI inserting the desiderated values of A and F_0.

The BPTI depends on: (i) the membrane separation performance which influences x_1, the choice of the stage-termination condition, which may also influence x_1, and the initial concentration of the feed mixture at t=0, *i.e.*, $x_{1,0}$.

$$BPTI = t\frac{\mathrm{A}}{F_0} = \int_{x_1}^{x_{1,0}} \frac{y_1}{y_1 - x_1}\frac{\exp(-z)}{j_1}\mathrm{d}x_1$$

Equation 19

Three versions of the batch pervaporation time index are used: (i) $BPTI_{rec,98}^{MM20}$ for separations (see Section 4.2 of Chapter 4) in which each stage ends once a constant value of stage-recovery of the component enriched in the permeate is reached (Table 3); (ii) $BPTI_{98}^{MM20}$ for separations (Section 4.3 of Chapter 4) in which each stage ends once a constant purity of the component enriched in the retentate is reached;

and (iii) a standardized version of the batch pervaporation time index ($BPTI_{98}^{o}$), for separations (Section 4.4 of Chapter 4) that start from an initial feed concentration of 50 mole% and end when the purity of the component enriched in the retentate reaches a value of 98 mole%.

Furthermore, the normalized permeate-product concentration is defined as follow: $y^{o} = (y_1 - x_{1,0})/(1 - x_{1,0})$. The $BPTI_{98}^{o}$ - y^{o} diagram is called the *batch pervaporation-membrane performance graph* and it is in this work compared with the results of a pervaporation separation index (PSI) analysis.

2.3.3. Extractive distillation system design and retrofitting simulations (Chapter 5)

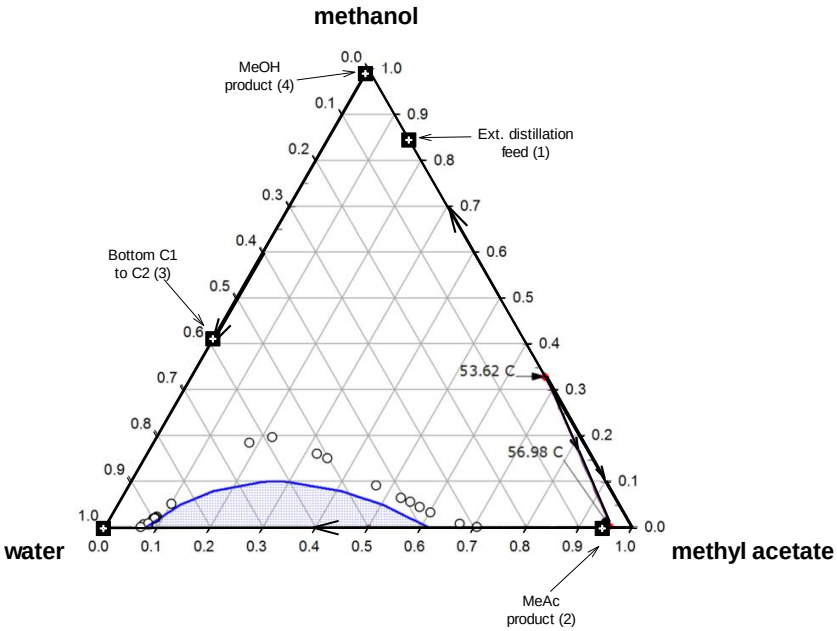

Figure 12. Methyl acetate/methanol/water ternary diagram (in molar concentrations), NRTL-HOC and immiscibility gap experimental (Iglesias et al., 1999) data (○) at 1 atm. Head/bottom products data (■) are also represented in order to help the reader in visualizing the extractive distillation separation studied in this work and discussed in the Results and Discussion of Chapter 5; the number under brackets refers to each stream of Figure 13a.

For all simulations discussed in Chapter 5, the NRTL-HOC property method was chosen (among others) since it gave the best estimation of the experimental thermodynamic data of the methyl acetate/methanol/water system, discussed elsewhere (Iglesias et al., 1999, Tu et al., 1997). Figure 12 shows the good fitting between the NRTL-HOC prediction and the immiscibility gap experimental data.

Figure 13a shows the extractive distillation unit studied in this thesis. It is composed of two columns. The first column (C1) produces methyl acetate

from the top and it is fed with the MM20 stream and pure water that extracts methanol. Then, from the bottom of column 1, methanol and water are sent to the second column (C2), where they are separated. Pure water is sent back to the first column.

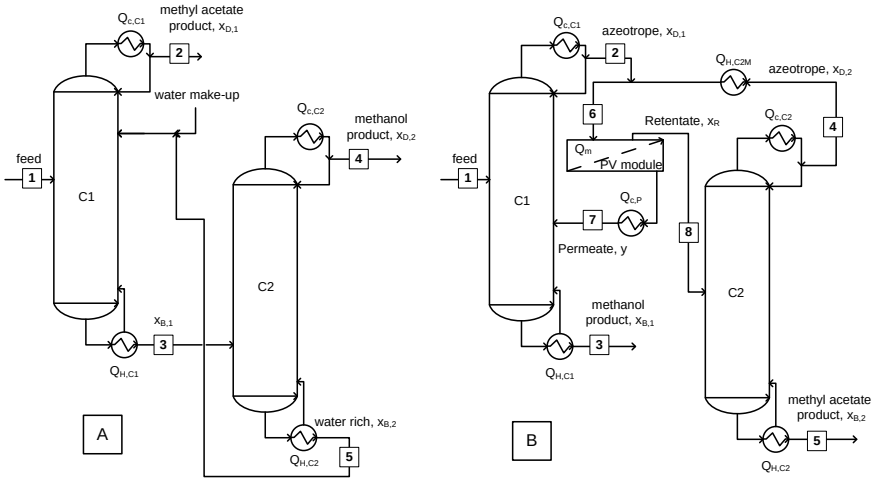

Figure 13. Extractive distillation system (a) and retrofitted unit (b) flow schemes. Information about all streams can be found in Chapter 5.

The design of the extractive distillation unit follows an iterative procedure. The two columns are first designed separately and then, an energetic optimization is done considering the whole system with close recycles. In particular, the design can be divided in two phases: (1) the determination of N_i (*i*-column number of stages), Nf_i, Ns (feed and solvent stage inlets) and the solvent to feed flow ratio (m), together with an initial guess on RR_i (*i*-column reflux ratio); and (2) obtaining the final values of RR_i and $(D/F)_i$, as result of an energetic optimization (*i.e.*, minimization of the energy required from the heating utility by the two reboilers of the two columns).

During the design of the first column, it was assumed that (1) no methyl acetate goes to the bottom, which (2) ensures the highest reasonable purity in methyl acetate chosen looking at the ternary diagram methyl acetate-methanol-water (*i.e.*, 94.4 mole% methyl acetate, see also Figure 12).

During the design of the second column, a distillate purity of about 99 mole% in methanol was arbitrary assumed.

The design of the extractive distillation and retrofitted systems was performed using the software Aspen Plus v7.3. The RADFRAC unit (equilibrium stage approach) was used for all simulations. A feed stream of about 17,900 kg/h was chosen in order to simulate a realistic industrial case.

Figure 13b shows the flow scheme of the retrofitted unit. The two columns, obtained during the design of the extractive system, were kept as a basis for retrofitting (*i.e.*, the number of stages is fixed). A pervaporation membrane module is inserted in between the two columns in order to treat the azeotropic mixture obtained as distillate from column 1. Methanol and methyl acetate products exit from the bottom of column 1 and 2, respectively. Methanol product has the same purity of the extractive distillation case (*i.e.*, 99 mole%). In this work, two cases of retrofitting were simulated: (1) with a concentration of 94.4 mole% in methyl acetate obtained, *i.e.*, the same purity obtained in the extractive system; and (2) with nearly pure methyl acetate produced (99.6 mole%).

Similarly to the extractive distillation design, the retrofitting procedure is iterative. Following this iterative procedure (better discussed in Chapter 5), RR_i and $(D/F)_i$ are varied in order to minimize A_{tot} (total area of the

membrane) and the sum of Q_m (heat supplied to the membrane module consumed during pervaporation) with $Q_{H,2}$ (duty of the heater working on the fraction of distillate of the second column recycled to the membrane module) and Qr_i (reboiler duties). In this simulation, the pervaporation module was implemented in Aspen Custom Modeler (Amelio et al., 2015) adding the energy balance (Wankat, 2006), in order to take the energy required for the permeation process into account. A pervaporation unit simulated using this model can be imagined as a plate and frame module (ideal mixing of the feed is assumed for each plate), in which heat is provided in between each plate in order to maintain a constant membrane inlet temperature of 40°C.

The energetic optimization of the two columns of the extractive distillation and retrofitted units was pursued using the Aspen Plus Optimization tool, selecting the SQP method (Sequence Quadratic Programming).

Finally, flow rate profiles of the columns and hot/cold utilities duties were used to determine the feasibility of the retrofitting from a hydraulic and energetic point of view.

2.3.4. Continuous methyl acetate conversion simulation methods (Chapter 6)

A. *Model, methods and procedure*

The pervaporation modules used for the simulation described in Chapter 6 are assumed to be composed of stacks in series for the retentate, as shown in Figure 14. Each stack is made of tubes of spiral wound membranes operating in parallel. Each tube has a membrane area of 20

m^2 and is 1 m long. The feed entering is divided into a series of sub-streams feeding each tube. Thus, in any point in the axial direction of the spiral wound the properties of the mixture being pervaporated are the same for each tube of the stack. Therefore, the term "cell" is used for each length of the stack in the axial direction of its tubes, in which a condition of perfect mixing can be assumed, *i.e.*, where the retentate exiting the cell has the same physico-chemical properties as the liquid present inside. The system is working in a condition of turbulence. A certain level of turbulence is necessary inside the cell in order to validate the perfect mixing assumption. Moreover, for pervaporation of organic-organic mixtures in the presence of high levels of turbulence, the polarization effect can be considered negligible (Baker, 2012).

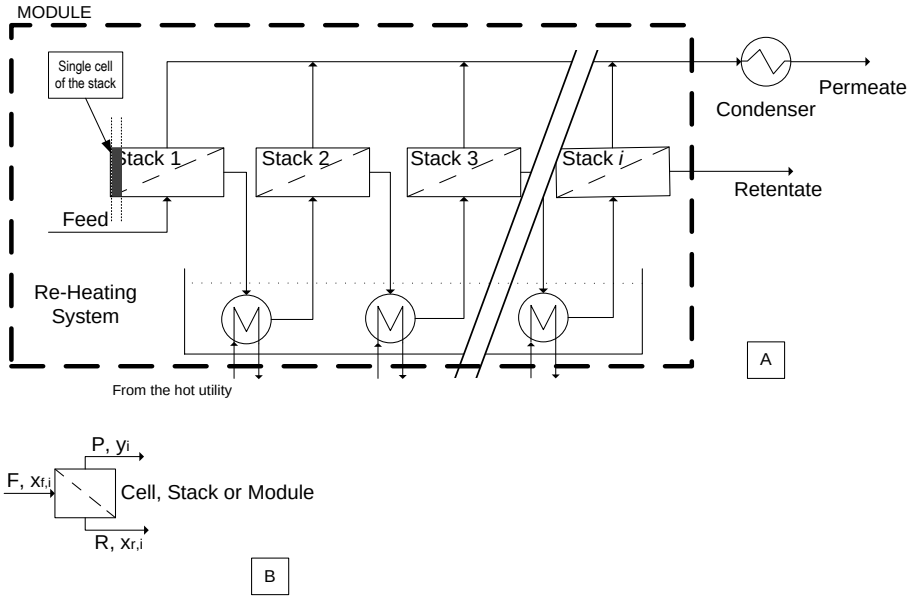

Figure 14. (a) configuration of each module employed during the simulations of this work; (b) a single cell of the stack.

The simulations of each module were performed in MATLAB and according to the code designed, the program calculates all the properties of each cell that become the input for the next cell until the retentate reaches a lower temperature limit of 37 °C. According to the membrane pervaporation behaviour (see Section 2.3.4D. where the membrane is described), this temperature was chosen in order to limit the increase of membrane area associated to the reduced permeance at low temperatures.

At the outlet of each stack, the retentate is re-heated and sent to the following stack. After a certain number of stacks, a desired (very low) concentration of methanol (or methyl acetate) in the retentate or permeate is reached and the simulation stops.

In order to be coherent with the perfect mixing assumption, a very low variation of the retentate concentration (*i.e.*, 0.0008%) is assumed for each cell. To this end, the program calculates retentate and permeate flow rates and concentrations by the mass balance of Equation 20 and Equation 21.

$$F * x_{f,i} = y_i * P + x_{r,i} * R$$

Equation 20

$$F = R + P$$

Equation 21

Assuming steady-state and adiabatic conditions, for the energy balance Equation 22 is used; which can be further elaborated to Equation 23, setting the temperature of the permeate (T_p) as reference temperature for enthalpies. In fact, due to the very small thickness of dense pervaporation membrane layers, it is possible to assume that permeate

and retentate are at the same temperature. Hence, from Equation 23, rewriting into Equation 24 and using Equation 25, where the cell-*cut* θ definition is given, it is possible to calculate T_p (Wankat, 2006).

$$F * h_f = P * H_p + R * h_r$$

Equation 22

$$F * c_{p,f}^{L} * \left(T_f - T_p\right) = P * \lambda_p$$

Equation 23

$$T_p = T_f - \frac{\lambda_p * \theta}{c_{p,f}^{L}}$$

Equation 24

$$\theta = \frac{P}{F} = \frac{c_{p,f}^{L} * \left(T_f - T_p\right)}{\lambda_p}$$

Equation 25

Since the retentate/permeate temperature is an unknown, the heat capacity ($c_{p,i}^{L}$) of the mixture inside each cell was calculated based on the feed inlet temperature. This approximation is sufficient, since for each cell the variation of temperature between feed inlet and retentate outlet is always very small.

Equation 26 and Equation 27 represent, respectively, permeate concentration and flux data of a given value of retentate concentration and temperature. These data are used by the program to calculate Equation 28 and Equation 29, *i.e.*, the values of the permeance activation energy (E_{att}) and permeance at infinite temperature ($\frac{P_i^{\infty}}{l}$). These two parameters are then implemented in the Equation 30 in order to calculate the permeance for the component selectively permeated.

$$y_i = f(x_{r,i}, T_p)$$

Equation 26

$$J = f(x_{r,i}, T_p)$$

Equation 27

$$E_{att} = f(x_{r,i})$$

Equation 28

$$\frac{P_i^{\infty}}{l} = f(x_{r,i})$$

Equation 29

$$\frac{P_i}{l} = \frac{P_i^{\infty}}{l} * \exp\left(-\frac{E_{att}}{R * T}\right)$$

Equation 30

Equation 31, derived from the definition of component permeance (Baker et al., 2010), permits to calculate the flux of the component selective for the membrane. For this equation vapour pressures (P_i^{sat}), activity coefficients (γ_i) and permeate concentration for the component selective for the membrane are of simple estimation since depend on the cell temperature T_p. Equation 32 is then used to calculate the value of total flux for each permeate temperature, dividing component flux for the corresponding permeate concentration.

$$j_i = \frac{P_i}{l} * \left(P_i^{sat} * x_{r,i} * \gamma_i - P_{cond} * y_i\right)$$

Equation 31

$$J = \frac{j_i}{y_i}$$

Equation 32

The area of the cell is then calculated dividing the permeate flow rate for the total flux of the cell.

In these module equations, all the heat capacities were calculated based on average temperatures. As a further approximation, molar concentration averaged heat capacities and heat of vaporization were used accounting the contribution of each component of the mixture.

For the estimation of condensers energy requirement, a simple energy balance was used. Average heat capacities calculated between condenser inlet and outlet and heat of vaporization (λ_i) estimated at the feed-cell temperature were used. In addition, during all the simulations, a condenser outlet temperature of -40 °C was set for the permeate.

Vapour pressures, the heat capacity of each component and the heat of vaporization were calculated using the correlations reported in Perry's Chemical Engineers' Handbook 8th edition (Perry and Green, 2008). The activity coefficients of each component were estimated using Aspen Plus® v7.2 UNIQUAC property method coefficients (Abrams and Prausnitz, 1975).

B. *Aspen Plus-Matlab coupled simulations*

Coupling Matlab pervaporation module simulations with Aspen Plus v7.3 it was possible to obtain all flow rates, concentrations, temperatures, energy consumptions and physical properties of all the streams of each pervaporation-based flow scheme. Three flow schemes were simulated in this way: (1) a system made of a reactor, a methanol selective module, a methyl acetate selective module and a *n*-butanol/butyl acetate service column (this system is denoted as SIM1); (2) a system made of a pressure swing pre-concentration step, reactor, methanol selective module, methyl

acetate selective module and a *n*-butanol/butyl acetate service column (SIM2); (3) and a system similar to SIM2, where the distillation based pre-concentration step is substituted by another methanol selective pervaporation module (SIM3). If for SIM1 the reactor is fed with the main feed having 60 mole% methyl acetate, for SIM2 the pre-treatment step produces a methyl acetate reactor feed of 94.4 mole% methyl acetate. This reagent concentration value was chosen to be not too high in order to reduce the energetic load for the first column of the distillation based pre-concentration step (see Chapter 6). This methyl acetate reagent stream concentration choice was maintained also for SIM3. In these schemes, the methanol selective membrane module working on the reaction medium exiting from the reactor is called Module1. Module2, instead, contains a methyl acetate selective membrane to treat the retentate of Module1. In addition for SIM3, the pre-concentration module working on the binary methanol/methyl acetate feed mixture is denoted as Module0.

All the distillation columns were dimensioned fixing a reflux ratio 1.3 higher than its minimum.

In all simulations, the two reagents are fed into the reactor with a BuOH/MeOAc molar ratio of 1.7. This value, higher than 1, was chosen in order to increase the equilibrium conversion of MeOAc. In fact, there is a direct proportionality between MeOAc equilibrium conversion and BuOH/MeOAc molar ratio (Bożek-Winkler and Gmehling, 2006).

The transesterification reaction model and parameters (equilibrium relations) were obtained based on the work of Bożek-Winkler and Gmehling (2006).

C. *The conventional system used for comparison*

The three pervaporation-based flow schemes were energetically compared with the two conventional process schemes studied by Luyben et al. (2004) and already introduced in Section 1.7 and Figure 8a-b.

D. *The membrane used*

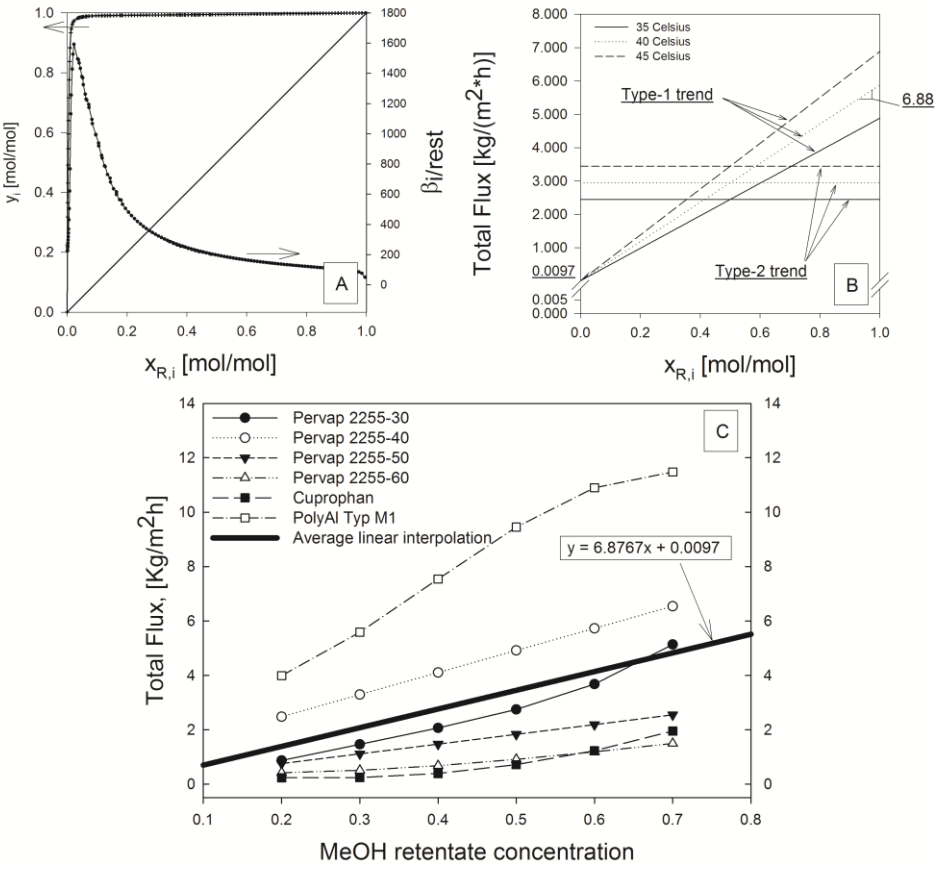

Figure 15. (a) permeate concentration/separation factor and (b) total flux vs. feed/retentate concentration variation in the component selective for the membrane for the two total flux trend cases. (c) average linear trend obtained from literature data of commercial membranes (Gorri et al., 2006, Sain et al., 1998, Steinigeweg and Gmehling, 2004, Abdallah et al., 2013) used during methanol/methyl acetate pervaporation.

Depending on the module that is simulated the membrane is methanol or methyl acetate selective. It was assumed that the methanol selective membrane and the methyl acetate selective membrane have the same values of permeate vs. retentate concentration and total flux vs. retentate concentration. For the *i*-component each time selective for the membrane, these separation data can be found in Figure 15a and b, respectively. A maximal value of separation factor of 1592 and an average value of 435 were chosen.

Despite flux and separation factor being the same for the two membranes, due to the effect of the driving force, the permeance trend of each component changes completely between the two membranes with different selectivity (see Chapter 6).

In order to assess the total flux trend effect on the membrane area and profitability of the conversion process, two different types of total flux behaviour were assumed for the membrane of *i*-component selectivity. Hence, in Figure 15b, it is then called type-1 (or simply M1) the total flux trend obtained from literature data. Figure 15c better shows how this trend was obtained, *i.e.*, by linear average of the polynomial fitting of fluxes of commercial membranes tested in literature (Gorri et al., 2006, Sain et al., 1998, Steinigeweg and Gmehling, 2004, Abdallah et al., 2013) for pervaporation of methanol/methyl acetate mixtures. The range of feed/retentate concentration of 20-70 mole% methanol and about 40°C were chosen in order to calculate this linear average. Starting from this average trend, assumed for a pervaporation temperature of 40°C, the total flux slope variation for the cases of 35 and 45°C, was arbitrary attributed (see Figure 15b).

The second type of total flux trend, denoted as type-2 (or simply M2), assumes a constant total flux in the entire range of retentate/feed concentrations (*i.e.*, the value that type-1 total flux has at 50 mole% methanol concentration in the retentate, as can be observed in Figure 15b).

In addition, it was assumed that the membrane data of Figure 15a-b were obtained by pervaporation experiments at constant permeate pressure of 1.5 mbar and three temperatures (35, 40 and 45°C). The limit of 45°C was chosen for two reasons: (i) in order to stay at least about 10°C lower than the azeotropic atmospheric temperature of the methanol/methyl acetate binary mixture [*i.e.*,~52 °C (Tu et al., 1997)]; and (ii) in order stay in the range of temperatures in which the reaction of methanolysis, which produces the MM20 stream, takes place. In fact, the methanolysis reaction of conversion of polyvinyl acetate into PVOH and MeOAc is industrially conducted at low temperatures, *e.g.*, in between room temperature and 60 °C (Snyder, 1960, Finch, 1973, Ter Jung et al., 1983).

E. *Energetic comparisons and energetic integrations*

For the energetic comparison, the energy requirement of condensers and reboilers of the conventional systems described by Luyben et al. (2004) and shown in Figure 8a-b, was compared with the energy consumption of the three PV-based flow schemes. This comparison is unfavourable for the PV-based schemes since the energy requirement of pre-heaters and coolers is also considered, whereas it is not for the conventional systems.

Finally, an energetic integration was pursued following the suggestion of Turton et al. (2003).

F. *Economical analysis*

The economic analysis was pursued following the indications reported by Turton et al. (2003), also applied in the program CAPCOST®. Information on material costs and energy costs is normally difficult to obtain, however, it was possible to find all major information for the year 2012 (listed in Table 4). Market prices of chemicals refer to the USA market averaging the prices for the period comprised between September and December 2012 (Tecnon-OrbiChem, 1 November 2013b, Bowen, 2013, Lane, 2013). Electricity, cooling water, refrigeration (-50 °C) and high pressure steam costs were obtained from the Dutch Association of Cost Engineers (Kiss, 2013), adding the indications of Turton et al. (2003). All this information together with additional data used during the profitability analysis, are listed in Table 4.

Table 4. Support information for the economic analysis.

Miscellaneous data for profitability analysis (year 2012)	
Electricity (110V - 440V)	29.5 $/GJ
Cooling Water (30°C to 45°C)	2.2 $/GJ
Refrigerated Water (15°C to 25°C)	9.7 $/GJ
High Pressure (41 barg, 254°C)	21.5 $/GJ
Very Low Refrigeration (-50°C)	28.8 $/GJ
Pump Efficiency	70%
Cost of Labour (per operator/year)	52,900.00 $
CEPCI	584.6
BuOH Price (late 2012)	2.06 $/kg
BuOAc Price (late 2012)	2.00 $/kg
MeOH Price (late 2012)	0.39 $/kg

Similarly to Oliveira et al. (2001), the purchased cost of each membrane module was calculated adding the cost of the module (calculated on the

base of 300 \$/stack) to the cost of the membrane (ranging between $50 \leq \$/m^2 \leq 725$). The bare module equipment cost (C_{BM}) of the membrane module was then estimated employing the bare module factor of 3 suggested by Hickey and Gooding (1994) .

The cost of each heat transfer system was estimated within CAPCOST using a heat transfer area calculated by the short cut method and overall heat coefficients (Sinnott, 1999). Based on simulation and simple pressure drop calculations for spiral wound modules (Oliveira et al., 2001, Hickey and Gooding, 1994, Fárková, 1991), the energy consumption for pervaporation module feed pumps was estimated. Aspen Plus simulation data were used for all other units cost assessments via CAPCOST.

For the economic analysis, two cases were studied: (i) the case in which the *n*-butyl acetate system is added to an existing plant producing the MM20 or MM80 waste stream (*e.g.*, polyvinyl alcohol plant); (ii) and the case in which the plant is built from scratch and fed with the MM20 stream. In the former case, the Fixed Capital Investment (FCI) is equal to the Total Module Cost (C_{TM}). In the latter case, the FCI is equal to the Grass Roots Cost (C_{GR}). Moreover, respecting the indications of Turton et al. (2003), the Grass Roots Cost was calculated with Equation 33 (Turton et al., 2003).

$$C_{GR} = C_{TM} + 0.4 * \sum C_{BM}$$

Equation 33

Concerning the COM (cost of manufacturing), the expression (see Equation 34) proposed by Turton et al. (2003), was modified (Equation 35) adding a further term that takes into account the cost of membrane

replacement (C_{MR}), assuming a membrane life of 3 years. However, with Equation 35 during the last years of work of the plant the COM is slightly overestimated, since the cost of membrane replacement is an unnecessary expense being the plant going to dismantling and selling.

$$COM_{Turto\,n} = 0.18 * FCI + 2.76 * C_{OL} + 1.23 * (C_{UT} + C_{WT} + C_{RM})$$

Equation 34

$$COM = COM_{Turton} + \left[1/3 * \left({Module\ Cost\ of\ PV\ Modules}/{C_{TM}}\right) * FCI\right]$$

Equation 35

Finally, a plant life of 15 years comprising of 1 year of construction and start up was assumed for all simulations. The Discounted Profitability Criterion parameters, used during results discussions, were obtained setting a 3 years MACRS (Modified Accelerated Cost Recovery System) depreciation.

Chapter 3

POLYVINYLIDENE FLUORIDE DENSE MEMBRANE FOR THE PERVAPORATION OF METHYL ACETATE-METHANOL MIXTURES

Adapted from: G. Genduso, H. Farrokhzad, Y. Latré, S. Darvishmanesh, P. Luis, B. Van der Bruggen, Polyvinylidene fluoride dense membrane for the pervaporation of methyl acetate–methanol mixtures, Journal of Membrane Science, Volume 482, 15 May 2015, Pages 128-136, ISSN 0376-7388, http://dx.doi.org/10.1016/j.memsci.2015.02.008.

3.1. Introduction

From an energetic point of view, the pervaporative separation of MeOAc from the MM20 stream should be conducted via a methyl acetate selective membrane; in fact, the MM20 stream contains only 16 mole% MeOAc in MeOH. In order to select the right material for a methyl acetate selective membrane, to be used during MM20 stream concentration, the applicability of the Hansen Solubility Parameters theory for the selection of polymers is described in Section 3.2. The methodology of selecting materials via the HSPs theory, already studied in literature for various mixtures (Buckley-Smith, 2006), is discussed here describing the pervaporation outcomes of three polymeric materials (polyvinyl alcohol, chlorinated polypropylene and polyvinylidene fluoride). These materials were chosen above many others, present in our laboratory, on the base of: (i) the HSPs theory (for what concerns polyvinyl alcohol and chlorinated polypropylene polymers) or (ii) on the basis of previous

experience (for what concern the polyvinylidene fluoride polymer). For these pervaporation tests, two reference alcohol/ester binary (MeOAc/MeOH) and quaternary (MeOAc/BuOAc/MeOH/BuOH) mixtures were used. According to the results, shown in Section 3.2, a more detailed discussion on the pervaporation performance of polyvinylidene fluoride dense membranes, for MeOAc/MeOH mixture separation, is given in Section 3.3. Finally, the effect of temperature on permeation of methyl acetate/methanol mixtures in polyvinylidene fluoride membranes is discussed in Section 3.4.

3.2. Selection of the membrane material

From the *solubility parameter distance* (R_a) analysis (summarized in Figure 16) it can be inferred that PVDF is the polymer with the highest affinity for methyl acetate, while PVOH has more affinity for methanol than for methyl acetate. If this analysis is extended on the basis of the *relative energy difference* (RED) ratio (which is shown in Table 5), it can be concluded that PVOH and ClPP are all suitable for methyl acetate pervaporation since this solvent lies inside the solubility sphere of these polymers and close to the edge. This is, in fact, the condition that makes a membrane suitable for pervaporation (Buckley-Smith, 2006) and the premise that led to the selection of these two materials. Even if PVDF is a potential polymer, it should be discarded since the RED value is higher than 1. However, the pervaporation tests on the quaternary reference mixture do not confirm this analysis. In reality, the ClPP and PVOH membranes provided a permeate richer in both methyl acetate and methanol, as shown in Table 6 (*i.e.*, $\beta_{MeOAc/rest}$ and $\beta_{MeOH/rest}$ are both higher than 1); moreover, when $\alpha_{MeOAc/MeOH}$ (methyl acetate/methanol selectivity) is considered, the PVOH membrane showed to be selective

toward methanol and ClPP slightly toward methyl acetate, as shown in Table 7 (first column). The PVDF membrane, instead, gave a $\beta_{MeOAc/rest}$ and $\alpha_{MeOAc/MeOH}$ higher than 1 (Table 6 and Table 7).

Table 5. Relative energy difference (RED, Equation 3) analysis results for the chosen polymers.

Polymeric material	RED methyl acetate	RED methanol	RED n-butanol	RED n-butyl acetate
polyvinylidene fluoride (PVDF)	1.68	2.40	1.92	2.33
chlorinated polypropylene (ClPP)	0.93	1.96	1.27	0.89
polyvinyl alcohol (PVOH)	0.97	0.73	0.84	1.30

Table 6. Pervaporation separation factors obtained after pervaporation (at 40°C) of the quasi-equimolar four component alcohols/esters mixtures.

		methyl acetate	methanol	n-butanol	n-butyl acetate
	Feed	0.21 [mol/mol]	0.26 [mol/mol]	0.27 [mol/mol]	0.26 [mol/mol]
PVDF	$\beta_{i\text{-component/all the rest}}$	1.77	1.02	0.48	1.03
	Feed	0.21 [mol/mol]	0.24 [mol/mol]	0.28 [mol/mol]	0.27 [mol/mol]
ClPP	$\beta_{i\text{-component/all the rest}}$	2.29	1.54	0.26	0.67
	Feed	0.19 [mol/mol]	0.23 [mol/mol]	0.30 [mol/mol]	0.28 [mol/mol]
PVOH	$\beta_{i\text{-component/all the rest}}$	1.13	1.21	0.85	0.89

Table 7. Pervaporation selectivities obtained after pervaporation (at 40°C) of the quaternary alcohols/esters mixture.

	α methyl acetate/methanol	α n-butanol/methanol	α n-butanol/methyl acetate	α n-butyl acetate/methyl acetate	α n-butyl acetate/ n-butanol	α n-butyl acetate/ methanol
PVDF	**1.25**	9.38	7.51	10.00	1.33	12.48
ClPP	**1.04**	4.50	4.35	6.22	1.43	6.45
PVOH	**0.65**	15.52	23.78	13.47	0.57	8.79

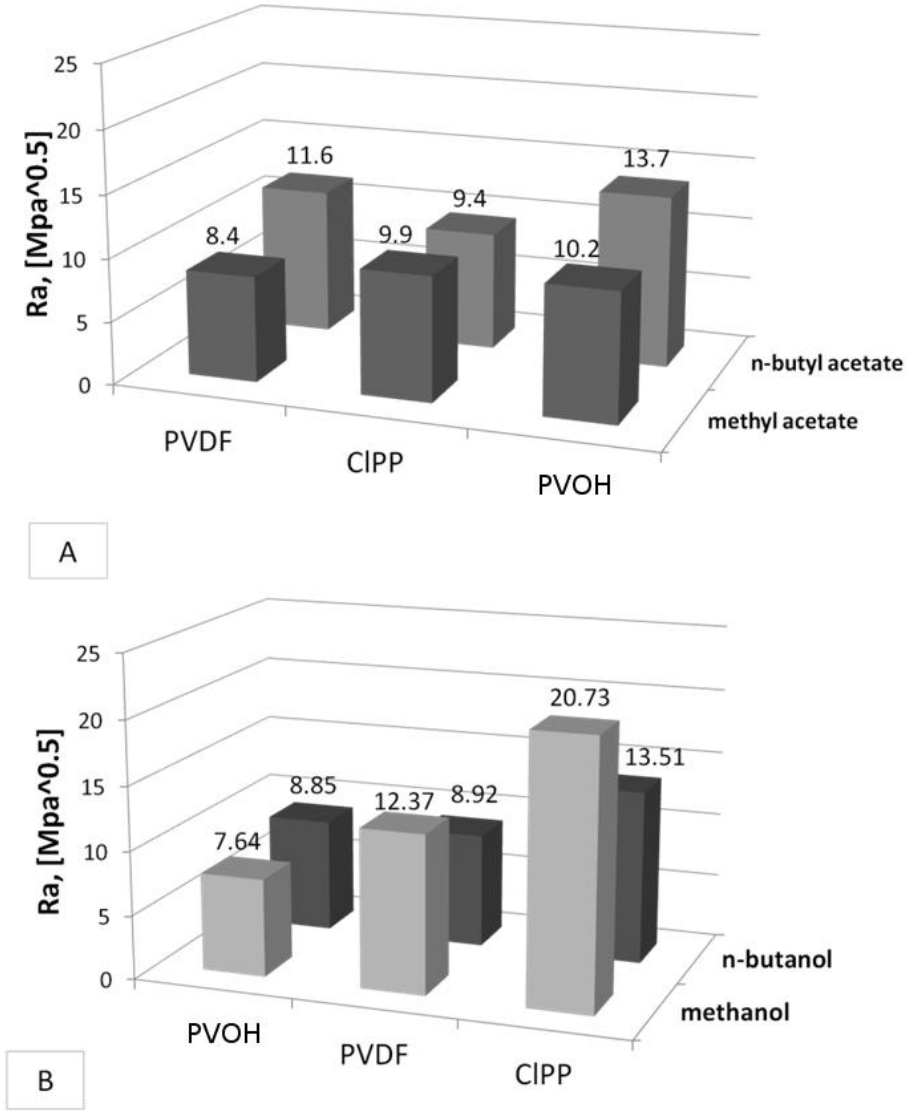

Figure 16. In (a) the solubility parameter distance (Ra, Equation 2) analysis is shown considering the two esters of the reference mixture (methyl acetate/methanol/n-butyl acetate/n-butanol); in (b) the same analysis considering the two alcohols.

Bell et al. (1988) described how for polymeric membranes in a glassy state, the contribution of component diffusion to the pervaporative separation is more relevant than component solubility. Hence, for both PVOH and ClPP membranes, in a glassy state at a working temperature of 40 °C (in fact according to the data of Table 1, the T_g of these two materials is higher than the working temperature), the HSPs theory is inadequate to predict their pervaporation behaviour, proving Bell et al.'s outcomes. Concerning the PVDF membrane that is in the rubbery state (in this case, T_g is lower than the working temperature) the HSPs assessment suggested a high affinity of PVDF toward methyl acetate (in terms of R_a) and a potential use of the same membrane in order to selectively pervaporate methyl acetate. In fact, for the PVDF membrane, in comparison with the REDs toward MeOH, BuOH and BuOAc, the RED toward MeOAc is the lowest and the closest to 1. However, even when the distance from the solubility sphere edge is not taken into account, this prediction can be considered in agreement with the experimental outcomes only when considering the selectivity of the membrane for a methyl acetate/methanol binary mixture ($\alpha_{MeOAc/MeOH}$, Table 7 first column). In fact, according to the data presented in Table 7, the HSPs assessment failed in predicting the PVDF potential over this pervaporative separation, and in general in predicting the membrane selectivity. This is probably due to many concurrent effects [*e.g.*, possible misestimation of the HSPs (Buckley-Smith, 2006), coupling phenomena effect on HSPs, swelling effect on HSPs, and others] that may indicate the inability of the HSPs method in being used in a membrane selection step for alcohol/ester mixtures pervaporation. There are other cases in which the HSPs methods failed when used as selection methods; Buckley-Smith (2006) already reported how the HSPs theory applied as a screening

method fails when halogenated/organic and xylene isomers mixtures are studied.

A similar situation was reported by Luis et al. (2013). In this case the so-claimed alcohol selectivity of many commercial membranes (*e.g.*, the PolyAl® membranes produced by PolyAn™) could be derived from the separation factor; however, when removing the driving force contribution, all these membranes resulted to be *n*-butyl acetate selective.

The ability of the PVDF membrane in selective pervaporating methyl acetate/methanol binary mixtures was further experimentally assessed, as discussed in the next section.

3.3. Methyl acetate-methanol pervaporative separation via PVDF membranes

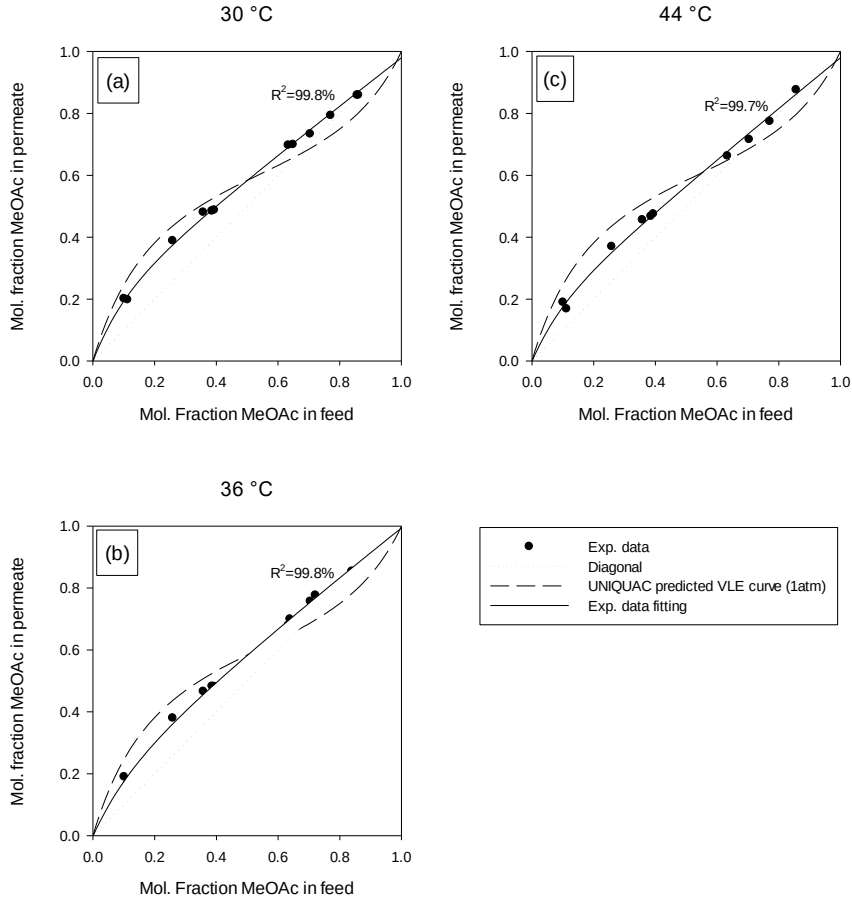

Figure 17. McCabe-Thiele diagrams resulted from the pervaporation experiments at 30 (a), 36 (b) and 44 °C (c). In the same figure, the methyl acetate/methanol VLE, UNIQUAC-predicted, data (1 atm) are reported together with the best fitting curves of the experimental data.

In Figure 17, permeate vs. retentate/feed concentration data at 30, 36 and 44 °C are shown. As it is possible to notice, the PVDF membrane permits to obtain a permeate richer in methyl acetate than the corresponding feed; these McCabe-Thiele data were fitted using Equation 36 and the estimated parameters reported in Table 8.

$$y = A + B * [1 - EXP(-C * x) - D * \frac{1 + \frac{C * EXP(-DD * x) - DD * EXP(-C * x)}{DD - C}}{DD}]$$

Equation 36

Table 8. Parameters of Equation 36 used in the fitting of the data shown in Figure 17.

Parameters	30 °C	36 °C	44 °C
A	-9.3E-4	-1.43E-3	-1.16E-3
B	31.7	18.3	34.4
C	8.2E-2	1.12E-1	6.7E-2
D	6.8	5.1	6.5
E	3.3	3.6	4.0
DD=D+E	10.2	8.7	10.5

Figure 18 reports the separation factor $\beta_{MeOAc/MeOH}$, and the selectivity $\alpha_{MeOAc/MeOH}$ as a function of the methyl acetate feed concentration on a molar basis. In this figure, $\beta_{MeOAc/MeOH}$ is always above 1, in agreement with the information shown in Figure 17. This is also the case when the membrane resulted to be methyl acetate selective only for feed concentrations higher than about 60 mole% methyl acetate. This is due to the combined contribution of driving forces to fluxes that allows to obtain permeates richer in methyl acetate than the corresponding feed in the entire range of feed concentrations. As a result, from low to high methyl acetate concentrations in the feed, the membrane changes its selectivity. The explanation for this can be found in the definition of selectivity, which takes into account the thermodynamic affinity of the components with the membrane and the kinetic aspect of the diffusion of these components across the dense layer of the membrane. As explained by Van Baelen et al. (2005), the membrane contribution to a pervaporative separation is a complex problem that depends on many variables and

contributions (*e.g.*, temperature and feed concentration variation, mutual component-membrane, component-component, component-membrane-component interactions, etc.). Therefore, selectivity as a single parameter fails in describing all these aspects. A modelling study may provide a more complete analysis (Heintz and Stephan, 1994); in this work, a first understanding of the selectivity behaviour and membrane contribution to the separation is described considering the temperature effect analysis proposed in Section 3.4.

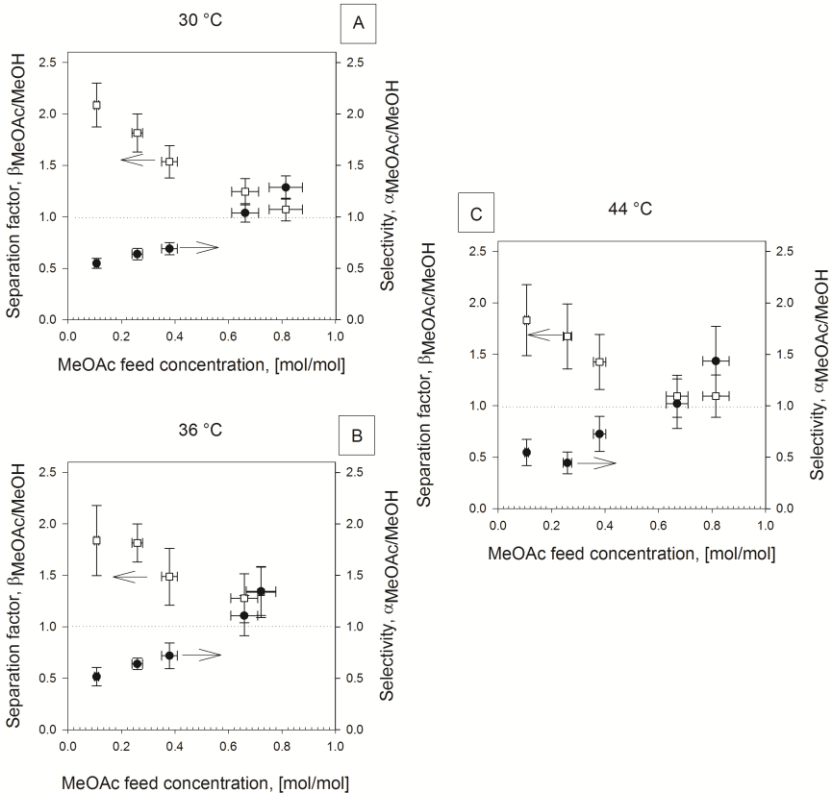

Figure 18. Separation factor and selectivity variation with methyl acetate molar concentration in the feed.

The bi-selectivity of the membrane explains also why for concentrations lower than 50 mole% methyl acetate, the permeate/retentate curve stays

below the vapour-liquid equilibrium curve (Figure 17). In fact in this concentration range, the membrane being methanol selective, it acts against the thermodynamics of the separation (*i.e.*, VLE curve). However, this contribution is insufficient to invert the separation and $\beta_{MeOAc/MeOH}$ remains higher than one.

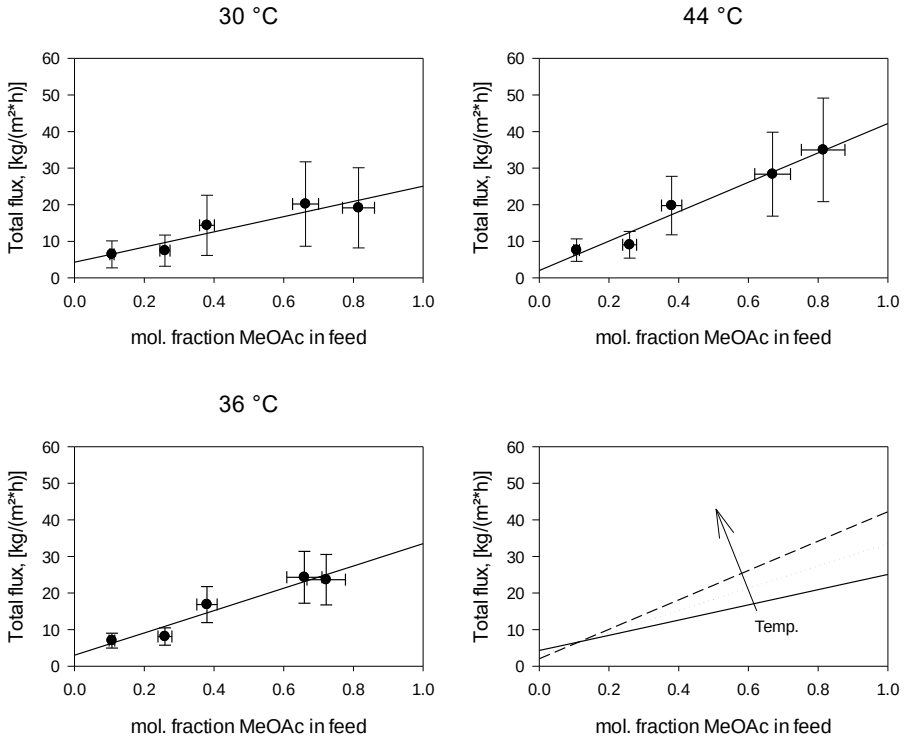

Figure 19. Total flux (weight basis) vs. molar feed concentration experimental outcomes.

In the entire feed concentration range the total fluxes increase with the methyl acetate concentration in the feed, as shown by the linear fitting of the experimental outcomes presented in Figure 19. However, pervaporation experiments at the same initial feed concentration, temperature and different pieces of the same membrane, resulted in average fluxes with a significant standard deviation. The difference in flux obtained with a different piece of the same membrane may be attributed

to the difference in average thickness between each employed PVDF membrane. The thickness of a used dense membrane was estimated by SEM imaging and resulted to be lower than 10 μm (Figure 20a). Figure 20b and c show two SEM images of two PVDF membranes (taken from the same prepared sheet) before and after pervaporation. It seems that the interaction of the two solvents with the membrane is so strong that after pervaporation the surface of the membrane results to be slightly deformed (in any case the membrane remains dense and transparent).

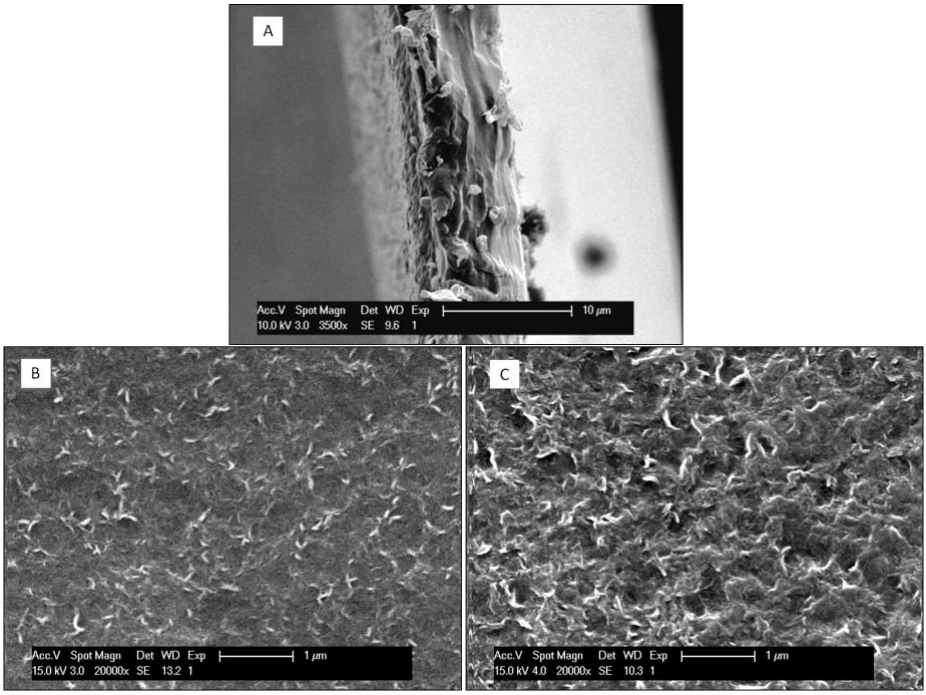

Figure 20. In (a) the cross-sections of the PVDF membrane is reported. In (b) and (c) the top view of a piece of the same membrane sheet, before and after pervaporation.

Table 9 reports the data of methyl acetate and methanol permeances as a function of methyl acetate feed concentration, for all explored temperatures. It is important to note that each error attributed to each point reported in this table was calculated on the basis of the maximal

value of calculated percentage standard deviation (*i.e.*, for some points the error may be overestimated). Thus, Table 9 shows how for concentrations in the feed higher than about 60 mole% in methyl acetate, the methanol permeance becomes lower than the methyl acetate permeance, supporting the conclusion arising from Figure 18.

Table 9. Component permeances in function of feed molar concentration. The column 'number of points' indicates how many times each concentration was tested.

Temperature	**Number of points**	**Feed, methyl acetate concentration**	**Methyl acetate permeance**	**Methanol permeance**
[°C]		*[mol/mol]*	*[GPU]*	*[GPU]*
30	**	0.814 ± 0.062	6765.3 ± 3957.9	5283.5 ± 3185.0
30	***	0.662 ± 0.051	7416.7 ± 4339.0	7157.2 ± 4314.5
30	***	0.380 ± 0.029	5554.2 ± 3249.4	8178.3 ± 4930.1
30	*	0.259 ± 0.020	3079.1 ± 1801.4	4817.2 ± 2903.9
30	**	0.107 ± 0.008	2980.2 ± 1743.5	5417.4 ± 3265.7
36	*	0.722 ± 0.055	6551.1 ± 3159.9	4872.2 ± 2381.5
36	***	0.659± 0.050	7004.7 ± 3378.7	6339.8 ± 3098.8
36	***	0.380 ± 0.029	4752.6 ± 2292.4	6684.9 ± 3267.5
36	*	0.259 ± 0.020	2513.5 ± 1212.4	3841.8 ± 1877.8
36	**	0.107 ± 0.008	2320.4 ± 1119.2	4535.0 ± 2216.7
44	**	0.814 ± 0.049	6834.2 ± 2659.5	4951.9 ± 1951.0
44	**	0.669± 0.041	5767.6 ± 2244.4	5654.0 ± 2227.6
44	***	0.380 ± 0.023	4138.7 ± 1610.5	5711.0 ± 2250.1
44	*	0.260 ± 0.016	1323.9 ± 515.2	2972.4± 1171.1
44	**	0.107 ± 0.006	1885.5 ± 733.7	3447.8 ± 1358.4

$1\ \text{GPU} = 1 \cdot 10^{-6} \text{cm}^3(\text{STP})/(\text{cm}^2 \cdot \text{s} \cdot \text{cmHg}) = 7.5005 \cdot 10^{-12} \text{m} \cdot \text{Pa}^{-1} \cdot \text{s}^{-1}$

3.4. Temperature effect on pervaporation

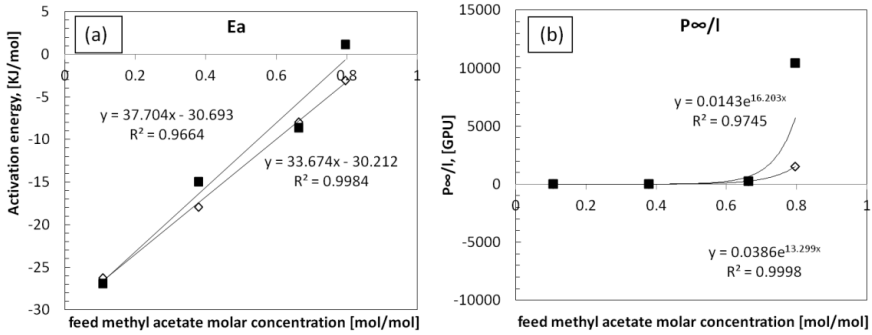

Figure 21. Methyl acetate (■) and methanol (◇) activation energy (a) and permeance at infinite temperature (b) in function of feed molar concentration in methyl acetate.

The data at about 26 mole% in methyl acetate were not considered for this temperature effect analysis (presented in Figure 21) since they consist of only three points (for the three temperatures). As described by Feng et al. (1996), the permeation activation energy can be considered mainly composed of two terms: the enthalpy of sorption, $\Delta H_{sorb,i}$ (generally negative for exothermic processes) and the activation energy of diffusion $E_{d,i}$ (positive value). Up to about 80 mole% methyl acetate, permeances activation energy values of both the components resulted negative (Figure 21a), meaning that the main contribution is an enthalpic contribution. This is in agreement with the results of Bell et al. (1988) concerning rubbery membranes. The negative activation energy favours permeation at low temperatures. This is not in disagreement with the flux results (Figure 19), where the driving force is also taken into account (*i.e.*, the effect of the temperature on components permeance counteracts the effect of temperature on driving force and then on the flux). Moreover, the two permeation activation energies (for methyl acetate and methanol) have a similar curve trend in the entire concentration range and similar values for low methyl acetate feed concentrations. Hence, in

particular in the region of retentate/feed concentrations in which for both compounds the activation energy presents close values and a very similar trend, it can be supposed that the presence of one of the two mixture components, affects the remaining component permeation. This may be related to unwanted swelling or coupling directly linked to the presence of methanol. In fact, when methanol concentration decreases the two activation energy curves diverge (*i.e.*, at high methyl acetate concentration) and the membrane becomes methyl acetate selective, as shown in Section 3.3. This is also confirmed by Figure 21b, which shows how the methyl acetate permeance at infinite temperature (*i.e.*, the pre-exponential factor P_∞/l) increases more than the methanol permeance at infinite temperature, exactly for concentrations above about 60 mole%, when the membrane starts to be methyl acetate selective. This means that a high concentration in methyl acetate (higher than 60 mole% methyl acetate) is beneficial for membrane selectivity toward methyl acetate.

3.5. Conclusions

In this chapter, PVDF membranes for the separation of methyl acetate/methanol mixture were developed and studied. The membranes have a selectivity up to 1.44 for methyl acetate and flux values up to 35 $kg.m^{-2}.h^{-1}$, at high concentrations of methyl acetate in the feed. However, the highest separation factor values were observed at lower methyl acetate concentrations in the feed (up to 2.1), as result of the mutual contribution of the two components fluxes-driving forces ratios. Furthermore, the PVDF membrane applied in this work has an outstanding flux compared to commercial membranes used in similar applications. The separation performance is still object of further

research in order to increase the selectivity for methyl acetate. This work has presented the first steps to the synthesis of novel PVDF membranes for the separation of ester/alcohol mixtures.

From the temperature effect analysis it resulted that up to 80 mole% methyl acetate, dissolution of the two organic solvents into the membrane is driving the pervaporative separation mechanism. This is in agreement with the general theory applied to polymeric membranes in rubbery state (Bell et al., 1988), and with the results of the Hansen Solubility Parameters analysis, which suggested the potential of PVDF for pervaporation of methyl acetate/methanol binary mixtures. However, the same assessment failed in describing the PVDF membrane affinity and pervaporation ability related to the components of the quaternary equimolar methyl acetate/methanol/*n*-butyl acetate/*n*-butanol mixture, used as reference, suggesting that the HSPs method is not suitable in order to be used in a rubbery membrane screening step, in the context of pervaporation of alcohol/esters mixtures.

Chapter 4

OVERCOMING ANY CONFIGURATION LIMITATION: AN ALTERNATIVE OPERATING MODE FOR PERVAPORATION AND VAPOUR PERMEATION

Adapted from: Genduso, G., Luis, P. and Van der Bruggen, B. (2015), Overcoming any configuration limitation: an alternative operating mode for pervaporation and vapour permeation. J. Chem. Technol. Biotechnol.. doi: 10.1002/jctb.4661

4.1. Introduction

In the previous chapter, the ability of Hansen Solubility Parameters theory in selecting a polymeric material for membrane synthesis, in the context of the pervaporative separation of methyl acetate/methanol mixtures, was assessed. In this study, it was also found that the PVDF membranes have the potential to selectively pervaporate methyl acetate; however, the industrial application of this membrane material is linked to a process of improvement of the separation performance.

The selection, synthesis and improvement of a membrane for a particular separation can require a large effort. In this chapter, a particular operating mode for pervaporation is assessed: the "*multi-stage-batch-pervaporation*" (MSBP), thought to be independent from modules configuration and membrane performances. The MSBP unit, simulated in this chapter, is a simplified version of Baker *et al.*'s apparatus (Baker et al., 1993) and it is made of three tanks. The simulations help revealing the

influence of different "*stage-termination conditions*" on the products quality and separation performance. In particular, as an example, two new stage-terminations, (1) at a fixed stage-recovery of the component enriched in the permeate and (2) at fixed retentate product purity, are discussed in Section 4.2 and 4.3, respectively. In Section 4.4, a new way of representing pervaporation membrane performances is shown, with the intent of introducing a new tool that may be applied in substitution of the PSI parameter analysis during selection of pervaporation membranes for a particular separation.

4.2. Stage-termination at a fixed stage-recovery of the component enriched in the permeate

Table 10 reports the number of stages, the $BPTI_{rec,98}^{MM20}$ (see definition Chapter 2, Section 2.3.2) and the final amount of permeate as a fraction of the initial feed, obtained by varying the stage-recovery of the component enriched in the permeate, *i.e.*, the stage-termination condition for the separation of the MM20 stream. Moreover, Figure 22a shows the permeate product final purity and Figure 22b the retentate product final purity as a function of the stage-recovery of the component enriched in the permeate.

From a theoretical point of view, all the membranes included in Figure 6 would be able to yield a permeate with the specified concentration. However, during intermediate stages, all the membranes that lead to very low separation performances consume almost all the feed in order to satisfy the stage-termination condition and the purity requirement for the permeate product, *i.e.*, the process-termination condition. This results

in very low permeate product amounts. Thus, in this case a non-feasible application is obtained. This is the case for the PolyAl TypM1 and the PVDF membranes, which were not able to reach the required specification, *i.e.* stage-recovery of the component enriched in the permeate of 0.3, 0.6, 0.75 or 0.9 together with 98 mole% purity for the permeate product; therefore, these simulation results are not reported in Table 10 and Figure 22. The same situation was found for the Pervap 2255-40, Pervap 2255-50 and Cuprophan membranes when setting a stage-recovery of the component enriched in the permeate of 0.3, as can be noticed looking at the final permeate/initial feed amount ratio in Table 10. These data are also not reported in Figure 22.

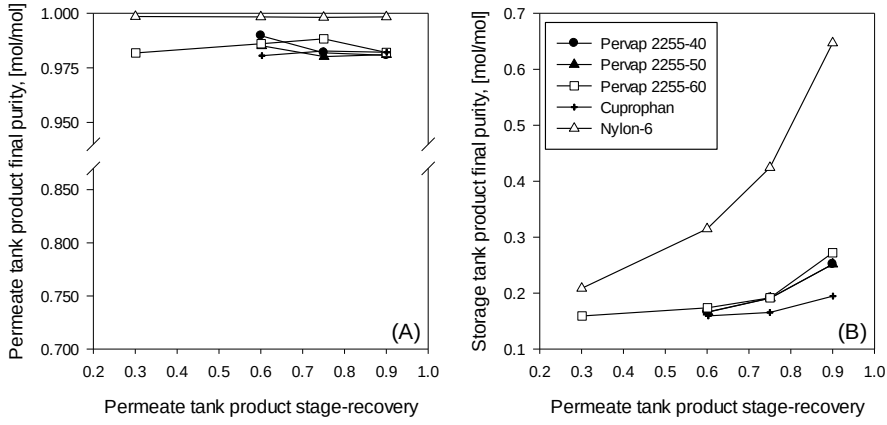

Figure 22. Purity of permeate (a) and retentate (b) products against variation in stage-recovery of the component selective for membrane (stop condition for each MSBP simulation). The data for PVDF and PolyAl TypM1 are not represented since the two membranes were not able to yield a separation.

Table 10 and Figure 22a show how high performance membranes, such as nylon-6, ensure a high permeate product purity (> 98 mole%) together with a high final permeate/initial feed amount ratio.

Table 10. Number of stages, BPTI and percentage of permeate product over initial feed amount for all simulated separations at different stage-recoveries of the component enriched in the permeate.

Membrane	No. stages	$BPTI_{rec,98}^{MM20}$	% of the total initial feed in the permeate tank at end of the process	Permeate-product stage recovery
Pervap 2255-40	4	1.80	0.70	0.3
	5	5.73	6.65	0.6
	5	9.48	20.44	0.75
	7	19.39	41.17	0.9
Pervap 2255-50	4	4.29	0.71	0.3
	5	13.60	6.71	0.6
	5	22.41	20.47	0.75
	7	45.51	41.17	0.9
Pervap 2255-60	3	6.74	2.34	0.3
	4	20.47	11.11	0.6
	5	35.22	20.29	0.75
	6	65.37	45.69	0.9
nylon-6	1	0.74	25.39	0.3
	1	1.57	50.73	0.6
	1	2.05	63.42	0.75
	1	2.58	76.09	0.9
Cuprophan	4	4.01	0.00	0.3
	7	12.68	2.43	0.6
	9	22.84	6.48	0.75
	13	51.14	21.90	0.9

In contrast, membranes with a medium separation performance, *i.e.*, Pervap 2255-40, Pervap 2255-50, Pervap 2255-60, and Cuprophan membranes, allow a smaller volume of permeate product with a high

purity and a higher retentate product amount with a lower purity to be obtained.

Figure 22b indicates that for low stage-recoveries, only membranes with high separation factors are able to ensure retentate products with sufficient purity. Moreover, it also indicates that for very high stage-recoveries it is also possible to obtain pure retentate products. In fact, in Figure 22b, a power-like trend can be observed for the curve concentration of the component enriched in the retentate vs. stage-recovery of the component enriched in the permeate.

4.3. Stage-termination at fixed retentate product purity

To obtain both products at the desired purity, each stage can be ended once a constant purity for the retentate product is reached, *i.e.*, the stage-termination mode described using Figure 11b in Chapter 2. In this case, Figure 23a and b show the variation of permeate product purity and total recovery of the component enriched in the retentate with the number of batch-stages, respectively. Figure 23c shows the relation between the number of stages and time expressed in the BPTI form. Table 11 shows the time expressed in the BPTI form and the number of stages needed to obtain both products with a purity of 98 mole%.

Theoretically, with a MSBP unit working at constant retentate product purity in the stage-termination condition, all membranes would be able to give both products at high purity; however, in practice the PolyAl TypM1, PVDF and Pervap 2255-40 membranes were not able to ensure the specification for the permeate product (*i.e.*, 98 mole% purity) even

after 1000 batch stages. This is indicated with the infinity (∞) symbol in the $BPTI_{98}^{MM20}$ row of Table 11.

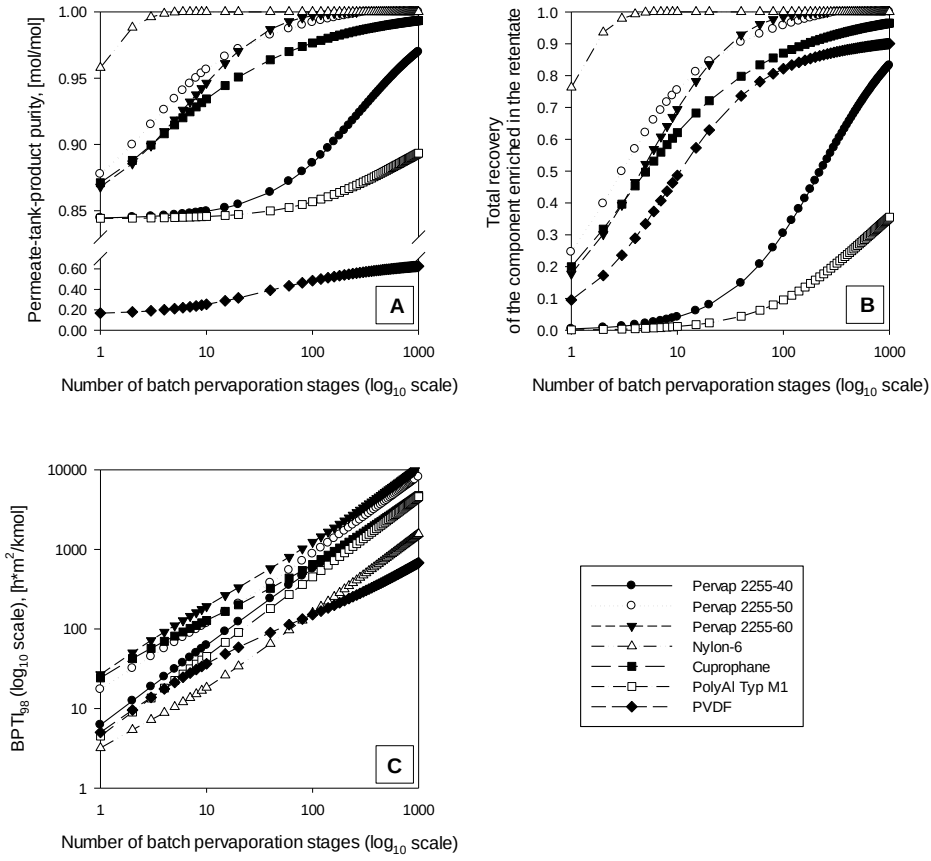

Figure 23. Variation of purity of the permeate product (a), total-recovery of the component enriched in the retentate (b) and pervaporation cumulative time (c) with the variation of the number of batch-stages for all the membranes treated in this work (with the only exception of the Pervap 2255-30 membrane) for a temperature of 40-45 °C (depending on the membrane).

Table 11. Number of stages, $BPTI_{98}^{MM20}$ and product recoveries estimated when both products reach a purity of 98 mole%.

Membrane	Nr. stages	$BPTI_{98}^{MM20}$	Retentate product recovery (methyl acetate basis)	Permeate product recovery (methanol basis)
Pervap 2255-40	>1000	∞	-	-
Pervap 2255-50	40	379	0.90	~1.00
Pervap 2255-60	40	575	0.93	~1.00
nylon-6	2	5	0.94	~1.00
Cuprophan	140	845	0.89	~1.00
PolyAl TypM1	>1000	∞	-	-
PVDF	>1000	∞	-	-

It has to be pointed out that the time depends on the membrane area and the initial amount of mixture in the feed tank (as seen from Equation 18 and Equation 19). The higher the membrane area, for fixed initial feed amounts, the shorter is the stage-time. Thus, membranes requiring a high number of stages to obtain the required purities may need a reasonable time to complete the separation, when an appropriate (even large) membrane area is used with an automatic system of valves and pumps needed to pass from one stage to the following one.

4.4. Batch pervaporation membrane performance representation (a new way)

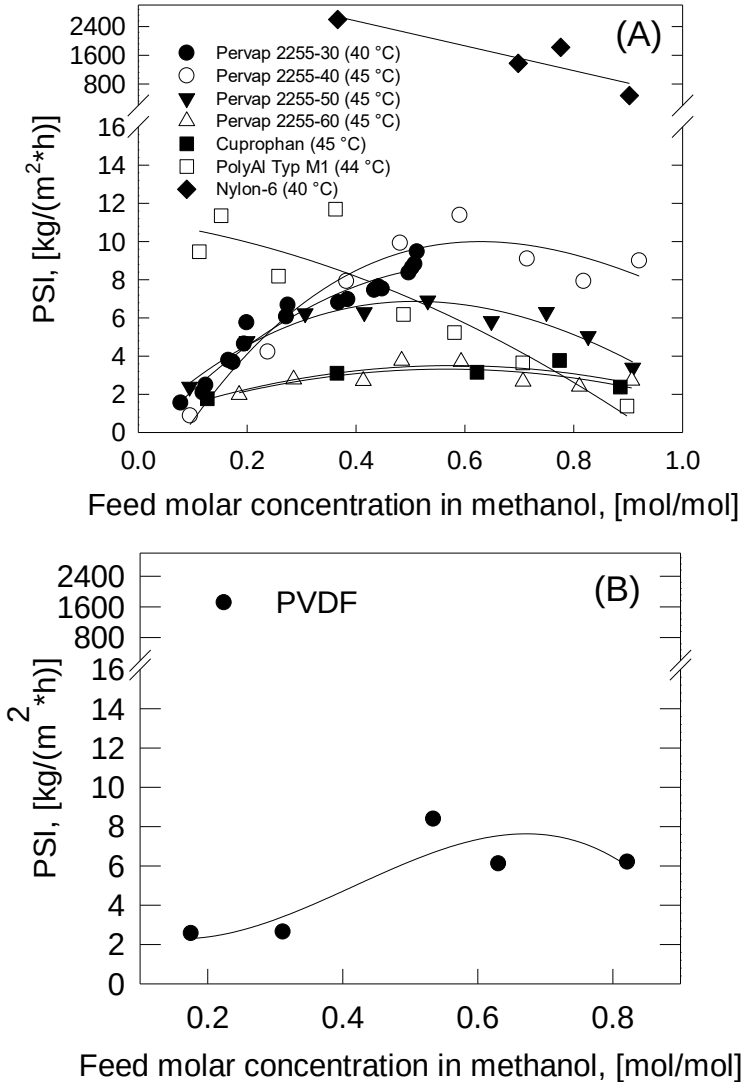

Figure 24. In (a) pervaporation separation indexes (PSI) values of all the commercial membranes reported in literature (Gorri et al., 2006, Sain et al., 1998, Steinigeweg and Gmehling, 2004, Abdallah et al., 2013); In (b) the PSI analysis for the only methyl acetate selective membrane (i.e., the PVDF membrane). Polynomial fitting curves are also shown in the figure as a guide to the eye.

Generally, during the selection of the right membrane for a batch pervaporation separation, the PSI analysis is often taken as a reference.

For the particular mixture presented in this text, the PSI analysis is shown in Figure 24a-b. If for example the feed mixture has a composition of 50 mole% in the feed, the membrane ranking in order of decreasing separation performance is:

Nylon-6 >> Pervap 2255-40 > PolyAl TypM1 ≈ Pervap 2255-50 > PVDF > Pervap 2255-60 ≈ Cuprophan

Ranking 1

However, for concentrations higher or lower than 50 mole% in the feed, the position of each membrane in the ranking may change completely. In particular from low to medium feed concentrations in the component selective for the membrane, which is the optimal range from an energetic point of view since the component selective for the membrane is present in a lower amount, the PSI analysis suggests the selection of nylon-6 membranes or PolyAl TypM1 membranes. Instead, when considering the medium-high feed concentration range, the best choices would be nylon-6 or Pervap 2255-40 membranes.

A different result is obtained when representing the normalized permeate product purity, obtained after a single stage, as a function of the $BPTI^{0}_{98}$, *i.e.*, the batch pervaporation time index obtained when (i) the feed tank product reaches a purity of 98 mole% and (ii) starting from a feed concentration of 50 mole% in the component selective for the membrane. This *batch pervaporation-membrane performance graph* is shown in Figure 25. In this case, when giving priority to the separation

ability of the membrane together with the contribution of the driving force, the following ranking is obtained:

Nylon-6 > Pervap 2255-50 ≈ Cuprophan > Pervap 2255-60 > PolyAl TypM1 > Pervap 2255-40 ≈ PVDF

Ranking 2

When giving priority to the BPTI, *i.e.*, the time to reach a desired separation:

Nylon-6 ≈ PVDF > PolyAl TypM1 > Pervap 2255-50 > Pervap 2255-60 > Cuprophan > Pervap 2255-40

Ranking 3

However, the latter ranking is not preferable since membranes that give very low permeate purity during each stage, tend to consume all the feed to respect the imposed conditions on permeate or component enriched in the retentate purity, making the separation unfeasible.

Thus, looking at Ranking 2 it can be noted that nylon-6 and Pervap 2255-50 membranes have top positions and should be selected for the separation. Conversely, PVDF, PolyAl TypM1, and Pervap 2255-40 membranes should be discarded. This outcome is perfectly consistent with the simulation data previously discussed, where PVDF, PolyAl TypM1, and Pervap 2255-40 membranes were not able to ensure any product specification even after a very high number of batch-stages, (Section 4.3) or gave a very poor separation performance (see Section 4.2) and nylon-6 and Pervap 2255-50 membranes gave the best performance.

This analysis demonstrates the inability of the PSI analysis to provide insights for membrane selection procedure for batch pervaporation applications when medium-low separation factor membranes are compared. In fact apart from the nylon-6 membrane, a very high performance membrane, the PSI analysis favours Pervap 2255-40 and PolyAl TypM1 membranes which instead come out as the worst choice during *batch pervaporation-membrane performance graph* analysis and MSBP simulations.

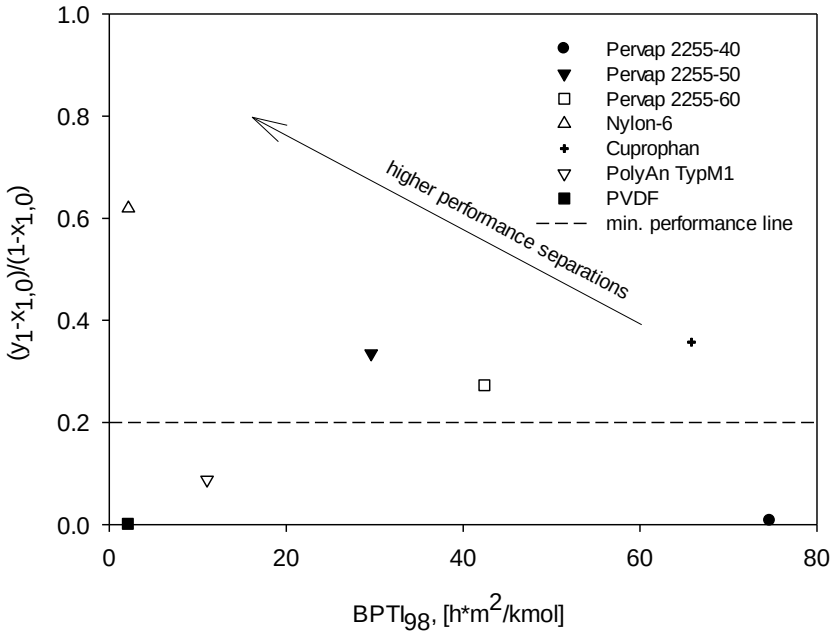

Figure 25. The batch pervaporation-membrane performance graph. In this graph the subscript '1' indicates the component selective for the membrane (e.g., for the PVDF membrane it is methyl acetate) that is the component enriched in the permeate.

In the *batch pervaporation-membrane performance graph,* it is possible to roughly draw a line that separates very low performance pervaporation membranes from the rest (dashed line of Figure 25) for a normalized

permeate concentration of 0.2; membranes that lie below this line should not be used during a real MSBP separation that requires high purity products.

Finally, it has also to be stressed that in certain cases, *i.e.*, for concentrations above 50 mole% in the component selective for the membrane, a more accurate prediction can be obtained when estimating the *batch pervaporation-membrane performance graph* starting from these actual feed concentrations, as shown in the case of the MM20 stream concentration.

4.5. Conclusions

In conclusion, when pursuing an MSBP separation it is possible to overcome the limitation due to the use of a condenser after each stage, necessary when enriching permeate streams by conventional pervaporation. In MSBP, the product purity is increased by recycling the condensed permeate to the feed tank. This means that just one condenser is needed for the unit. Moreover, theoretically this unit operation is also able to overcome any membrane limitation since the separation performance of the membrane is bypassed by increasing the number of MSBP stages, as any membrane is able to give permeates and retentates with high purities. However, from a practical point of view it was demonstrated that membranes with very low pervaporation ability tend to consume all the feed in order to reach the required product purity.

Medium performance membranes gave permeate and retentate products with high purity when terminating each stage at a constant value of retentate product purity. On the other hand, in this case the number of

stages can be very high. This number can be decreased significantly when working at constant stage-recovery of the component enriched in the permeate. However in this case, for stage-recoveries of the component enriched in the permeate that are not very high, the purity of the retentate product is limited by the membrane separation ability.

It is important to note that these two operational modes can be further elaborated to fit any specific product requirement. Furthermore, the storage tank can be connected to a secondary system of separation that helps reducing the concentration of the component selective for the membrane, even during MSBP operation. In the MSBP proposed in this work a *static* storage vessel was used.

In this chapter it is also shown how, apart from consideration of very high performance membranes, the PSI analysis gave an incorrect prediction of the membrane performance during the MSBP process with two of the three best membrane choices actually performing worst in the simulations. A new and more accurate performance analysis was proposed, based on the *batch pervaporation-membrane performance graph*. In this case the permeate product purity is shown as a function of a time index, the BPTI (defined independent from initial amount of the feed and membrane area), needed to obtain a retentate product with certain specification by a single pervaporation stage. In this way a complete description of the membrane ability during pervaporation is given.

What has been shown in this chapter may lead to some interesting conclusions about the applicability of MSBP units. An MSBP unit could be the natural substitute of all stand-alone batch distillation processes, in

particular for azeotropic mixtures. Moreover, the removal of bottlenecks in batch pervaporation separations could also be another application.

Production of pharmaceuticals and in general all small batch productions could benefit from the use of an MSBP unit, even with the use of medium-low performance pervaporation membranes.

Finally, treatment of small fractions of continuous productions could also be suitable for MSBP systems.

Chapter 5

RETROFITTING OF EXTRACTIVE DISTILLATION COLUMNS WITH HIGH FLUX, LOW SEPARATION FACTOR MEMBRANES: A WAY TO REDUCE THE ENERGY DEMAND?

Adapted from: G. Genduso, A. Amelio, E. Colombini, P. Luis, J. Degrève, B. Van der Bruggen, Retrofitting of extractive distillation columns with high flux, low separation factor membranes: A way to reduce the energy demand? Chemical Engineering Research and Design, Volume 109, May 2016, Pages 127-140, http://dx.doi.org/10.1016/j.cherd.2016.01.013.

5.1. Introduction

Pre-concentration of the MM20 stream can be obtained via conventional advanced distillation methods (*e.g.* extractive distillation). The same separation may be also pursued: (i) via pervaporation with an improved version of the polyvinylidene fluoride membrane (Chapter 3) or (ii) via MSBP, in the case in which the process is carried out in batch (Chapter 4).

Another interesting case can be explored. In a polyvinyl alcohol plant, methyl acetate contained in the MM20 waste is usually converted into acetic acid by reaction with water. However, *n*-butyl acetate has a much higher market price than acetic acid: 2.00 $/kg against the 0.50 $/kg for acetic acid during late 2012 in USA (Tecnon-OrbiChem, 1 November 2013a, Lane, 2013). Therefore, the modification of the process, from MM20 to acetic acid into MM20 to *n*-butyl acetate, may be an interesting opportunity.

In the context of the MM20 to acetic acid conversion, the pre-concentration step to higher methyl acetate reagent concentrations is normally pursued via extractive distillation with water. As described in the following text of this chapter, the resulting methyl acetate head product contains a non-negligible amount of water. Water is the second reagent during acetic acid production but it is not necessary in the *n*-butyl acetate production. In view of modifying the plant in order to produce *n*-butyl acetate instead of acetic acid, the retrofitting of this type of extractive distillation units is assessed in this chapter. Retrofitting via the insertion of a pervaporation module may allow reducing the energy consumption of the system, producing a methyl acetate reagent stream lacking of water since no solvent extractor is needed anymore.

In this chapter, Section 5.2 and 5.3 are dedicated to the description of the PolyAl TypM1 membrane performance, also in comparison with the literature of other commercial membranes. Then, respectively in Section 5.4 and 5.5, the design of the methanol/methyl acetate extractive distillation unit fed with water and its retrofitting with the PolyAl TypM1 membrane, are discussed. Finally, in Sections 5.6 and 5.7, the retrofitting is judged both from a hydraulic and energetic point of view, in order to explore the real potential of this operation.

5.2. Methyl acetate/methanol pervaporative separation using the PolyAl TypM1 membrane

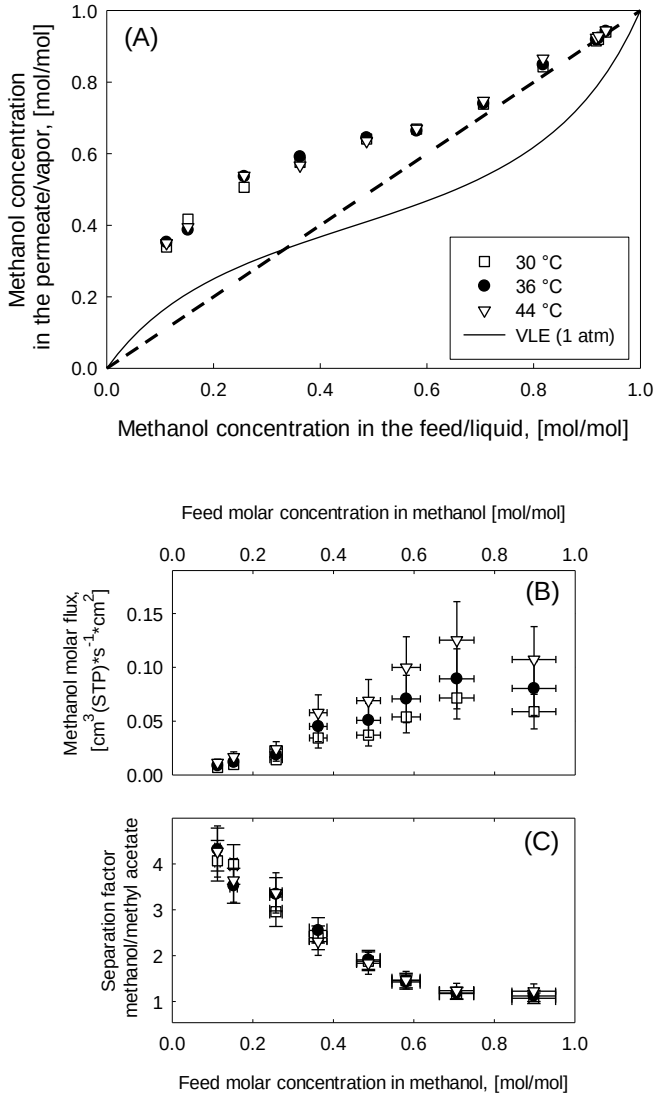

*Figure 26. (a) PolyAl TypM1 permeate-feed data at 30 and 36 and 44 °C, together with the vapour-liquid equilibrium (VLE) curve obtained using the UNIQUAC property method. (b) methanol molar flux and (c) separation factor variation with feed molar concentration in methanol basis. In this figure the molar flux is given in [cm³(STP)/(s*cm²)] and can be converted into weight flux [kg/(m²*h)] employing the factor (3600/100)*PMᵢ/v_i^G.*

Figure 26a compares vapour-liquid equilibrium data with the composition of the feed and permeate; Figure 26b and c show the corresponding variation of the methanol flux and the methanol/methyl acetate separation factor. For feed concentrations close to the azeotropic composition the membrane offers an alternative, as the permeate composition differs from the feed composition. The highest separation factor value registered is about 4, in the lower range of methanol feed concentrations. For increasing methanol feed concentrations, the separation factor decreases; the variation of temperature did not have any influence on the separation factor. The methanol molar flux (Figure 26b) increases to a maximum at about 70 mole% methanol in the feed, and then decreases again. As can be expected, the temperature has a positive effect on the methanol flux.

Figure 27a-b shows total molar fluxes and methanol/methyl acetate selectivity for the pervaporation temperatures of 30, 36 and 44 °C. Similarly to Figure 26b, in Figure 27a a maximum trend can be observed. When the total flux has the maximum (at about 70 mole% methanol in the feed), the methanol/methyl acetate selectivity (Figure 27b) is still confined in a plateau region. The membrane recovers its methanol selectivity for low concentrations in methyl acetate in the feed mixture. This may suggest that swelling associated to methyl acetate presence is detrimental for the separation performance of the membrane. Figure 27c-d illustrates the variation of *i*-component permeance with feed molar concentration in methanol. The decreased selectivity due to membrane swelling can also explain why methanol and methyl acetate permeances have a similar trend, although in a different range of permeances: the

methanol permeance is almost 3 times higher than the methyl acetate permeance.

In addition to these figures it is also shown how temperature has a positive effect on total flux and a negative effect on selectivity, as expected from the free volume theory (Mulder, 1998).

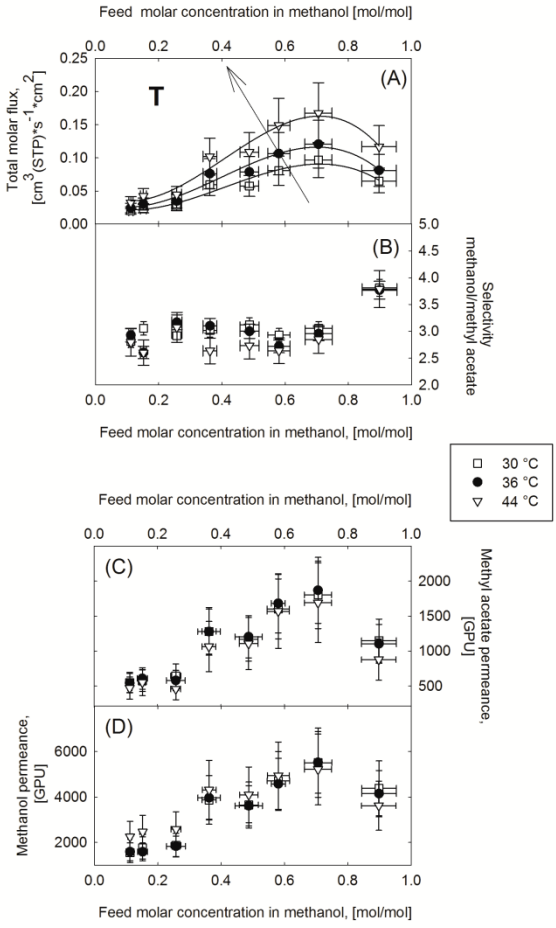

Figure 27. For all the three temperatures explored, in (a) the total, methyl acetate and methanol molar fluxes variation and (b) selectivity methanol/methyl acetate variation with methanol feed molar concentration. In (c) methyl acetate and (d) methanol permeance variation with feed molar concentration are shown, respectively.

5.3. Comparison with other membranes reported in the literature

In this section, the PolyAl TypM1 membrane is compared with other commercial membranes reported in the literature, for the range of pervaporation temperature of 40-45 °C. The purpose is to select a commercial membrane ready to be used during an industrial retrofitting. To do so, Figure 6 (Chapter 1) and Figure 24 (Chapter 4) are needed. From Figure 6c it can be seen that for almost the entire feed concentration range, the PolyAl TypM1 membrane has separation factors lower than the other membranes. Figure 6a shows that the PolyAl TypM1 and Pervap 2255-40 commercial membranes have the highest total fluxes.

Figure 24a shows that PolyAl TypM1 and Pervap 2255-40 and 2255-30 are the commercial membranes with the highest PSI at the azeotropic composition. However, the PSI parameter gives the same weight to membranes of high selectivity and low flux and membranes of low selectivity and high flux. This means that membranes with poor separation ability can have the highest PSI, as for example the PolyAl TypM1 for the separation here under examination.

However, for the purpose of this study (*i.e.*, to simulate the worst retrofitting possibility in term of energy consumption), having the highest flux and moderate separation factor, the PolyAl TypM1 was used for the retrofitting simulations discussed in the next sections.

5.4. Iterative procedures for the design of the extractive distillation unit

Figure 28 contains the iterative procedure followed during the design of the extractive distillation unit, together with the reproduction of Figure 13a (*i.e.*, the extractive distillation flow scheme).

Figure 29a-d show column 1 head concentration vs. reflux ratio at fixed number of stages (*i.e.*, for the five numbers of stage arbitrary chosen, N_1=15;26;39;52;75), created in order to analyze the separation behaviour of column 1 of the extractive distillation unit. These five graphs can be obtained using the Sensitivity Analysis tool of Aspen Plus. In practice, as also shown in the left side of the iterative procedure (Figure 28), for each value of N_1, RR_1 is varied in order to obtain the concentration of the distillate of column 1 (x_{D1}). During this procedure, the solvent to feed flow ratio serves as parameter [m=0.3;1;2;3;4, chosen following information from literature (Finch, 1973, Langston et al., 2005)]. It is important to note that during iterations on loop 1 and 2, Nf_1 and Ns vary in order to minimize column 1 reboiler duty, meaning that two different couples of RR_1 and N_1 can have different values of Nf_1 and Ns. In each of the five graphs of Figure 29a-d (*i.e.*, for each the five chosen values of N_1), it is possible to find the minimum value of RR_1 (RR^m_1) that allows to respect the limit condition x_{D1}=94.4 mole% methyl acetate. The exact value of RR^m_1 was estimated using the DesignSpec tool of Aspen Plus. Figure 29f contains all estimated couples RR^m_1-N_1, with the exception of the data at m=0.3 and for m=1 at 26 stages, for which Aspen simulations did not respect column 1 distillate purity condition of 94.4 mole% methyl acetate (see Figure 29a-d).

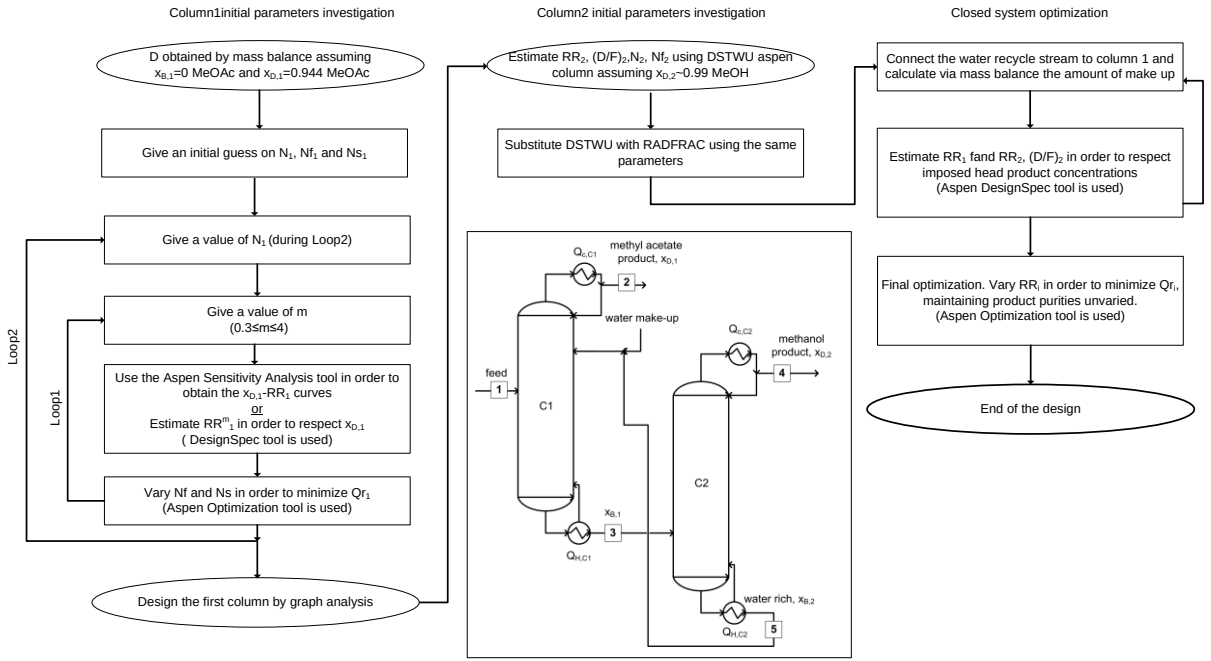

Figure 28. Sequential procedure employed during column 1 and column 2 designs. The solvent to feed ratio varied in the range 0.3≤m≤4, as reported in literature (Finch, 1973, Langston et al., 2005). Concentrations are in mole basis. Figure 13a is also reproduced in this iterative scheme of the extractive distillation unit design.

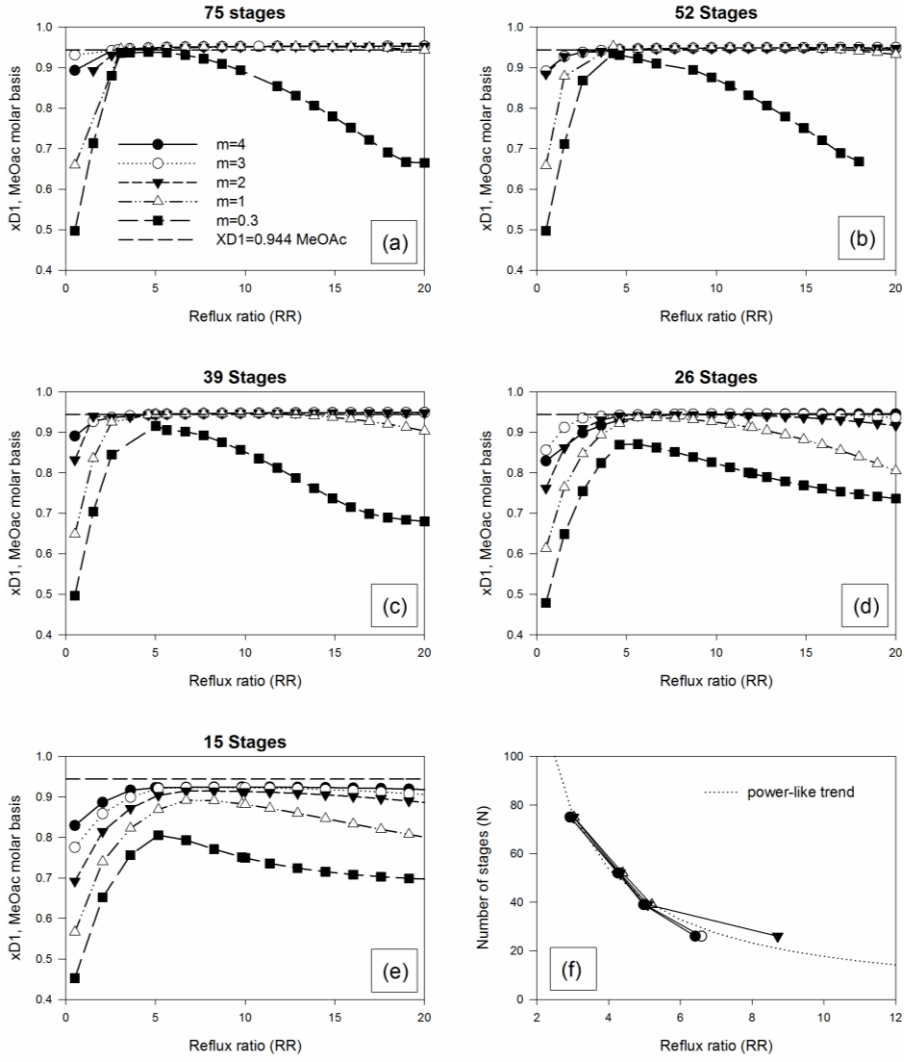

Figure 29. From (a) to (e), column 1 distillate purity (x_{D1}) vs. reflux ratio at constant number of stages (i.e., N_1=15;26;39;52;75) and using the solvent to feed flow ratio as parameter [m=0.3(■);1(◊);2(▼);3(○);4(●)]. Based on these five graphs and on the limit condition on the methyl acetate head product (i.e., x_{D1}=94.4 mole%), in (f) it is represented the variation of number of stages with reflux ratio for all solvent-feed amount ratios (an average power like trend was also included to drive reader's eyes).

The neck of the curves of Figure 29f reveals the best operative condition in terms of reflux ratio, solvent-feed ratio and number of stages (Pribic et al., 2006, Amelio et al., 2015). Considering a safe value of 1.5 times the

minimum solvent-feed ratio (*i.e.*, m=1), in order to answer to possible process variations, the following optimal values were chosen for column 1 of the extractive distillation system: N_1=39, m=1.5 and, RR_1=5.3 (this last value is still an initial guess since the reflux ratio of column 1 undergoes variation in the following steps of this procedure).

Subsequently, once the initial design parameters of column 2 were obtained, as described in the central part of Figure 28, the optimization of the overall system was possible (right side of Figure 28), leading to the final design specifications of column 1 and 2. These are reported in Section 5.6.

The extractive distillation unit design procedure, just described, differs from what can be found in the literature (Wankat, 2006, de Figueirêdo et al., 2011, Wang et al., 2012, Langston et al., 2005, Brüggemann and Marquardt, 2004) since it is based on the graph: number of stages vs. reflux ratio (*i.e.*, Figure 29f). This graph is the result of the initial part of the design procedure and permits to define a unit with minimized investment costs (selecting lower N_1) or minimized operating costs (selecting lower $RR^m{}_1$).

5.5. Iterative procedures for the retrofitted unit design

The retrofitted unit was designed using the procedure of Figure 30 (where the flow scheme of the retrofitted unit of Figure 13b can also be found). As can be noticed in Figure 30, the iterative procedure is initiated without considering internal recycles streams (*i.e.*, from the head of column 2 to the module and from the module to column 1). This open-recycle phase is necessary in order to provide all initial values used during the optimization of the closed-recycle system.

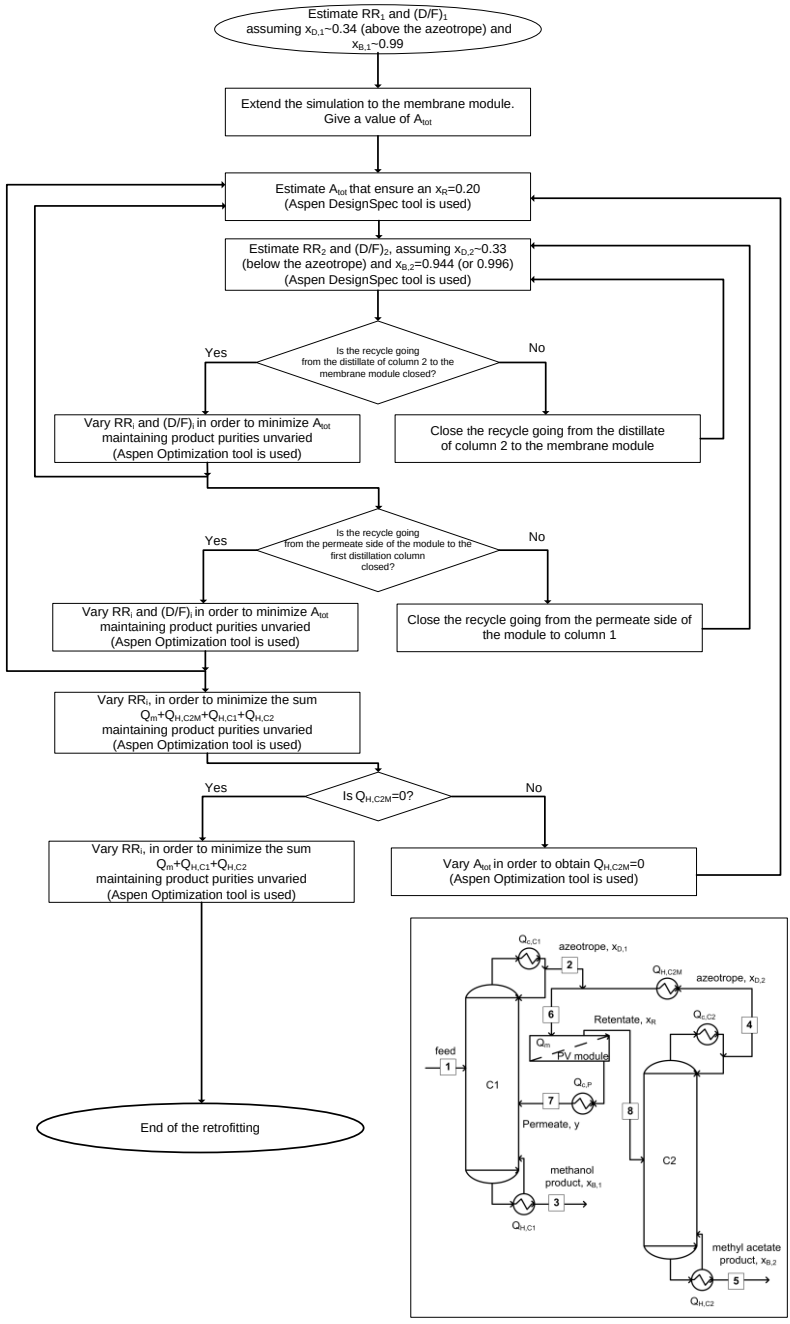

Figure 30. Sequential procedure employed during retrofitting. Concentrations are in methanol mole basis with the exception of $x_{B,2}$ given in methyl acetate mole basis. Figure 13b is also reproduced in this iterative scheme of retrofitting.

In the third step of this iterative procedure of retrofitting, the retentate concentration is set to a value of 20 mole% methanol. However, with the iteration steps that follow, this concentration varies in order to respect imposed product purities and in order to minimize membrane area and energy requirements of all heating utilities.

5.6. Outcomes of the design of the methanol/methyl acetate extractive distillation and the corresponding retrofitted systems

Table 12. Design specifications of the extractive distillation system and the hybrid system (this last both in the retrofitted and optimal design variation).

	Extractive distillation system		**Retrofitted hybrid case, 94.4mole%**		**Retrofitted hybrid case, 99.6mole%**	
	Col.1	Col.2	Col.1	Col.2	Col.1	Col.2
N_i	39	22	39	22	39	22
Nf_i	35	14	35	19	35	19
Ns or Np	18	-	10	-	10	-
RR_i	5.14	1.33	1.11	2.22	1.62	8.19
M	1.5	-	-	-	-	-
$(D/F)_i$	0.16	0.42	0.45	0.42	0.51	0.24
Memb. Area [m^2]	-	-	758		1433	

The design specifications of the extractive distillation system and the retrofitted system, are reported in Table 12. All compositions, flow rates and temperatures of the streams of Figure 13, are shown in Table 13.

Figure 31 reports feeds, permeate, retentate, head and bottom outlets concentrations in the McCabe-Thiele diagram at 1 atm, for the retrofitting case ensuring a methyl acetate product of 94.4 mole%. Table 13 and Figure 31 show how the pervaporation module permits to bypass the azeotrope.

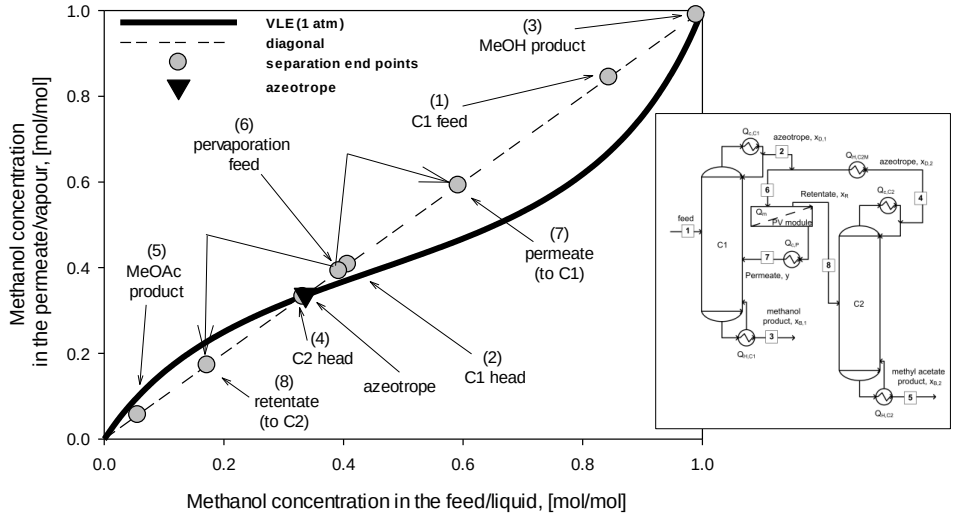

Figure 31. McCabe-Thiele diagram (VLE at 1 atm) with feeds, permeate, retentate, head and bottom outlets concentrations for the retrofitting case ensuring a methyl acetate product of 94.4 mole%. The numbers under brackets refer to the streams of the retrofitted unit flow scheme, also reproduced (from Figure 13b) on the right side of the graph.

As can be noted from Table 12, an increase of 5% purity of the methyl acetate outlet stream produces quite an increase of the membrane area; this is due to the fact that now all methyl acetate entering with the main feed stream, needs be recovered in the retentate of the module and sent to column 2. For the retrofitting case ensuring a methyl acetate product of 99.6 mole%, the area required is equal to the area of an ideal module made of 12 stacks (all in parallel) each composed of 6 spiral wound tubes (in parallel) of 20 m^2 of area each (which is a common value for commercial spiral wound membrane tubes). In addition, it has to be taken into account that membranes of higher separation factor would require a drastically lower membrane area for the same separation.

Table 13. Stream purities, flow rates and temperatures obtained from the three simulations described in this chapter (each stream position can be found in Figure 13).

Stream number	**1**	**2**	**3**	**4**	**5**	**6**	**7**	**8**
Ext. Dist. 94.4% methyl acetate	Feed	methyl acetate product		methanol product				
Mole Frac								
Methanol	0.844	0	0.412	0.988	0	-	-	-
methyl acetate	0.156	0.944	0.001	0.002	0	-	-	-
Water	0	0.056	0.587	0.010	1	-	-	-
Total Flow kmol/s	0.129	0.021	0.264	0.110	0.154	-	-	-
Total Flow kg/s	4.978	1.494	6.295	3.524	2.771	-	-	-
Temperature [°C]	25.0	57.0	75.2	64.6	100.0	-	-	-
Hyb. 94.4% methyl acetate	Feed		methanol product		methyl acetate product			
Mole Frac								
Methanol	0.844	0.407	0.990	0.332	0.056	0.392	0.592	0.172
methyl acetate	0.156	0.593	0.010	0.668	0.944	0.608	0.408	0.828
Total Flow kmol/s	0.129	0.059	0.109	0.015	0.020	0.073	0.038	0.035
Total Flow kg/s	4.978	3.334	3.532	0.877	1.446	4.211	1.889	2.322
Temperature [°C]	25.0	53.5	63.9	53.4	55.5	53.4	47.0	47.0
Hyb. 99.6% methyl acetate	Feed		methanol product		methyl acetate product			
Mole Frac								
Methanol	0.844	0.356	0.996	0.333	0.004	0.355	0.505	0.050
methyl acetate	0.156	0.644	0.004	0.667	0.996	0.645	0.495	0.950
Total Flow kmol/h	0.129	0.066	0.109	11.531	0.020	0.070	0.047	0.023
Total Flow kg/s	4.978	3.927	3.517	0.192	1.460	4.119	2.467	1.653
Temperature [°C]	25.0	53.4	64.3	53.4	56.9	53.4	41.4	41.4

5.7. Columns hydraulic after retrofitting

In case the purpose is the retrofitting of an acetic acid, *n*-butyl acetate or ethyl acetate production line, the case of retrofitting that ensures pure methyl acetate (99.6% methyl acetate) should be the reference for the hydraulic comparison with the original extractive system, since methanol is an unwanted compound. For the two studied cases of retrofitting (*i.e.*, 94.4 mole% and 99.6 mole% methyl acetate product), Figure 32 shows the volumetric flow rates profiles for column 1 and column 2 of the extractive distillation unit. As can be noticed, in the two cases of retrofitting, the volumetric flow rate profiles of vapour inside column 1 are of the same order of magnitude but higher than in the extractive distillation case. As a result, column 1 flooding is possible, above all for the 99.6 mole% methyl acetate product case. This may be the major problem of this retrofitting operation. A solution might be the substitution of column 1 plates with a packing material that allows a higher flooding limit or in the worst case the replacement of column 1. It is, however, important to understand that the use of membranes with a higher separation factor would solve all main hydraulic problems of the column 1. A higher membrane selectivity reduces the permeate flow sent back to column 1, lowering column 1 hold up and reducing the risk of flooding.

Furthermore, the vapour flow rate of column 2 is much lower than in the extractive distillation case, leading to potential problems of weeping. The solution of this side effect of the retrofitting is the modification of plate holes diameter or the use of valve type trays (Sinnott, 1999).

Moreover, the liquid flow rate of both columns resulted to be scaled down in both cases of retrofitting. The residence time could not be

verified after retrofitting, which may affect the plate efficiency (Sinnott, 1999). This could lead to the replacement of all trays with a structured packing, or even increasing the number of stages of the column.

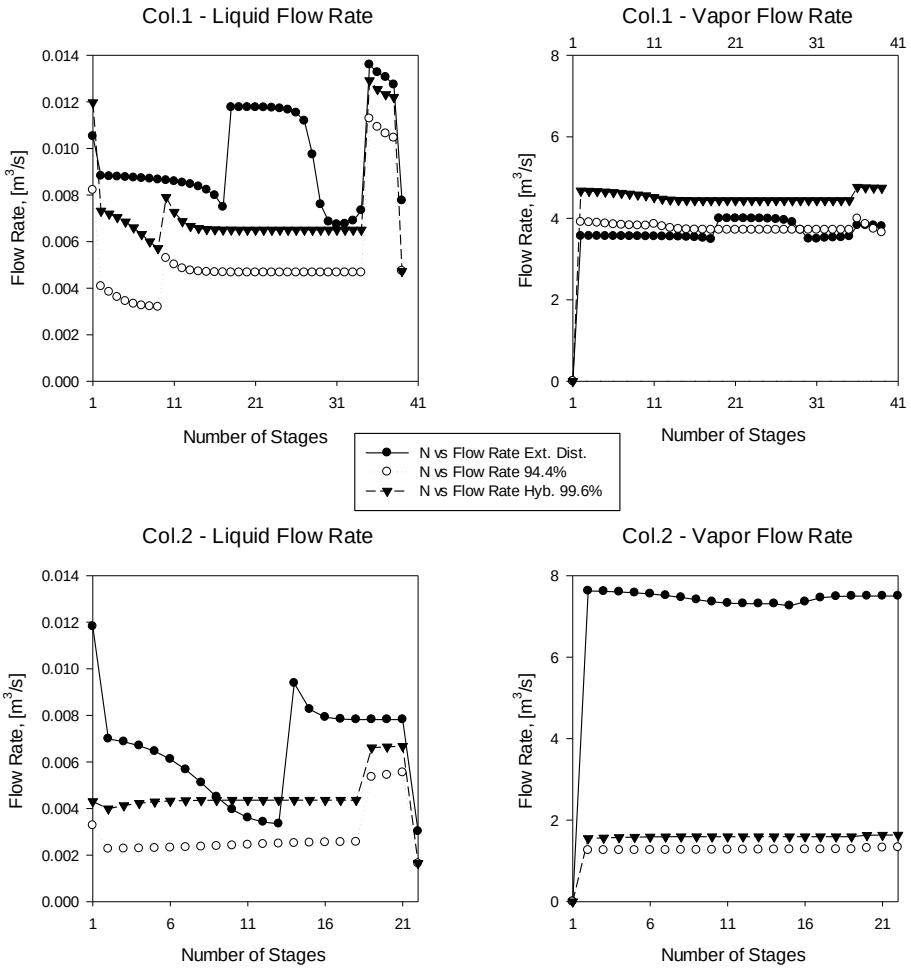

Figure 32. Liquid and vapour volumetric flow rates profiles for column 1 and column 2 of the extractive distillation unit and the two studied cases of retrofitting.

5.8. Energetic analysis

From an energetic point of view, the comparison between the extractive distillation system and its retrofitting should be done on the basis of an equal methyl acetate product concentration, *i.e.*, the retrofitting giving 94.4 mole% methyl acetate product. Table 14 reports all power requirements of all utilities (both cooling and heating) of the three simulated cases. As can be observed the retrofitting permits a consistent reduction of energy consumption; for example, retrofitting the extractive distillation system maintaining the same methyl acetate product, for the heating utilities the reduction of energy is ~23% (about ~38% considering also the cold utilities). Even when retrofitting toward 99.6% methyl acetate product, it is possible to obtain an overall power reduction of ~10%.

It has to be emphasised that a vapour permeation module would be preferable in order to take advantage of the enthalpy of the vapour phase exiting column 1. Hence, the energy requirement of the retrofitted units are overestimated, proving even more the supremacy of the hybrid system over the extractive system from an energetic point of view.

In this context it is also important to stress that both the extractive distillation and the retrofitted system were designed on the basis of a similar optimization of the energy required in the heating utilities. This procedure was chosen in order to prove the concept. However, when this type of retrofitting is applied, a profitability analysis-design should take into account the effect of the energy consumption of the condenser of the pervaporation module. This is even more important when organic compounds of high volatility are permeated, since sub-zero temperatures may be required during condensation.

Table 14. Comparison of power requirement for all heating and cooling utilities. The sum is calculated using the absolute value of each entry.

Utility	Extractive	Hybrid 94,4%	Hybrid 99,6%	
$Q_{H,C1}$	4.01E+06	4.51E+06	6.02E+06	[W]
$Q_{H,C2}$	9.33E+06	5.97E+05	1.84E+06	[W]
$Q_{C,C1}$	-3.93E+06	-3.93E+06	-5.55E+06	[W]
$Q_{C,C2}$	-8.92E+06	-5.66E+05	-1.81E+06	[W]
$Q_{H,C2M}$	0	0	0	[W]
Qm	0	5.15E+06	6.79E+06	[W]
$Q_{C,P}$	0	-1.45E+06	-1.52E+06	[W]
Sum (abs.)	2.62E+07	1.62E+07 (**-38%**)	2.35E+07 (**-10%**)	[W]
sum Hot	1.33E+07	1.03E+07 (**-23%**)	1.46E+07 (**+10%**)	[W]
sum cold	-1.29E+07	-5.95E+06 (**-54%**)	-8.88E+06 (**-31%**)	[W]

5.9. Conclusions

In this chapter, computer assisted simulations of a chosen industrial case of extractive distillation of methanol/methyl acetate azeotropic waste mixtures, were reported. A new, energy optimized, graphic-assisted iterative procedure of design of extractive distillation systems was successfully used. The first investigation of retrofitting of extractive distillation units by a pervaporation module was described in two cases: the first, maintaining the value of methyl acetate product concentration of the extractive distillation system and the second obtaining almost pure methyl acetate.

The commercial PolyAl TypM1 membrane used during retrofitting simulation was found to have the highest separation factor methanol/methyl acetate (up to about 4.3) in the middle-low range of methanol feed concentrations. The highest total flux (11.5 $kg*m^{-2}*h^{-1}$) was registered at about 71 mole% methanol in the feed and 44 °C.

This membrane was chosen for retrofitting by comparison with other membranes reported in the literature. As resulted from this comparison, at the methanol/methyl acetate azeotropic composition (at 1 atm), the PolyAl TypM1 showed the highest flux and medium low separation factor values. This corresponds to a very challenging condition of retrofitting from an energetic and hydraulic point of view.

The retrofitting operation resulted to be successful from an energetic point of view, estimating an overall energy saving up to 38% (23% when considering only the heating utilities). These savings can be substantially increased using a vapour permeation module instead of pervaporation.

From a hydraulic point of view, due to the variation of the vapour flow rate after retrofitting, weeping in column 2 and flooding in column 1 could be encountered. If tray weeping can be avoided by a simple modification of plate holes, column 1 flooding could lead to major structural changes of the unit. However the use of column packings and pervaporation/vapour permeation membranes with a high separation factor (in order to reduce column 1 hold up) could be beneficial and reduce the number of column 1 modifications.

In addition, after retrofitting the liquid flow rates in column 1 and 2 were lower; this may not verify the required residence time for the liquid. In this case the solution may be the replacement of the plates by a structured packing.

In conclusion, once a suitable pervaporation (vapour permeation) membrane is developed on a commercial scale for the separation of a mixture of organics, even if the membrane has medium/low separation factors, it would be viable from an energetic point of view to retrofit an

existing extractive distillation unit, making the use of any solvent unnecessary. However, from a hydraulic point of view, the use of higher separation factor membranes would reduce column modifications after retrofitting.

Chapter 6

TECHNO-ECONOMICAL ASSESSMENT OF A PERVAPORATION BASED PRODUCTION OF *N*-BUTYL ACETATE FROM A METHYL ACETATE WASTE STREAM: A COMPARISON WITH OTHER CONVENTIONAL PROCESSES

Adapted from: Genduso G., Luis, P. and Van der Bruggen, B., Techno-economical assessment of a pervaporation based production of *n*-butyl acetate from methyl acetate waste streams, (submitted for publication).

6.1. Introduction

In Chapters 3, 4 and 5, different ways to address the MM20 stream concentration issue were discussed. In particular, in Chapter 3 this stream was separated using the first methyl acetate selective membrane; a procedure for membrane selection was also assessed in this chapter. Separation of the same binary mixture was discussed in Chapter 4 using a batch pervaporation methodology meant to be independent from membrane performance and unit configuration. Then, in Chapter 5 the retrofitting of an extractive distillation unit, used in order to concentrate the MM20 waste into high purity methyl acetate reagent stream, was discussed.

Apart from the concentration of the MM20 stream, the scope of this thesis is also to propose an alternative to the MM20 to the acetic acid conversion process. This is done in Chapter 6, where the conversion of a

methyl acetate/methanol stream into *n*-butyl acetate using pervaporation-based process flow schemes, is considered. In particular, Section 6.2 offers a short review on commercial and laboratory-synthesized membranes that could be used during the design of pervaporation-based MM20 to *n*-butyl acetate process flow schemes. Assuming an appropriate methanol and methyl acetate membrane, in Section 6.3, the simulation of three pervaporation-based schemes is discussed. In the same section, the results of these simulations are energetically compared with two distillation-based flow schemes simulated by Luyben et al. (2004) introduced in Section 1.7 (Chapter 1). In order to be coherent with the choices made by Luyben et al. (2004), the inlet stream is the MM80 stream (*i.e.*, 60 mole% methyl acetate in methanol) and the output products have a purity of 99 mole%. Of the three PV-based flow schemes, proposed in Chapter 6, the system being able to combine high energy saving and process flow scheme simplicity, is selected for heat integration, which is discussed in Section 6.4. In Section 6.5, the same PV-based flow scheme, this time fed with the MM20 stream, is analyzed from a profitability point of view in order to evaluate the real potential of the MM20 to *n*-butyl acetate conversion process.

6.2. A discussion on the membranes assumed: the nylon-6 membrane case

For the simulations discussed in this chapter a methanol and a methyl acetate selective membrane, were assumed. Both these membranes have a total flux typical for methyl acetate/methanol pervaporations (see Figure 15 in Chapter 2). Moreover, a separation factor high enough to obtain a product 99 mole% as permeate was assumed. To date, there are no methyl acetate selective membranes with such features. On the other

hand, looking at Figure 6 (which summarizes the literature of pervaporation of methyl acetate/methanol mixtures), the nylon-6 membrane seems to be applicable for the separation of methanol from methyl acetate. In Appendix I, pervaporation of methanol from the quaternary transesterification mixture composed of methanol/methyl acetate/*n*-butanol/*n*-butyl acetate, for many of the membranes encountered in this thesis and summarized in Figure 6, is reported. It can be noticed that the nylon-6 membrane gave a quite low separation factor (*i.e.*, 3.15). For the purposes of the chapter the nylon-6 membrane is therefore of no use.

The discrepancy in performance of the nylon-6 membrane, during pervaporations of the binary and quaternary mixture, may be attributed to swelling provoked by contact with *n*-butanol or *n*-butyl acetate compounds. Further research is needed in order to confirm this hypothesis.

6.3. Simulation of the three pervaporation-based flow schemes and energetic comparison with the literature

Figure 33a shows the variation of the methanol, methyl acetate, *n*-butanol and *n*-butyl acetate permeance with the concentration in methanol in the retentate at 40 °C, for type-1 total flux trend and data reported in Figure 15. Since the methanol permeance is one order of magnitude higher than the permeance of the other components, it can be concluded that the membrane is highly selective for methanol. For the same membrane, it can be noted in Figure 33c that the permeance of each component decreases with increasing permeation temperature.

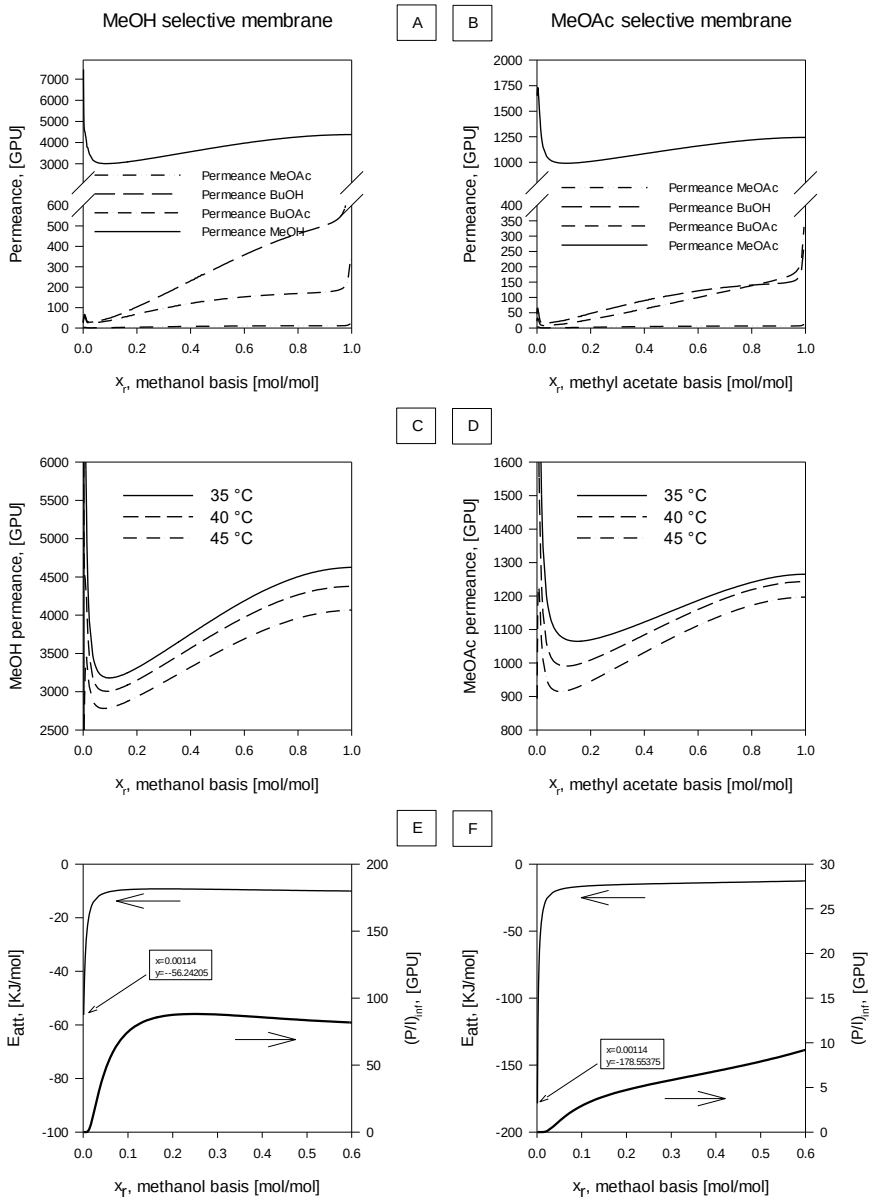

Figure 33. For the type-1 total flux trend, in (a) and (b) components permeance variation with retentate concentration of the component selective for the membrane, in the case of methanol and methyl acetate selective membrane, respectively, at 40 °C. In (c) and (d) variation of methanol or methyl acetate permeance (respectively) with retentate concentration of the component selective for the membrane at three temperatures of 35, 40 and 45 °C. In (e) and (f), activation energy and permeance at infinite temperature for the methanol selective membrane and methyl acetate selective membrane, respectively. In all graphs, data are calculated on the base of the four components transesterification mixture.

Similar conclusions arise from the analysis of component permeances data of the methyl acetate selective membrane, as shown in Figure 33b and Figure 33d.

For the two membranes, Figure 33e-f reports the variation of permeation activation energy and permeance at infinite temperature with the retentate concentration of the component selective for the membrane. These trends are used in the pervaporation model with Equations 28-29.

Similar figures can be obtained for methanol and methyl acetate membranes characterized by a type-2 total flux trend (not shown).

In Figure 34, the three block flow pervaporation-based schemes developed in this study to obtain both methanol and methyl acetate products at the same concentration of 99 mole%, are shown. For each block flow scheme output and inputs are independent of the total flux trend (type-1 or type-2), since for equal separation factors the separation outcome does not depend on the total flux trend. The first pervaporation-based system (SIM1), shown in Figure 34a, is made of a reactor, two pervaporation modules and a support *n*-butanol/butyl acetate column. In order to increase the conversion in the reactor and reduce the system-hold up (due to the presence of unwanted methanol), a pre-concentration step has been considered in both SIM2 and SIM3 (Figure 34b and Figure 34c, respectively). In first instance, a pressure swing system was used (SIM2), then substituted in SIM3 by a methanol selective membrane module that requires >90% less energy from the utilities (both cold and hot). Figure 35a-c demonstrates that SIM3 is the best option from an energetic point of view. At the same time, SIM3 suffers from the higher number of stacks (and re-heaters), in comparison with the SIM1 case, due to the use of the pre-concentration module0. Thus, even if the membrane

area requirement is very similar for both SIM1 and SIM3, there is quite a gap of complexity between the two options.

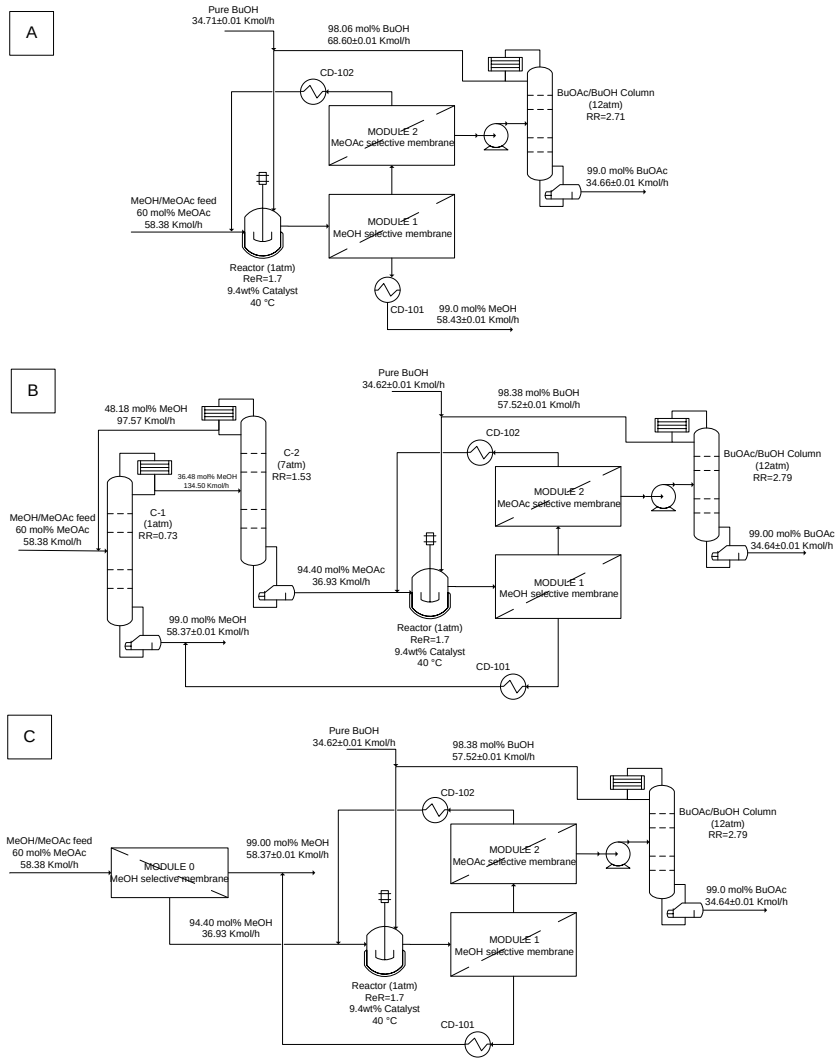

	Membrane Area MODULE nr.0	Membrane Area MODULE nr.1	Membrane Area MODULE nr.2	TOT Area	Nr. Stacks MODULE nr.0	Nr. Stacks MODULE nr.1	Nr. Stacks MODULE nr.2	Nr. Tubes MODULE nr.0	Nr. Tubes MODULE nr.1	Nr. Tubes MODULE nr.2
	[m*m]	[m*m]		[m*m]						
SIM1_Mx_40	-	3.81E+03	3.06E+03	6.87E+03	0	10	5	-	196	156
SIM2_Mx_40	-	2.99E+03	2.96E+03	5.95E+03	0	8	4	-	153	150
SIM3_Mx_40	8.21E+02	2.99E+03	2.96E+03	6.77E+03	16	8	4	51	153	150

Figure 34.In (a) the block flow diagram of the first pervaporation-based system (SIM1). In (b) the block flow diagram of the second pervaporation-based system (SIM2). In (c) the block flow diagram of the third pervaporation-based system (SIM3).

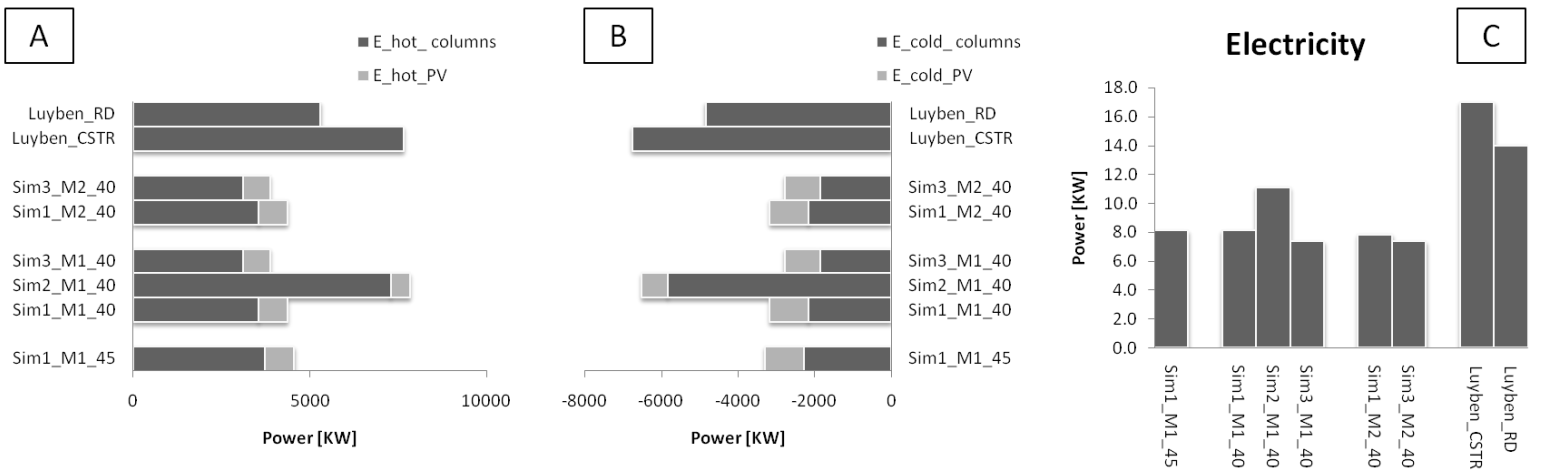

Figure 35. (a) heating utility energy requirement, (b) cooling utility energy requirement and electric energy requirement for three pervaporation-based systems and the two process units studied by Luyben et al. (2004). For each data label, SIMx refers to the flow scheme simulated (see Figure 34), M1 or M2 refer to the total flux trend-type and the last number (i.e., 40 or 45) to the reaction temperature assumed.

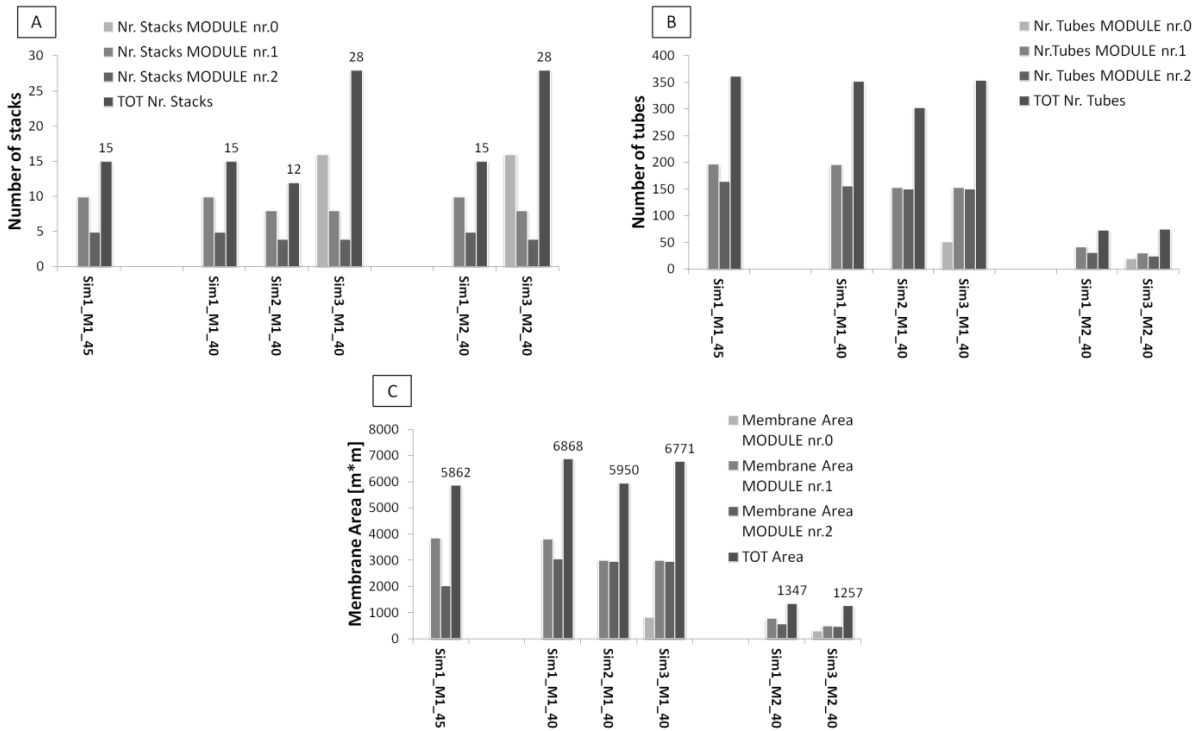

Figure 36. The number of stacks (a), number of tubes (b) and membrane area (c) for each module of the three pervaporation-based systems discussed in this work.

In Figure 35 and Figure 36, the comparison between SIM1_M1_40 (*i.e.*, SIM1 with type-1 membrane trend and reaction temperature of 40°C) and SIM1_M1_45 is made. For the same system an increase of the reaction temperature from 40 to 45°C yields a slight increase of the overall energy duty and a considerable decrease of the membrane area requirement (about 1000 m^2).

In Figure 35 and Figure 36 two other cases are presented as well: SIM1_M2_40 and SIM3_M2_40 based on type-2 total flux trend to be compared with the respective simulations based on type-1 total flux trend (*i.e.,* SIM1_M1_40 and SIM3_M1_40). If the energy requirements remain the same, a methanol or methyl acetate selective membrane with type-2 (flat) total flux permits a tremendous reduction of the membrane area requirement. Figure 37a and b can be used to understand how the total flux trend (and not the average total flux value) can drastically affect the membrane area. In fact, Figure 37a reports the example of module1 of SIM3 in both cases of total flux trend type-1 and 2. For a decreasing concentration of methanol in the retentate (methanol is in this case the component selective for the membrane), the membrane area requirement in the stack increases exponentially for trend type-1 and remains unvaried for trend type-2. Figure 37b clarifies this, showing the PSI behaviour in both cases. For low concentrations of the component selective for the membrane in the retentate, in the case of a type-1 trend, the PSI starts decreasing already for concentrations where the PSI for a type-2 trend is still increasing. This directly affects the membrane area requirement since for the same concentration a membrane with a lower PSI requires a higher membrane area to achieve the same separation. In addition, from Figure 37b a powerful field of application for the PSI parameter is noticed. The inability of the PSI parameter in determining

the right membrane for a certain separation has already been demonstrated in Chapter 4 and 5. However, from the analysis made in Figure 37b it results that the PSI parameter is a powerful tool to be used in order to map the separation performance within a determinate separation (even along a module). For example, for the membrane with total flux trend type-2, this analysis shows how the membrane has a PV-performance that increases with decreasing concentrations in the component selective for the membrane.

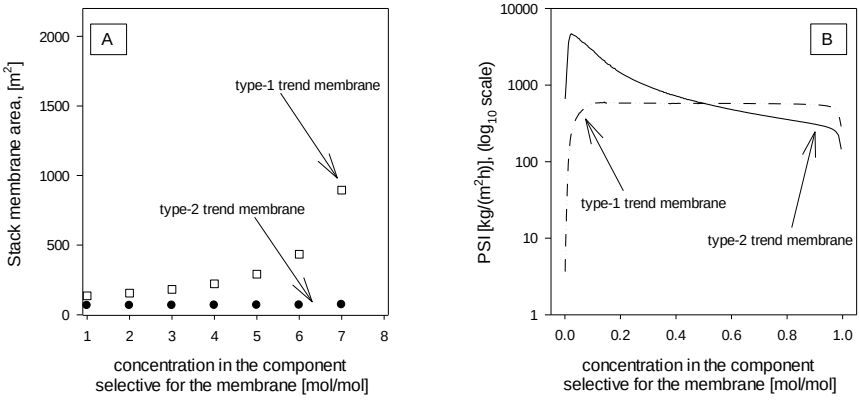

Figure 37. In (a) the stack membrane area variation for module1 of SIM3 employing both membrane-type 1 and membrane-type 2. In (b) PSI variation with retentate concentration in the component selective for the membrane using both membrane types.

6.4. Energetic integration of the chosen PV-based system

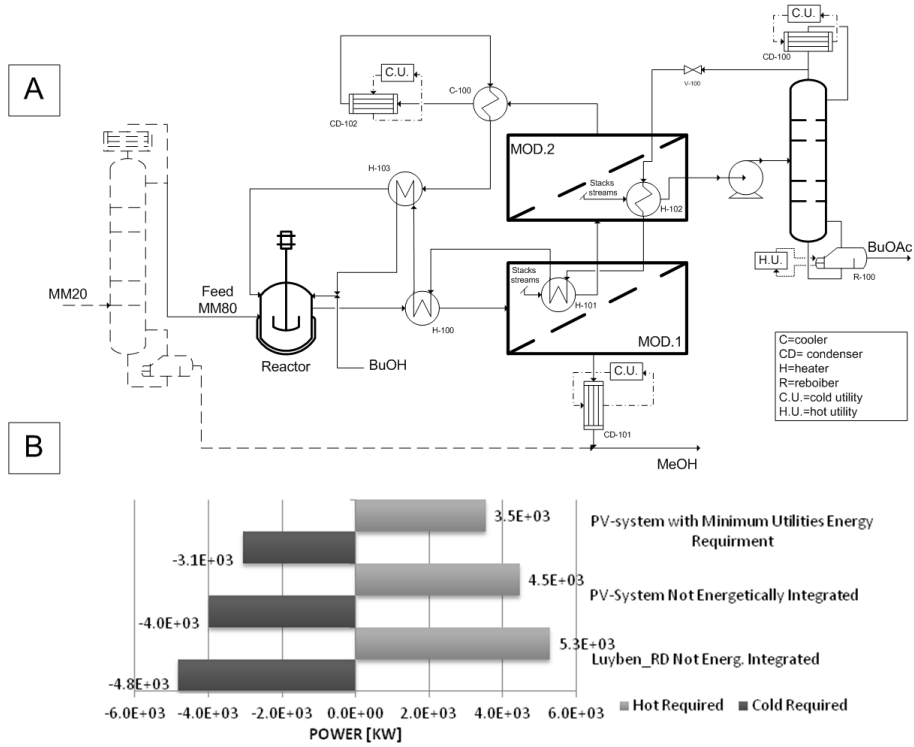

Figure 38. (a) energetically integrated system that requires the minimum energy from the utilities (dashed units and stream-lines were not taken into account during heat integration). (b) comparison between the minimum energy, the original energy requirements for SIM1 and the energy required by the Luyben_RD system (Figure 8b, Chapter 1).

Even if SIM3 resulted to be the best option from an energetic point of view, considering that the difference with SIM1 is low both from an energetic and a membrane area point of view and taking into account that SIM3 requires a re-heating system, a condensation system and 13 stacks more than SIM1, it was not considered for further heat integration. The heat integrated scheme of SIM1 system is presented in Figure 38a (dashed units and dashed stream-lines were not taken into account during this heat integration; their function is clarified in the Economic Analysis section). The heat transported by the distillate of the *n*-

butanol/butyl acetate column is used to heat up all inter-stacks streams of module1 and 2 (this system of heat exchangers is indicated with H-101 and H-102) and pre-heat the feed of module1 to 45 °C. This distillate stream is finally cooled down to 40°C by the condensed permeate of module2. From this heat integration it was found that it was possible to reduce the utility energy load of about 1000 kW both for the hot and cold utility (Figure 38b).

6.5. Economic Analysis

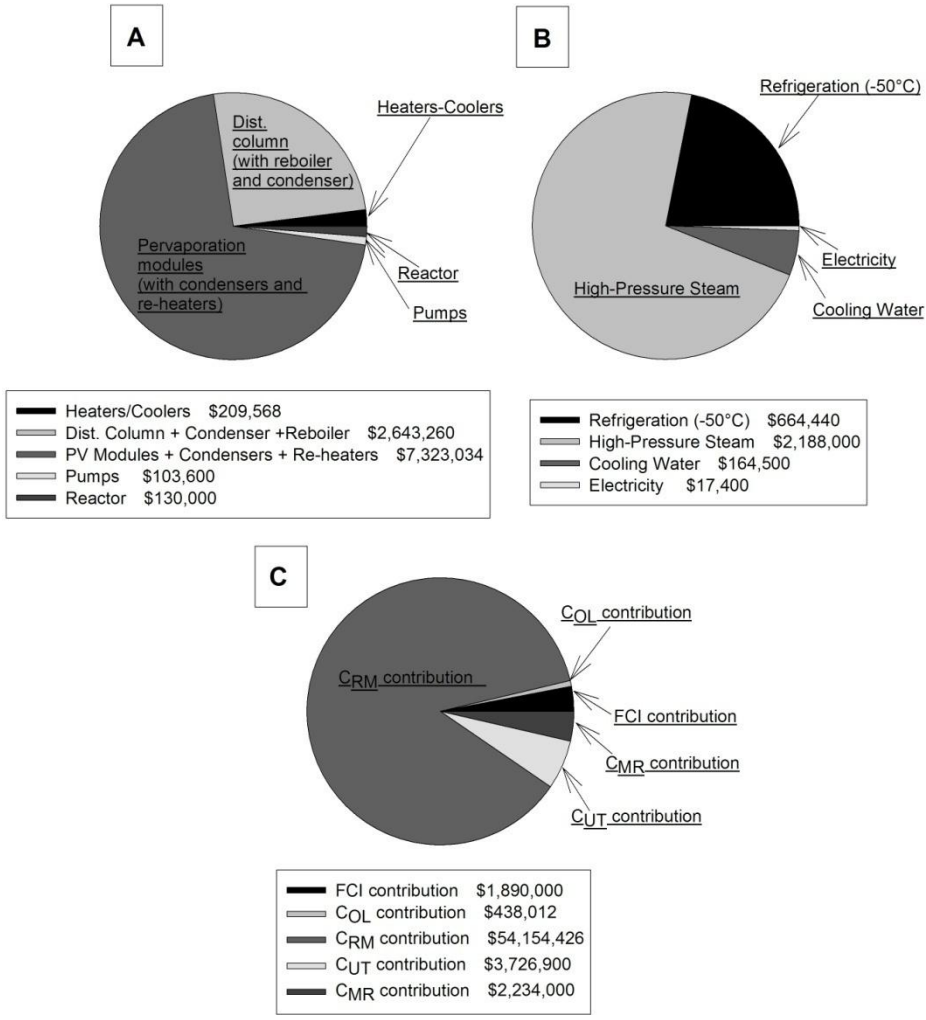

Figure 39. In (a) total module costs, (b) utility costs and (c) the COM of the pervaporation-based plant (heat integrated SIM1) for the case of expansion of a existing plant, employment of the MM80 waste mixture and cost of membrane of 275 $/m². More details about COM contributions can be found in Equation 34 and Equation 35.

The flow rate of the stream entering module1 is very high (~12800 kg/h); using typical feed spacers [d_h<1.4 mm, (Schock and Miquel, 1987)] the pressure drop becomes unrealistic. Hence, in order to estimate the pressure drop in each module and the energy consumptions of the feed

pump (to be inserted in CAPCOST), tailored values of hydraulic diameters were used. In any case, even overestimating feed pumps costs and energy consumption costs (which is the case in this work), this contribution resulted to be very small when compared to other costs. Figure 39a, b and c shows three pie diagrams for total module cost, utility cost and cost of operations, respectively, in the case in which the system treating the MM80 waste stream (C_{MM80}=0) is built as an expansion of an existing plant (FCI=C_{TM}) and the membrane cost is of 275 \$/m^2 [slightly higher than typical values of membrane cost reported in the literature (O'Brien et al., 2000, Oliveira et al., 2001)]. In this case, the main contributions to plant costs are given by pervaporation modules and the distillation column (Figure 39a); high pressure steam and refrigeration costs are the main contributions to the utility costs (Figure 39b). Furthermore, Figure 39c shows how the cost of operations is almost completely dominated by the cost of raw materials (C_{RM}=C_{BuOH}). This means that the ratio between the two reagents (in this work chosen very high, *i.e.*, 1.7 BuOH/MeOAc molar ratio) sent to the reactor, can strongly affect the profitability of this process.

Finally, the economic analysis was extended to the case in which the feed of the system has the MM20 composition. To do so, the MM20 distillation column (dashed in Figure 38a) was rigorously designed (RADFRAC column simulations in Aspen Plus v7.3) in order to obtain from the top the MM80 stream already discussed in this chapter and from the bottom 99 mole% pure MeOH (sold to the market). For this analysis, an expansion of an existing plant (FCI=C_{TM}) and C_{MM20}=0 (waste mixture) was assumed. As can be noticed from Figure 39a and b, even for very high values of membrane cost the process that starts from MM20 waste and yields 99 mole% pure *n*-butyl acetate is very profitable. In the same

images, the profitability varies in a fashion that strongly depends from the membrane total flux trend.

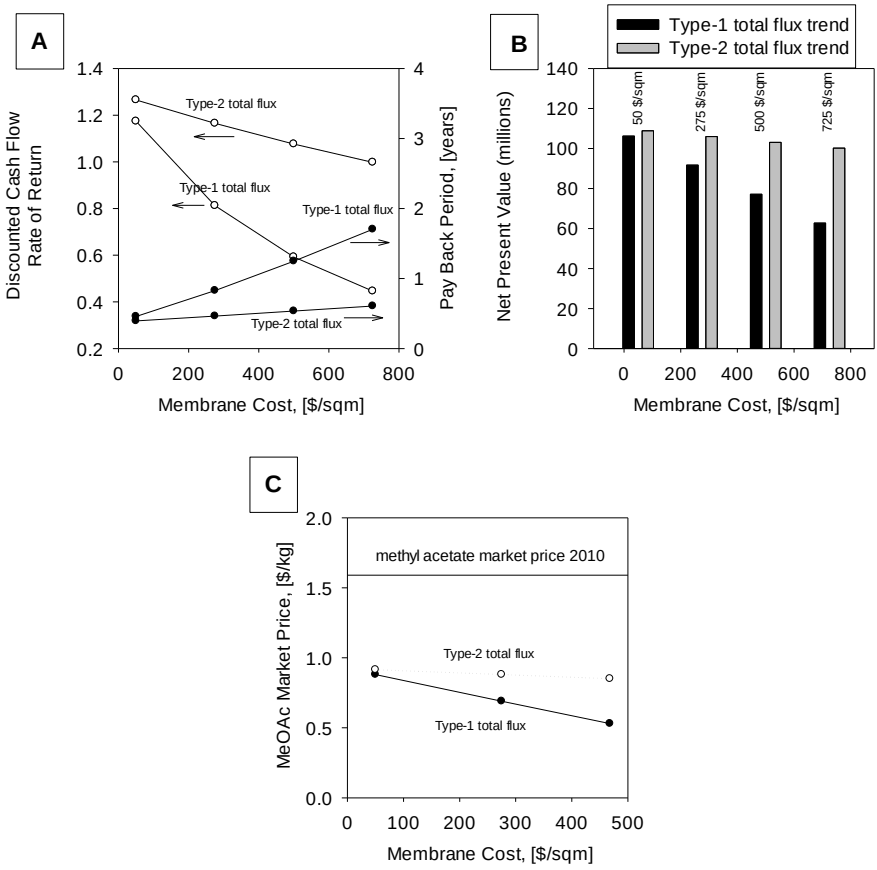

Figure 40. For the case of expansion of an existing plant, employment of the MM20 waste mixture and variable membrane cost, the DCFROR/PBP and the NPV variations are shown in (a) and (b), respectively. In (c), for fixed DCFROR=15%, the price of MeOAc fed to the plant shown in Figure 38a and comprising of the MM20 distillation column; the plant is considered to be built from scratch (FCI=C_{GR}).

On the other hand, the same plant fed with market-origin MeOAc is not profitable. In fact, Figure 39c shows how expensive should MeOAc be in order to build the plant from scratch (FCI=C_{GR}) and obtain a DCFROR of 15% (*i.e.*, the minimum value used in industry to discern between projects with good or bad profitability). In this condition, the price of

MeOAc is calculated to be 31% lower than the MeOAc-market price during 2010 (Haro et al., 2013). In order words, the project is only profitable if the plant is fed with an inexpensive waste stream (*e.g.*, the MM20 stream).

6.6. Conclusions

In this chapter, pervaporation is proven to be a very low energy consumption technology for specific applications: it was estimated that in order to perform the same methanol/methyl acetate separation pervaporation requires over 90% less energy to the utilities in comparison with distillation.

For membranes with similar separation factors, it was also demonstrated how the design of pervaporation modules mainly depends on the total flux trend. In particular, for similar average values of total flux (in the entire feed concentration range), membranes that present a higher total flux for lower concentrations in the component selective for the membrane, require a lower total area, a lower number of stacks and a lower plant complexity in order to perform the same separation. In addition, for membranes with similar separation factors the PSI parameter can be used in order to map the separation behaviour of each membrane along the module and better design the PV system (this suggests a proper way of using this performance indicator).

Among the three pervaporation-based flow schemes initially proposed, the design chosen (*i.e.*, the design in which the reactor precedes the PV-modules) to be heat integrated and analyzed by profitability analysis resulted to require 18, 15 and 42% less hot utility, cold utility energy and electrical energy, respectively, than the best conventional system based

on distillation technology. Moreover, after heat integration it was possible to ensure a further ~22% energy saving for hot and cold utilities.

The profitability analysis of the heat integrated system fed with a waste stream of 60 mole% methyl acetate in methanol (MM80 stream), showed how for PV-based plants the total module is strongly dependent on the membrane cost. The cost of refrigeration can have a large impact on the cost of utilities. Moreover, the cost of raw materials (*i.e.*, *n*-butanol) dominates the cost of manufacturing suggesting that the reagent ratio needs to be taken in opportune account during the design procedure of this process.

Finally, it was demonstrated how a process using the MM20 waste stream is very profitable even for membrane costs higher than 700 $\$/m^2$ (DCFROR always >20% and very short payback periods). This means that once a membrane of good performance exists the conversion by PV-based systems is a very remunerative investment for any MM20 stream producer such as the polyvinyl alcohol industry.

On the other hand, the same PV-based system employing market-origin methyl acetate and built from scratch is not profitable.

Chapter 7

CONCLUSIONS AND FUTURE RESEARCH SUGGESTIONS

7.1. Conclusions

The membrane is the Achilles' heel for methyl acetate and methanol pervaporation from alcohol/ester mixtures. For example, the results of pervaporation of quaternary (see Appendix I) and binary (see Figure 6 in Chapter 1) alcohol/ester mixtures, show how commercial membranes (much of which denoted as "alcohol selective") gave low separation factors during pervaporation. A similar case was found in Chapter 3, where the first case of a methyl acetate selective membrane made of PVDF for pervaporation of methyl acetate/methanol mixtures was discussed. Despite the very high total fluxes (up to 35 $kg*m^{-2}*h^{-1}$) ensured, the PVDF membrane gave a maximal $\beta_{MeOAc/MeOH}$ of 2.1 at 11 mole% methyl acetate in the feed, for pervaporation of the binary mixture; and a $\beta_{MeOAc/rest}$ of 1.77 for pervaporation of the quaternary equimolar transesterification mixture.

Accordingly, both the "alcohol selective" commercial membranes and the PVDF membrane gave an insufficient separation performance for any industrial application, which includes pervaporation of methanol/methyl acetate/*n*-butanol/*n*-butyl acetate mixtures.

The nylon-6 membrane (Abdallah et al., 2013), also reported in Figure 6, stood out in comparison with the other membranes for the separation of methyl acetate/methanol mixtures, suggesting a possible applicability.

However, the outcomes of the analysis made in Appendix I, got things into the right perspective since the $\beta_{MeOH/rest}$ for pervaporation of the quaternary equimolar alcohol/ester mixture, resulted in a value of 3.15. This value is quite far from the $\beta_{MeOH/rest}$ ~395 (estimated from Figure 15 of Chapter 2) that is necessary to produce a ~99 mole% pure methanol.

In order to synthesize membranes of high quality for pervaporation or vapour permeation separations, a method of selection of materials is necessary. In Chapter 3 it was demonstrated that the Hansen Solubility Parameters theory may fail if used as a predictive selection method for membrane materials.

Taking into account the difficulties in choosing a material, synthesizing a membrane and consequently improving its separation performances, with the intent of defining a pervaporation-based unit operation independent from stack configurations and membrane selectivity, in Chapter 4 the MSBP (Multi-Stage-Batch-Pervaporation) operation mode was presented. Simulations of this unit operation permits to conclude that three tanks and a condenser are enough to overcome any configuration limitation, allowing the obtainment of both permeate and retentate products at the desiderated concentration. Theoretically independent from the separation performance of the membrane, a MSBP unit showed a limited applicability when membranes with very low separation factor are used. In fact, for very low separation factors, the number of cycles needed in order to respect product concentrations and flow rates constrains, tends to infinite.

In Chapter 4, the inadequacy of the PSI analysis for selection of membranes to be used in a particular separation was discussed. The analysis of the *batch pervaporation-membrane performance graph* was

found to be a better selection procedure. In this graph, data of permeate product purity (*y*-axis) vs. a time index made independent from initial amount of the feed and membrane area (*x*-axis), are shown. This allows a complete description of the membrane performance during pervaporation.

Chapter 5 dealt with the concentration of the MM20 mixture (~16 mole% methyl acetate in methanol) via retrofitting of extractive distillation units. From an energetic point of view, this operation has a very high added value. In fact, an overall energy requirement reduction of 38% was estimated. This value is quite underestimated since the retrofitting was simulated using (i) a membrane of limited separation performances and high fluxes (the higher the flux the higher the energy requirement for condenser and re-heaters of the module) and (ii) using pervaporation instead of a vapour permeation module. In the case of retrofitting with a vapour permeation module, the feed is a part of the vapour exiting the two columns; this allows to save the energy of condensation of the distillate and, above all, to use the enthalpy of vaporization of the distillate for components permeation saving in energy for the re-heating system of the membrane module.

Evaluating the feasibility of this retrofitting operation, it was also found that the selectivity of the membrane can have a crucial impact on structural modifications required for the two distillation columns after retrofitting.

In Chapter 6, using PV-based flow schemes, the overall process that starts from the MM20 stream and produces a 99 mole% pure *n*-butyl acetate was studied from an energetic and economic point of view. The outcomes of this chapter allow concluding that this conversion alternative keeps its

very high remunerability quite independently from the cost of the membrane. However, being this process orphan of appropriate methanol and methyl acetate selective membranes, an industrial application is postponed; *i.e.*, a methanol and a methyl acetate membrane of good performances need to be designed, synthesized and commercialized first.

In different sections of this thesis, the influence of membrane parameters on the applicability of pervaporation was described. Accordingly, in the conclusive part of this text, an outline of the most important characteristics that a membrane should exhibit in order to be suitable for industry, is made. First of all a high selectivity is necessary. High selectivity is also the basic condition for any sustainable process (Vanneste, 2013), *i.e.*, the higher the selectivity of the membrane, the lower the energy required for condensation and the lower the number of design constraints. The question is of course how high should this selectivity be. In Chapter 6 a selectivity "high enough" to produce a permeate with the desiderated concentration in the component selective for the membrane, was assumed for the methanol and methyl acetate membranes. This also permitted to avoid working in series on the permeate minimizing condensers number, complexity and energy requirements. However, in view of an industrial application, a membrane of appropriate selectivity and very low average value of total flux (in the entire retentate/feed concentration range) is of no use. In fact, the lower the total flux, the higher the membrane area required for the separation. Yet this is not enough, since in Chapter 6 it was also found that for constant selectivity and average value of total flux, the total area critically depends on the total flux trend in the regions of low concentration in the component selective for the membrane. Apart from economic

considerations, the lower the membrane area, the less space and membrane material are consumed.

Adding to all these considerations the definition that Ready (2008) gave of process intensification: "*any engineering development that leads to a substantially smaller, cleaner, safer and more energy-efficient technology*", it is possible to conclude that selectivity, the average total flux and total flux trend at low concentrations in the component selective for the membrane, are crucial characteristics to be taken into account during the design of pervaporation-vapour permeation membranes; especially when the intent is to intensify and increase the sustainability of a certain conversion process.

7.2. Recommendations for future research

In this thesis, it is shown how the necessity of a procedure for material selection is a very urgent issue in order to give the opportunity to certain membrane processes, such as the conversion described throughout this work, to become applicable. For this reason, the study of a robust predictive selection method, which may also include the Hansen Solubility Parameters theory, is the first recommendation for future research. This would be a quite challenging study, since in the case of diffusion of molecules inside a dense membrane, many parameters need to be taken into account; most of the time these parameters depend on the way in which the membrane is synthesized.

The PVDF membranes demonstrated to have the capability of selectively pervaporate methyl acetate with high total fluxes; the study of the improvement of these membranes is also recommended. In particular, in

this case, the insertion of fillers or the synthesis of a PVDF based membrane made in a blend with other polymers should be assessed.

Since the operability of MSBP units is strictly linked to the stage termination condition, an interesting future research topic is the assessment of the effect of the stage termination condition on profitability and energetic consumption.

In this thesis, the MSBP unit operation was described considering batch operation. However, mainly for small productions it would be possible to use this technology also for semi-batch or even continuous productions. For instance, if a residence time-like parameter is introduced in the design, it would be possible to design an appropriate membrane module and tanks that work with a feed continuously sent to the feed tank; in this semi-batch mode the products are removed after a certain operation time. A continuous version could also be studied when a product and by-product stream are continuously taken from the product-tanks; in this case, a further tank may be required allowing continuously discharge of the two products without compromising the performance of the separation. Therefore, the simulation (or even implementation in a small scale) of this semi-batch or continuous version of the MSBP unit, is also suggested as future research.

The study of the influence of PV-membrane selectivity on the number of modifications, the extent of these modifications and profitability of the retrofitting of extractive distillation units, is also recommended as future research.

The literature about PV and the results of this thesis have demonstrated that the synthesis of pervaporation membranes, for separation of

mixtures consisting of similar small molecules, is very challenging and that its absence postpones the application of interesting processes (e.g., the PV-based flow scheme proposed in Chapter 6) to an undefined future. According to that, it would be interesting to explore the concept of extractive pervaporation, in which, during the separation of two similar A and B small molecules (of relatively intense mutual interaction), a larger solvent extractor component (E) is used to drag the A-molecule out. The separation of the A-E/B mixture depends mainly on the type and intensity of the interactions between these compounds in solution. For example, physical interactions may lead to two liquid phases, *i.e.*, A-E rich liquid and B rich liquid, which can be separated by decantation or in general by means of any liquid-liquid extraction unit operation. Another possibility is that, similarly to extractive distillation, the E solvent extractor alters the relative volatility of the A/B mixture, increasing the efficiency of the vapour permeation of the B compound. In any case, in series with this initial stage in which pure B is obtained, pervaporation is used to separate the A/E mixture, producing pure A and recovering E. Moreover, both A and B compounds are small, hence, it is reasonable that commercial dense membranes A and/or B selective already exist and may perform well during an extractive pervaporation unit operation. Therefore, in order to investigate this unit operation, the methanol/methyl acetate separation may be used as a challenging case-study; solvent extractors, energy requirements and economics of the operation can also be assessed.

Another future research suggested, is the study of a porous layer being highly hydrophobic or hydrophilic, to be inserted on the feed-side surface of the membrane. This layer induces the formation of a gradient of concentrations, advantaging the component selective for the membrane.

In this way, the separation factor of commercial membranes used during separations of similar small compounds may be increased. Moreover, this layer can be designed to be able to locally increase feed/retentate turbulence, minimizing the polarization phenomenon. The shape, length and diameter of the channels of this porous layer, together with the interaction of the polarization phenomenon, can be explored via computer assisted simulations coupled with experimental validation.

APPENDIX I

PERVAPORATION OF THE EQUIMOLAR TRANSESTERIFICATION MIXTURE

For most of the membranes encountered in this thesis, in Figure 41a-b, total flux and the methanol or methyl acetate separation factors for pervaporation of the equimolar quaternary mixture of transesterification between methyl acetate and *n*-butanol, are represented. The majority of these membranes were tested supposing to obtain separation factor methanol/rest of the mixture ($\beta_{MeOH/rest}$) higher than the unity. From the same figure it can be noted how the PolyAl Typ M2, denoted as "alcohol selective", gave a separation factor methyl acetate/rest of the mixture ($\beta_{MeOAc/rest}$) higher than one. In general, $\beta_{MeOH/rest}$ resulted to be lower than ~11; *i.e.*, less than one order of magnitude the value (*i.e.*, $\beta_{MeOH/rest} \sim 395$) necessary in order to obtain a permeate product of concentration of 99 mole% in methanol. This $\beta_{MeOH/rest}$ ideal value was estimated from Figure 15 of Chapter 2.

From Figure 41a-b it can be clearly concluded that, even if the method of synthesis of all the membranes is generally not known (these membranes are mostly commercial), the total flux has a trend inversely proportional to the $\beta_{MeOH/rest}$ trend. This can be attributed to a swelling effect, *i.e.*, membranes that swell more in contact with the quaternary feed solution have a lower capability in separating methanol from the other compounds. It should be taken into account that all pervaporation experiments were conducted in the same way (*i.e.*, the same thermodynamic condition for all the membranes), hence the discussion

on separation factor is also a discussion on separation ability of each membrane.

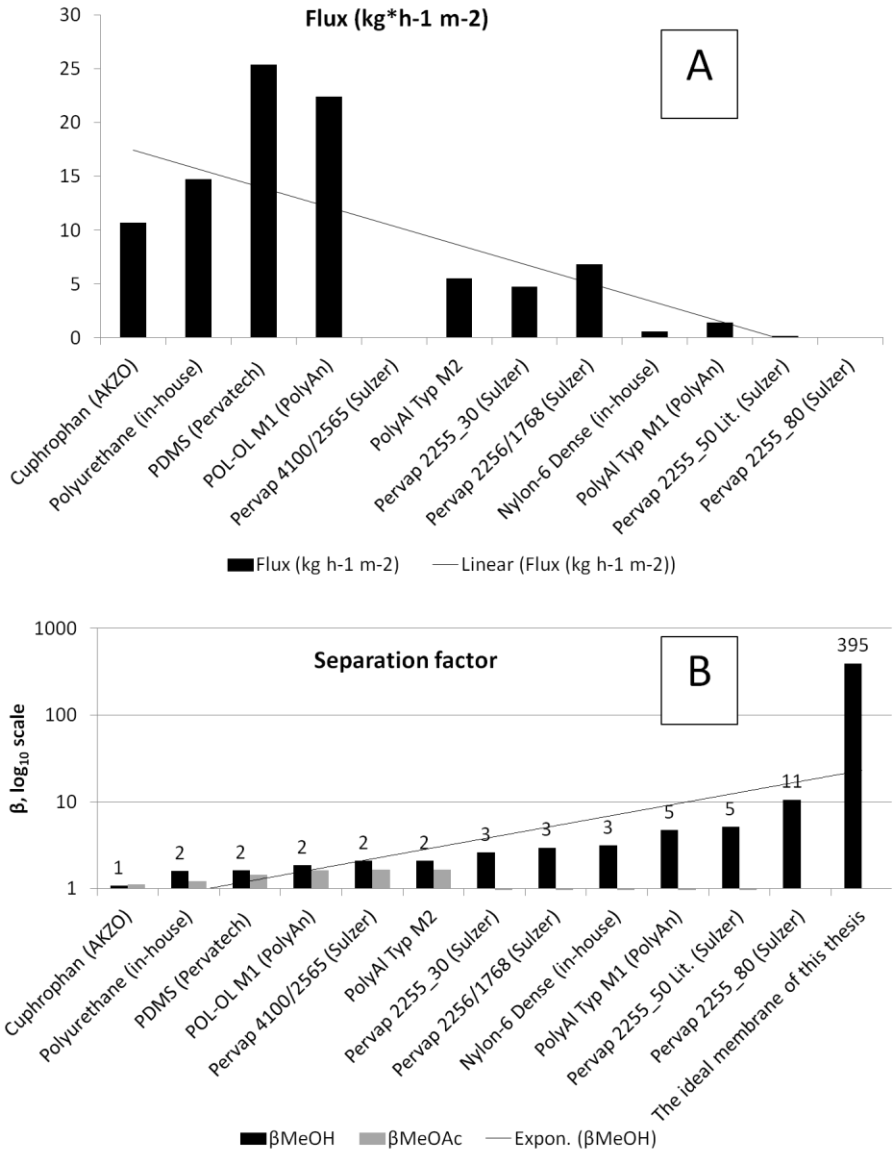

Figure 41. (a) total flux and (b) separation factor methanol/rest and methyl acetate rest, for commercial and in-house synthesized membranes. The data of the membrane Pervap 2255-50 were obtained from the work of Luis and Van der Bruggen (2015).

The nylon-6 membrane is a particular case. During the pervaporation of the quaternary alcohol/ester mixture, it was not possible to confirm the outstanding performances discussed by Abdallah et al. (2013) and reported in Figure 6. This was not understood since the nylon-6 membrane tested in this thesis was prepared on a Petri-dish and is completely dense, *i.e.*, the difference in performances cannot be attributed to a difference in synthesis conditions/procedures. A possibility is that nylon-6 suffers from *n*-butanol or *n*-butyl acetate swelling; however this should be proven by further testing.

REFERENCES

ABDALLAH, H., EL-GENDI, A., EL-ZANATI, E. & MATSUURA, T. 2013. Pervaporation of methanol from methylacetate mixture using polyamide-6 membrane. *Desalination and Water Treatment,* 51**,** 7807-7814.

ABRAMS, D. S. & PRAUSNITZ, J. M. 1975. Statistical thermodynamics of liquid mixtures: A new expression for the excess Gibbs energy of partly or completely miscible systems. *AIChE Journal,* 21**,** 116-128.

AMELIO, A., CURCIO, E., LUIS, P., CALABRÓ, V., DEGRÈVE, J., DARVISHMANESH, S. & VAN DER BRUGGEN, B. 2015. A complete study of pervaporation: experiments, modelling and simulation for the separation of MTBE and methanol. *submitted for publication*.

ANJALI DEVI, D., SMITHA, B., SRIDHAR, S. & AMINABHAVI, T. M. 2005. Pervaporation separation of isopropanol/water mixtures through crosslinked chitosan membranes. *Journal of Membrane Science,* 262**,** 91-99.

AOI, K., TAKASU, A. & OKADA, M. 1997. New Chitin-Based Polymer Hybrids. 2. Improved Miscibility of Chitin Derivatives Having Monodisperse Poly (2-methyl-2-oxazoline) Side Chains with Poly (vinyl chloride) and Poly (vinyl alcohol) 1. *Macromolecules,* 30**,** 6134-6138.

BAKER, M. I., WALSH, S. P., SCHWARTZ, Z. & BOYAN, B. D. 2012. A review of polyvinyl alcohol and its uses in cartilage and orthopedic applications. *Journal of Biomedical Materials Research Part B: Applied Biomaterials,* 100B**,** 1451-1457.

BAKER, R. W. 2012. *Membrane Technology and Applications*.

BAKER, R. W., KASCHEMEKAT, J. & WIJMANS, J. G. 1993. *Pervaporation apparatus and process*. WO 1993012865 A1.

BAKER, R. W., WIJMANS, J. G. & HUANG, Y. 2010. Permeability, permeance and selectivity: A preferred way of reporting pervaporation performance data. *Journal of Membrane Science,* 348**,** 346-352.

BELL, C. M., GERNER, F. J. & STRATHMANN, H. 1988. Selection of polymers for pervaporation membranes. *Journal of Membrane Science,* 36**,** 315-329.

BERG, L. & YEH, A.-I. 1986. *Separation of methyl acetate from methanol by extractive distillation*. US 4597834.

BOLTO, B., HOANG, M. & XIE, Z. 2011. A review of membrane selection for the dehydration of aqueous ethanol by pervaporation. *Chemical Engineering and Processing: Process Intensification,* 50**,** 227-235.

BOWEN, B. 2013. N-butanol. *ICIS Chemical Business,* 284**,** 47.

BOŻEK-WINKLER, E. & GMEHLING, J. 2006. Transesterification of Methyl Acetate and n-Butanol Catalyzed by Amberlyst 15. *Industrial & Engineering Chemistry Research,* 45**,** 6648-6654.

BRÜGGEMANN, S. & MARQUARDT, W. 2004. Shortcut methods for nonideal multicomponent distillation: 3. Extractive distillation columns. *AIChE Journal,* 50**,** 1129-1149.

BUCKLEY-SMITH, M. 2006. *The use of solubility parameters to select membrane materials for pervaporation of organic mixtures.* The University of Waikato.

CHAPMAN, P. D., OLIVEIRA, T., LIVINGSTON, A. G. & LI, K. 2008. Membranes for the dehydration of solvents by pervaporation. *Journal of Membrane Science,* 318**,** 5-37.

CHEMTECH, S. 2004. Pervaporation and vapor permeation technology. *Application of pervaporation (brochure). Sulzer Chemtech, Switzerland*.

CHEN, M. S., ENG, R. M., GLAZER, J. L. & WENSLEY, C. G. 1988. Pervaporation process for separating alcohols from ethers. Google Patents.

CHEN, M. S. K., MARKIEWICZ, G. S. & VENUGOPAL, K. G. 1989. Development of membrane pervaporation TRIM process for methanol recovery from CH3OH/MTBE/C4 mixtures. *AIChE Symposium Series,* 85**,** 82-88.

DE FIGUEIRÊDO, M. F., GUEDES, B. P., DE ARAÚJO, J. M. M., VASCONCELOS, L. G. S. & BRITO, R. P. 2011. Optimal design of extractive distillation columns—A systematic procedure using a process simulator. *Chemical Engineering Research and Design,* 89**,** 341-346.

EL-ZAHER, N. A. & OSIRIS, W. G. 2005. Thermal and structural properties of poly(vinyl alcohol) doped with hydroxypropyl cellulose. *Journal of Applied Polymer Science,* 96**,** 1914-1923.

ELICECHE, A. M., CAROLINA DAVIOU, M., HOCH, P. M. & ORTIZ URIBE, I. 2002. Optimisation of azeotropic distillation columns combined with pervaporation membranes. *Computers & Chemical Engineering,* 26**,** 563-573.

ENCYCLO.CO.UK. 2014. *Meaning of debottlenecking* [Online]. http://www.encyclo.co.uk/meaning-of-debottlenecking: Encyclo©2014 [Accessed 06-05-2015 2015].

FÁRKOVÁ, J. 1991. The pressure drop in membrane module with spacers. *Journal of Membrane Science,* 64**,** 103-111.

FENG, X. & HUANG, R. Y. M. 1996. Estimation of activation energy for permeation in pervaporation processes. *Journal of Membrane Science,* 118**,** 127-131.

FINCH, C. A. 1973. *Polyvinyl alcohol: properties and applications*, Wiley London.

FUCHIGAMI, Y. 1990. Hydrolysis of methyl acetate in distillation column packed with reactive packing of ion exchange resin. *Journal of Chemical Engineering of Japan,* 23**,** 354-359.

GENDUSO, G., AMELIO, A., LUIS, P., VAN DER BRUGGEN, B. & VREYSEN, S. 2014. Separation of methanol-tetrahydrofuran mixtures by heteroazeotropic distillation and pervaporation. *AIChE Journal,* 60**,** 2584–2595.

GOETHAERT, S., DOTREMONT, C., KUIJPERS, M., MICHIELS, M. & VANDECASTEELE, C. 1993. Coupling phenomena in the removal of chlorinated hydrocarbons by means of pervaporation. *Journal of Membrane Science,* 78**,** 135-145.

GONZALEZ, B. & ORTIZ, I. 2002. Modelling and simulation of a hybrid process (pervaporation–distillation) for the separation of azeotropic mixtures of alcohol–ether. *Journal of Chemical Technology and Biotechnology,* 77**,** 29-42.

GONZÁLEZ GONZÁLEZ, B. & ORTIZ URIBE, I. 2001. Mathematical modeling of the pervaporative separation of methanol-methylterbutyl ether mixtures. *Industrial & Engineering Chemistry Research,* 40**,** 1720-1731.

GORRI, D., IBANEZ, R. & ORTIZ, I. 2006. Comparative study of the separation of methanol-methyl acetate mixtures by pervaporation and vapor permeation using a commercial membrane. *Journal of Membrane Science,* 280**,** 582-593.

HANSEN, C. M. 1967. *The three dimensional solubility parameter and solvent diffusion coefficient. Their importance in surface coating formalation.* Danish Technical Press.

HANSEN, C. M. 1971. Solubility in the coatings industry. *Skandinavisk Tidskriftfoer Faergoch Lack,* 17**,** 69-77.

HANSEN, C. M. 2012. *Hansen Solubility Parameters: A User's Handbook*, CRC press.

HARO, P., OLLERO, P., VILLANUEVA PERALES, A. L. & GÓMEZ-BAREA, A. 2013. Thermochemical biorefinery based on dimethyl ether as intermediate: Technoeconomic assessment. *Applied Energy,* 102**,** 950-961.

HEINTZ, A. & STEPHAN, W. 1994. A generalized solution—diffusion model of the pervaporation process through composite membranes Part I. Prediction of mixture solubilities in the dense active layer using the UNIQUAC model. *Journal of Membrane Science,* 89**,** 143-151.

HENLEY, E. J., SEADER, J. D. & ROPER, D. K. 2011. *Separation process principles*, Wiley.

HICKEY, P. J. & GOODING, C. H. 1994. The economic optimization of spiral wound membrane modules for the pervaporative removal of VOCs from water. *Journal of Membrane Science,* 97**,** 53-70.

HIROSHI, Y. 2010. *Hansen Solubility Parameters (HSP) and Poly(vinylidene fluoride) swelling* [Online]. Available: http://pirika.com/NewHP/PirikaE2/PVdF.html [Accessed 24-04-2014 2014].

HO, W. W. & SIRKAR, K. K. 1992. *Membrane handbook*, Springer Science & Business Media.

HOCH, P., DAVIOU, M. & ELICECHE, A. 2003. Optimization of the operating conditions of azeotropic distillation columns with pervaporation membranes. *Latin American Applied Research,* 33**,** 177-183.

HUANG, R. Y. M. & YEOM, C. K. 1991. Pervaporation separation of aqueous mixtures using crosslinked polyvinyl alcohol membranes. III.

Permeation of acetic acid-water mixtures. *Journal of Membrane Science,* 58**,** 33-47.

IGLESIAS, M., MARINO, G., ORGE, B., PIÑEIRO, M. M. & TOJO, J. 1999. Liquid-Liquid Equilibria, and Thermodynamic Properties of the System Methyl Acetate+ Methanol+ Water at 298.15 K. *Physics and Chemistry of Liquids,* 37**,** 193-213.

IHS-CHEMICAL. 2013. *Polyvinyl Alcohols* [Online]. Available: http://www.ihs.com/products/chemical/planning/ceh/polyvinyl-alcohols.aspx.

JAFAR, J. J. & BUDD, P. M. 1997. Separation of alcohol/water mixtures by pervaporation through zeolite A membranes. *Microporous Materials,* 12**,** 305-311.

JIMÉNEZ, L. & COSTA-LÓPEZ, J. 2002. The Production of Butyl Acetate and Methanol via Reactive and Extractive Distillation. II. Process Modeling, Dynamic Simulation, and Control Strategy. *Industrial & Engineering Chemistry Research,* 41**,** 6735-6744.

JIMÉNEZ, L., GARVÍN, A. & COSTA-LÓPEZ, J. 2002. The production of butyl acetate and methanol via reactive and extractive distillation. I. Chemical equilibrium, kinetics, and mass-transfer issues. *Industrial & Engineering Chemistry Research,* 41**,** 6663-6669.

JULLOK, N., DARVISHMANESH, S., LUIS, P. & VAN DER BRUGGEN, B. 2011. The potential of pervaporation for separation of acetic acid and water mixtures using polyphenylsulfone membranes. *Chemical Engineering Journal,* 175**,** 306-315.

KHAJAVI, S., JANSEN, J. C. & KAPTEIJN, F. 2010. Application of a sodalite membrane reactor in esterification—Coupling reaction and separation. *Catalysis Today,* 156**,** 132-139.

KIRSCHNER, M. 2007. Polyvinyl alcohol. *In:* AMERICAS, I. C. B. (ed.) *Chemical Profile.*

KISS, A. A. 2013. *Advanced distillation technologies: design, control and applications*, John Wiley & Sons.

KOPEĆ, R., MELLER, M., KUJAWSKI, W. & KUJAWA, J. 2013. Polyamide-6 based pervaporation membranes for organic–organic separation. *Separation and Purification Technology,* 110**,** 63-73.

KREIS, P. & GÓRAK, A. 2006. Process Analysis of Hybrid Separation Processes: Combination of Distillation and Pervaporation. *Chemical Engineering Research and Design,* 84**,** 595-600.

KUJAWSKI, W. 2000. Application of pervaporation and vapor permeation in environmental protection. *Polish Journal of Environmental Studies,* 9**,** 13-26.

LANE, K. 2013. Butyl acetate. *ICIS Chemical Business,* 283**,** 43.

LANGSTON, P., HILAL, N., SHINGFIELD, S. & WEBB, S. 2005. Simulation and optimisation of extractive distillation with water as solvent. *Chemical Engineering and Processing: Process Intensification,* 44**,** 345-351.

LIPNIZKI, F., FIELD, R. W. & TEN, P.-K. 1999. Pervaporation-based hybrid process: a review of process design, applications and economics. *Journal of Membrane Science,* 153**,** 183-210.

LIU, F., HASHIM, N. A., LIU, Y., ABED, M. R. M. & LI, K. 2011. Progress in the production and modification of PVDF membranes. *Journal of Membrane Science,* 375**,** 1-27.

LUIS, P., DEGRÈVE, J. & VAN DER BRUGGEN, B. 2013. Separation of methanol–n-butyl acetate mixtures by pervaporation: Potential of 10 commercial membranes. *Journal of Membrane Science,* 429**,** 1-12.

LUIS, P. & VAN DER BRUGGEN, B. 2015. The driving force as key element to evaluate the pervaporation performance of multicomponent mixtures. *Separation and Purification Technology,* 148**,** 94-102.

LUYBEN, W. L. 2010. Design and Control of the Butyl Acetate Process†. *Industrial & Engineering Chemistry Research,* 50**,** 1247-1263.

LUYBEN, W. L., PSZALGOWSKI, K. M., SCHAEFER, M. R. & SIDDONS, C. 2004. Design and Control of Conventional and Reactive Distillation Processes for the Production of Butyl Acetate. *Industrial & Engineering Chemistry Research,* 43**,** 8014-8025.

MANDAL, S. & PANGARKAR, V. G. 2002. Separation of methanol-benzene and methanol-toluene mixtures by pervaporation: effects of thermodynamics and structural phenomenon. *Journal of Membrane Science,* 201**,** 175-190.

MATUSCHEWSKI, H. & SCHEDLER, U. 2008. MSE—modified membranes in organophilic pervaporation for aromatics/aliphatics separation. *Desalination,* 224**,** 124-131.

MCCABE, W. L., SMITH, J. C. & HARRIOTT, P. 2005. *Unit operations of chemical engineering*, McGraw-Hill Book Company New York.

MORIGAMI, Y., KONDO, M., ABE, J., KITA, H. & OKAMOTO, K. 2001. The first large-scale pervaporation plant using tubular-type module with zeolite NaA membrane. *Separation and Purification Technology,* 25**,** 251-260.

MULDER, M. 1998. *Basic Principles of Membrane Technology*, Kluwer Academic Publishers.

O'BRIEN, D. J., ROTH, L. H. & MCALOON, A. J. 2000. Ethanol production by continuous fermentation–pervaporation: a preliminary economic analysis. *Journal of Membrane Science,* 166**,** 105-111.

OLIVEIRA, T. A., COCCHINI, U., SCARPELLO, J. T. & LIVINGSTON, A. G. 2001. Pervaporation mass transfer with liquid flow in the transition regime. *Journal of Membrane Science,* 183**,** 119-133.

PENG, Y., CUI, X., ZHANG, Y., FENG, T., TIAN, Z. & XUE, L. 2014. Kinetics of Transesterification of Methyl Acetate and Ethanol Catalyzed by Ionic Liquid. *International Journal of Chemical Kinetics,* 46**,** 116-125.

PENKOVA, A. V., POLOTSKAYA, G. A. & TOIKKA, A. M. 2013. Separation of acetic acid-methanol-methyl acetate-water reactive mixture. *Chemical Engineering Science,* 101**,** 586-592.

PERRY, R. H. & GREEN, D. W. 2008. *Perry's Chemical Engineers' Handbook*, McGraw-Hill.

PRIBIC, P., ROZA, M. & ZUBER, L. 2006. How to Improve the Energy Savings in Distillation and Hybrid Distillation-Pervaporation Systems. *Separation Science and Technology,* 41**,** 2581-2602.

RAUTENBACH, R. & ALBRECHT, R. 1989. *Membrane Processes,* New York, John Wiley & Sons

REAY, D. 2008. The role of process intensification in cutting greenhouse gas emissions. *Applied Thermal Engineering,* 28**,** 2011-2019.

SAIN, S., DINÇER, S. & SAVAŞÇYı, Ö. T. 1998. Pervaporation of methanol–methyl acetate binary mixtures. *Chemical Engineering and Processing: Process Intensification,* 37**,** 203-206.

SAMPRANPIBOON, P., JIRARATANANON, R., UTTAPAP, D., FENG, X. & HUANG, R. Y. M. 2000. Pervaporation separation of ethyl butyrate and isopropanol with polyether block amide (PEBA) membranes. *Journal of Membrane Science,* 173**,** 53-59.

SCHIFFMANN, P. & REPKE, J.-U. 2015. Experimental Investigation and Simulation of Organophilic Pervaporation in Laboratory and Pilot Scale. *Chemical Engineering & Technology,* 38**,** 879-890.

SCHOCK, G. & MIQUEL, A. 1987. Mass transfer and pressure loss in spiral wound modules. *Desalination,* 64**,** 339-352.

SIGMA-ALDRICH. 2014. *Polypropylene, chlorinated* [Online]. http://www.sigmaaldrich.com/. Available: http://www.sigmaaldrich.com/catalog/product/aldrich/450391?lang=fr&region=BE [Accessed 07-07-2014.

SINNOTT, R. K. 1999. *Coulson & Richardson's Chemical Engineering* Butterworth-Heinemann.

SMITHA, B., SUHANYA, D., SRIDHAR, S. & RAMAKRISHNA, M. 2004. Separation of organic–organic mixtures by pervaporation—a review. *Journal of Membrane Science,* 241**,** 1-21.

SNYDER, J. M. 1960. *Alcoholysis of polyvinyl acetate.* US 2,950,271.

SOLVAY. 2014. *Solef 6020 polyvinylidene fluoride* [Online]. Solvay Speciality Polymers. Available: http://catalog.ides.com/Datasheet.aspx?I=92041&U=0&FMT=PDF&E=111434 2014].

STEINIGEWEG, S. & GMEHLING, J. 2004. Transesterification processes by combination of reactive distillation and pervaporation. *Chemical Engineering and Processing: Process Intensification,* 43**,** 447-456.

TECNON-ORBICHEM 1 November 2013a. Chem-Net Facts - Chemical Market Insight And Foresight - On A Single Page - Acetic Acid.

TECNON-ORBICHEM 1 November 2013b. Chem-Net Facts - Chemical Market Insight And Foresight - On A Single Page - Methanol.

TER JUNG, H., REIHS, L. & ROH, G. 1983. *Process for the manufacture of polyvinyl alcohol by alcoholysis of a polyvinyl ester*. US 4,401,790.

TU, C.-H., WU, Y.-S. & LIU, T.-L. 1997. Isobaric vapor-liquid equilibria of the methanol, methyl acetate and methyl acrylate system at atmospheric pressure. *Fluid Phase Equilibria,* 135**,** 97-108.

TURTON, R., BAILIE, R. C., WHITING, W. B. & SHAEIWITZ, J. A. 2003. *Analysis, synthesis and design of chemical processes,* Upper Saddle River (New Jersey), Pearson Education Inc.

URAGAMI, T., SUMIDA, I., MIYATA, T., SHIRAIWA, T., TAMURA, H. & YAJIMA, T. 2011. Pervaporation Characteristics in Removal of Benzene from Water through Polystyrene-Poly (Dimethylsiloxane) IPN Membranes. *Materials Sciences and Applications,* 2**,** 169.

VAN BAELEN, D., REYNIERS, A., VAN DER BRUGGEN, B., VANDECASTEELE, C. & DEGRÈVE, J. 2005. Pervaporation of binary and ternary mixtures of water with methanol and/or ethanol. *Separation Science and Technology,* 39**,** 563-580.

VAN DER BRUGGEN, B., JANSEN, J. C., FIGOLI, A., GEENS, J., VAN BAELEN, D., DRIOLI, E. & VANDECASTEELE, C. 2004. Determination of parameters affecting transport in polymeric membranes: parallels between pervaporation and nanofiltration. *The Journal of Physical Chemistry B,* 108**,** 13273-13279.

VAN HOOF, V., VAN DEN ABEELE, L., BUEKENHOUDT, A., DOTREMONT, C. & LEYSEN, R. 2004. Economic comparison between azeotropic distillation and different hybrid systems combining distillation with pervaporation for the dehydration of isopropanol. *Separation and Purification Technology,* 37**,** 33-49.

VANDI, L.-J., HOU, M., VEIDT, M., TRUSS, R., HEITZMANN, M. & PATON, R. Interface diffusion and morphology of aerospace grade epoxy co-cured with thermoplastic polymers. 28th International Congress of the Aeronautical Sciences (ICAS 2012), 2012. International Council of the Aeronautical Sciences (ICAS).

VANNESTE, J. 2013. *Development of integrated membrane techniques for advanced separations* Doctor in Engineering Science, KULeuven.

WANG, Q., YU, B. & XU, C. 2012. Design and Control of Distillation System for Methylal/Methanol Separation. Part 1: Extractive Distillation Using DMF as an Entrainer. *Industrial & Engineering Chemistry Research,* 51**,** 1281-1292.

WANG, S.-J., HUANG, H.-P. & YU, C.-C. 2011. Design and Control of a Heat-Integrated Reactive Distillation Process to Produce Methanol and n-Butyl Acetate. *Industrial & Engineering Chemistry Research,* 50**,** 1321-1329.

WANG, S.-J., WONG, D. S. H. & YU, S.-W. 2008. Design and control of transesterification reactive distillation with thermal coupling. *Computers & Chemical Engineering,* 32**,** 3030-3037.

WANG, Y.-C., LI, C.-L., HUANG, J., LIN, C., LEE, K.-R., LIAW, D.-J. & LAI, J.-Y. 2001. Pervaporation of benzene/cyclohexane mixtures through aromatic polyamide membranes. *Journal of Membrane Science,* 185**,** 193-200.

WANKAT, P. C. 2006. *Separation process engineering*, Pearson Education, Inc.

WIJMANS, J. G. & BAKER, R. W. 1995. The solution-diffusion model: a review. *Journal of Membrane Science,* 107**,** 1-21.

YANG, Z., CUI, X., YU, X., ZHANG, Y., FENG, T., LIU, H. & SONG, K. 2015. Transesterification of Methyl Acetate with n-Butanol Catalyzed by Single and Mixed Ionic Liquids. *Catalysis Letters,* 145**,** 1281-1289.

ZHANG, S.-J. & YU, H.-Q. 2004. Radiation-induced degradation of polyvinyl alcohol in aqueous solutions. *Water Research,* 38**,** 309-316.

INFORMATION ABOUT THE AUTHOR

Curriculum Vitae

Giuseppe Genduso was born on July 29th, 1986 in Petralia Sottana (Italy). He obtained a B. Sc. in Chemical Engineering at the University of Palermo (UNIPA) in 2009 and a M. Sc. in Chemical Engineering at the same university in 2012, cum laude. He conducted his master thesis study at the Helmholtz-Zentrum-Berlin für Materialien und Energie (HZB) about deposition of indium sulphide buffer layers on metallic template nano-wires substrates (preliminary study to the development of the next generation of solar cells).

In 2013 he started working in the group of prof. Bart Van der Bruggen investigating the applicability of pervaporation for organic-waste mixtures valorisation.

List of Publications

Articles in international peer reviewed academic journals

Genduso G., Luis P., Van der Bruggen B. Techno-economical assessment of a pervaporation based production of n-butyl acetate from methyl acetate waste streams; (submitted for publication).

Genduso G., Amelio A., Colombini E., Luis P, Degrève J, Van der Bruggen B. (2016). Retrofitting of extractive distillation columns with high flux, low separation factor membranes: a way to reduce the energy demand? *Chemical Engineering Research and Design, 109, 127 - 140.*

Genduso G., Luis, P., Van der Bruggen B. (2015). Overcoming any configuration limitation: an alternative operation mode for pervaporation and vapour

permeation. *Journal of Chemical Technology and Biotechnology. n/a* (n/a), n/a-n/a

Genduso G., Farrokhzad H., Latré Y., Darvishmanesh S., Luis P. and Van der Bruggen B. (2015). Polyvinylidene fluoride dense membrane for the pervaporation of methyl acetate-methanol mixtures. *Journal of Membrane Science, 482, 128-136.*

Farrokhzad H., Darvishmanesh S., Genduso G., Van Gerven T., Van der Bruggen B. (2015). Development of bivalent cation selective ion exchange membranes by varying molecular weight of polyaniline. *Electrochimica Acta*, 158, 64-72.

Genduso G., Amelio A., Luis P., Van der Bruggen B., Vreysen S. (2014). Separation of methanol-tetrahydrofuran mixtures by heteroazeotropic distillation and pervaporation. *AIChE Journal, 60* (7), 2584-2595.

Amelio A., Genduso G., Vreysen S., Luis P., Van der Bruggen B. (2014). Guidelines based on life cycle assessment for solvent selection during the process design and evaluation of treatment alternatives. *Green Chemistry, 16*, 3045-3063.

Genduso G., Inguanta R., Sunseri C., Piazza S., Kelch C., Saez-Araoz R., Zykov A., Fischer C. H. (2013). Deposition of very thin uniform indium sulfide layers over metallic nano-rods by the Spray-Ion Layer Gas Reaction method. *Thin Solid Films, 548*, 91-97.

Piazza S., Genduso G., Inguanta R., Sunseri C., Lux-Steinerb M., Fischerb C.-H. Nickel-Indium Sulphide Core-Shell Nanostructures obtained by Spray-ILGAR Deposition. (2013). *Chemical Engineering Transactions.* 32.

Book chapters

G. Genduso, P. Luis and B. Van der Bruggen, *19 - Pervaporation membrane reactors (PVMRs) for esterification*, In Woodhead Publishing Series in Energy, edited by Angelo Basile, Luisa Di PaolaFaisal l. Hai and Vincenzo Piemonte, Woodhead Publishing, 2015, Pages 565-603, *Membrane Reactors for Energy Applications and Basic Chemical Production.*

Scientific Conferences-symposia Proceedings

Genduso G., Farrokhzad H., Colombini E., Latré Y., Darvishmanesh S., Luis P., Van der Bruggen B. (2014). Two relevant pervaporation membranes for the separation of methyl-acetate-methanol industrial streams. *4th International Scientific Conference on Pervaporation, Vapor Permeation and Membrane Distillation*. International Scientific Conference on Pervaporation, Vapor Permeation and Membrane Distillation. Torun, Poland, 21-24 Sep 2014 (art.nr. SL 18).

Genduso G, Inguanta R, Sunseri C, Piazza S, LuxSteiner M, Kelch C, et al., editors. (2013). Electrodeposition and ILGAR process to obtain Ni-In_2S_3 core-shell nanowires. *GEI 2013 Giornate dell'elettrochimica Italiana*.